

**FACULDADE DE ENGENHARIA DA UNIVERSIDADE DO PORTO**

# **Robot Self-Localization in Dynamic Environments**

**Carlos Miguel Correia da Costa**



Mestrado Integrado em Engenharia Informática e Computação

Supervisor: Armando Jorge Miranda de Sousa (Ph.D.)

Second Supervisor: Germano Manuel Correia dos Santos Veiga (Ph.D.)

January 26, 2015

© Carlos Miguel Correia da Costa, 2015

# **Robot Self-Localization in Dynamic Environments**

**Carlos Miguel Correia da Costa**

Mestrado Integrado em Engenharia Informática e Computação

Approved in oral examination by the committee:

Chair: Doctor Name of the President

External Examiner: Doctor Name of the Examiner

Supervisor: Doctor Name of the Supervisor



# Abstract

Mobile robot platforms capable of operating safely and accurately in dynamic environments can have a multitude of applications, ranging from simple delivery tasks to advanced assembly operations. These abilities rely heavily on a robust navigation stack, which requires a stable and accurate localization system.

This dissertation describes an efficient, modular, extensible and easy to configure 3/6 [Degrees of Freedom \(DoF\)](#) localization system, capable of operating on a wide range of mobile robot platforms and environments. It is able to reliably estimate the global position using feature matching and is capable of achieving high accuracy pose tracking using point cloud registration algorithms. It can use several point cloud sensing devices (such as [Light Detection And Ranging \(LIDAR\)](#) or RGB-D cameras) and requires no artificial landmarks. Moreover, it can update the localization map at runtime and dynamically adjust its operation rate based on the predicted robot velocity in order to use the minimum amount of hardware resources. It also offers a detailed analysis of each pose estimation, providing information about the percentage of registered inliers, the root mean square error of the inliers, the angular distribution of the inliers and outliers, the pose corrections that were performed in relation to the expected position and in case of initial pose estimation it also gives the distribution of the acceptable initial poses, which can be very valuable information for a navigation supervisor when the robot is in ambiguous areas that are very similar in different parts of the known environment.

The [Robot Operating System \(ROS\)](#) implementation was tested in several dynamic indoor environments using two mobile robot platforms equipped with [LIDARs](#) and RGB-D cameras. Overall tests using sensor data from simulation and retrieved from the robot platforms performed in a high end laptop with an Intel Core i7 3630QM processor, 16GB DDR3 of memory and NVIDIA GTX680M graphics card, demonstrated high accuracy in complex dynamic environments, with less than 1 cm in translation error and less than 1 degree in rotation error. Execution times ranged from 5 to 30 milliseconds in a 3 [DoF](#) setup and from 50 to 150 milliseconds in a full dynamic 6 [DoF](#) configuration.

The sub centimeter accuracy achieved by the proposed localization system along with the dynamic map update capability and the need of no artificial landmarks will allow the fast deployment of mobile robot platforms capable of operating safely and accurately in cluttered environments. Moreover, the resilience to dynamic objects will grant the possibility to use robots as coworkers, helping humans perform their work more efficiently and thus reducing the overall production costs.



# Resumo

Plataformas móveis robóticas capazes de operar com precisão e de forma segura em ambientes dinâmicos têm um alargado espetro de aplicações, desde simples entregas de objetos até operações complexas de montagem. Para atingir estes requisitos de operação é necessário um sistema de navegação robusto, que por sua vez requer um módulo de localização preciso e estável.

Esta dissertação descreve um sistema de localização para 3/6 graus de liberdade (DoF), que é eficiente, modular, extensível e fácil de configurar, capaz de operar num alargado conjunto de plataformas móveis e ambientes. É capaz de estimar a posição inicial de um robô usando métodos de associação de características geométricas e consegue seguir a sua pose com alta precisão através de algoritmos de registo de nuvens de pontos. A sua implementação consegue tirar partido de vários sensores laser e câmaras RGB-D e não necessita de marcadores artificiais ou modificação do ambiente. Possui ainda a capacidade de atualizar o mapa incrementalmente e ajustar a sua frequência de funcionamento de acordo com a velocidade do robô de forma a usar o mínimo de recursos computacionais possível. Para facilitar a avaliação da qualidade da localização para operações críticas, cada estimativa da pose do robô é acompanhada com a análise do registo da nuvem de pontos, contendo informação acerca da percentagem de pontos corretamente registados, a raiz quadrada do erro quadrático médio, a distribuição angular dos pontos classificados como pertencentes e não pertencentes ao mapa de referência, as correções aplicadas à estimativa da pose e no caso de ser efetuada localização global também é disponibilizada a distribuição das poses iniciais aceitáveis, o que pode ser informação bastante útil para um supervisor de navegação quando o robô está em posições ambíguas do ambiente nas quais existe geometria semelhante em sítios diferentes do mapa.

A implementação em ROS foi testada em vários ambientes dinâmicos recorrendo a duas plataformas móveis equipadas com LIDARs e câmaras RGB-D. Os resultados obtidos usando dados de simulação e recolhidos das plataformas robóticas realizados num portátil com CPU Intel Core i7 3630QM, 16GB DDR3 de memória e placa gráfica NVIDIA GTX680M demonstraram que o sistema consegue fazer a estimativa da pose do robô com um erro de translação inferior a 1 centímetro e um erro de rotação abaixo de 1 grau. Os tempos de execução oscilaram entre 5 e 30 milissegundos para uma configuração 3 DoF e entre 50 e 150 milissegundos para 6 DoF.

A alta precisão disponibilizada pelo sistema de localização proposto em conjunto com a sua capacidade para atualizar o mapa incrementalmente e de não necessitar marcadores artificiais, irá permitir o desenvolvimento de plataformas robóticas móveis capazes de operar em ambientes não estruturados. Por outro lado, a sua robustez em relação a objetos dinâmicos abre a possibilidade dos robôs colaborarem com humanos para melhorar a produtividade global de uma dada tarefa e assim reduzir os custos de produção.



# Acknowledgments

I would like to express my gratitude to my supervisors and the INESC team, for their helpful contributions. Their experience and expertise significantly improved the quality of this dissertation.

I am also very grateful for the knowledge and experiences that I gather from my friends, teachers and colleagues over the years and for the brilliant work developed by the ROS and PCL community.

And of course, to my family, for their continuous support.

Carlos Miguel Correia da Costa



*“Perfection is achieved, not when there is nothing more to add,  
but when there is nothing left to take away.”*

Antoine de Saint-Exupéry



# Contents

<b>1</b>	<b>Introduction</b>	<b>1</b>
1.1	Context . . . . .	1
1.2	Project . . . . .	1
1.3	Motivation and objectives . . . . .	2
1.4	Contributions . . . . .	2
1.5	Dissertation outline . . . . .	2
<b>2</b>	<b>Localization methods</b>	<b>3</b>
2.1	Proprioceptive methods . . . . .	3
2.1.1	Odometry . . . . .	3
2.1.2	Dead reckoning . . . . .	4
2.2	Exteroceptive methods . . . . .	4
2.2.1	Trilateration methods . . . . .	4
2.2.1.1	Global Navigation Satellite System (GNSS) . . . . .	4
2.2.1.2	Differential Global Positioning System (DGPS) . . . . .	5
2.2.1.3	Assisted Global Positioning System (AGPS) . . . . .	5
2.2.1.4	Signal strength geolocation methods . . . . .	6
2.2.2	Celestial navigation . . . . .	6
2.2.3	Landmark methods . . . . .	7
2.2.4	Point cloud methods . . . . .	7
2.2.5	Probabilistic methods . . . . .	8
2.2.5.1	Monte Carlo Localization (MCL) . . . . .	8
2.2.5.2	Kalman filters . . . . .	9
2.2.5.3	Perfect Match . . . . .	10
2.2.6	Simultaneous Localization And Mapping (SLAM) . . . . .	10
2.3	Summary . . . . .	11
<b>3</b>	<b>Relevant software / hardware technologies</b>	<b>13</b>
3.1	ROS . . . . .	13
3.1.1	Architecture . . . . .	13
3.1.1.1	Nodes . . . . .	14
3.1.1.2	Nodelets . . . . .	15
3.1.1.3	Topics . . . . .	15
3.1.1.4	Services . . . . .	15
3.1.1.5	Actions . . . . .	16
3.1.2	Build system . . . . .	16
3.1.3	Development tools . . . . .	16
3.1.3.1	Graphical User Interface tools . . . . .	16

## CONTENTS

3.1.3.2	Command line tools . . . . .	17
3.2	PCL . . . . .	17
3.3	Gazebo . . . . .	18
3.4	Point cloud acquisition . . . . .	19
3.4.1	Structured light methods . . . . .	19
3.4.2	Time of Flight methods . . . . .	20
3.4.2.1	Light waves . . . . .	20
3.4.2.2	Radio waves . . . . .	21
3.4.2.3	Sound waves . . . . .	22
3.4.3	Stereo vision . . . . .	23
<b>4</b>	<b>Localization system</b>	<b>25</b>
4.1	Overview . . . . .	25
4.2	Pipeline configuration . . . . .	27
4.3	Reference map . . . . .	27
4.4	Point cloud assembly . . . . .	28
4.5	Point cloud search data structures . . . . .	28
4.5.1	Voxel grids . . . . .	29
4.5.2	Octrees . . . . .	29
4.5.3	k-d trees . . . . .	30
4.6	Filtering and down sampling . . . . .	30
4.6.1	Point cloud downsampling . . . . .	31
4.6.1.1	Voxel grid sampling . . . . .	31
4.6.1.2	Random sampling . . . . .	31
4.6.1.3	Covariance sampling . . . . .	31
4.6.2	Outlier removal . . . . .	32
4.6.2.1	Distance filter . . . . .	32
4.6.2.2	Passthrough filter . . . . .	32
4.6.2.3	Radius outlier removal filter . . . . .	33
4.6.2.4	Statistical outlier removal filter . . . . .	33
4.6.3	Surface and object reconstruction and resampling . . . . .	33
4.7	Normal estimation . . . . .	34
4.7.1	Line normal estimation . . . . .	35
4.7.2	Surface normal estimation . . . . .	35
4.8	Keypoint detection . . . . .	35
4.9	Keypoint description . . . . .	36
4.10	Cloud registration . . . . .	36
4.10.1	Initial alignment with keypoints descriptor matching . . . . .	36
4.10.2	Final alignment with point cloud error minimization . . . . .	37
4.11	Outlier detection . . . . .	37
4.12	Localization validation . . . . .	38
4.13	Dynamic map update . . . . .	38
<b>5</b>	<b>Localization system evaluation</b>	<b>39</b>
5.1	Testing platforms . . . . .	39
5.1.1	Jarvis platform . . . . .	39
5.1.2	Guardian platform . . . . .	40
5.2	Testing environments . . . . .	41
5.2.1	Jarvis in RoboCup field . . . . .	41

## CONTENTS

5.2.2	Guardian in structured environment . . . . .	42
5.3	3 DoF localization system tests . . . . .	43
5.3.1	Overview . . . . .	43
5.3.2	Jarvis robot tests . . . . .	45
5.3.2.1	Rounded path using Jarvis robot at 5 cm/s . . . . .	45
5.3.2.2	Complex path using Jarvis robot at 5 cm/s . . . . .	48
5.3.3	Jarvis simulator tests . . . . .	51
5.3.3.1	Rounded path using Jarvis simulator at 5 cm/s . . . . .	51
5.3.3.2	Rounded path using Jarvis simulator at 50 cm/s . . . . .	53
5.3.3.3	Rounded path using Jarvis simulator at 100 cm/s . . . . .	55
5.3.3.4	Complex path using Jarvis simulator at 5 cm/s . . . . .	57
5.3.3.5	Complex path using Jarvis simulator at 50-30-50-20 cm/s . . . . .	59
5.3.3.6	Complex path using Jarvis simulator at 200-30-200-30 cm/s . . . . .	61
5.3.4	Guardian simulator tests . . . . .	63
5.3.4.1	Wall follower path using Guardian simulator at 5 cm/s in static environment . . . . .	63
5.3.4.2	Wall follower path using Guardian simulator at 30 cm/s in static environment . . . . .	65
5.3.4.3	Wall follower path using Guardian simulator at 5 cm/s in static cluttered environment . . . . .	67
5.3.4.4	Wall follower path using Guardian simulator at 30 cm/s in static cluttered environment . . . . .	69
5.3.4.5	Wall follower path using Guardian simulator at 5 cm/s in dynamic cluttered environment . . . . .	71
5.3.4.6	Wall follower path using Guardian simulator at 30 cm/s in dynamic cluttered environment . . . . .	73
5.3.5	Initial pose estimation tests . . . . .	75
5.3.6	Results discussion . . . . .	76
5.4	6 DoF localization system tests . . . . .	77
5.4.1	Overview . . . . .	77
5.4.2	Results . . . . .	77
5.4.3	Results discussion . . . . .	77
6	Conclusions and future work	79
References		81

## CONTENTS

# List of Figures

2.1	Different types of optical encoders used to measure distances . . . . .	4
2.2	Trilateration technique in a global localization system . . . . .	5
2.3	Circle of position in celestial navigation . . . . .	6
2.4	ICP point cloud matching . . . . .	7
2.5	MCL particle distribution animation . . . . .	8
2.6	MCL redistribution of particles . . . . .	8
2.7	MCL position refinement . . . . .	8
2.8	MCL position estimation . . . . .	8
2.9	Unscented Kalman Filter . . . . .	9
2.10	Position estimates . . . . .	10
2.11	Positions associated error . . . . .	10
3.1	ROS logo . . . . .	13
3.2	PCL logo . . . . .	17
3.3	Point Cloud Library . . . . .	17
3.4	Gazebo logo . . . . .	18
3.5	Integration of ROS and Gazebo . . . . .	18
3.6	Structured light system diagram . . . . .	19
3.7	Kinect 2 sensor . . . . .	19
3.8	Structure IO sensor . . . . .	19
3.9	LIDAR scan . . . . .	20
3.10	Time of Flight system diagram . . . . .	21
3.11	Mesa SR4000 sensor . . . . .	21
3.12	2D SICK NAV 350 sensor . . . . .	21
3.13	3D Velodyne HDL-64E sensor sensor . . . . .	21
3.14	RADAR scan of two ships . . . . .	22
3.15	QT50R-AFH RADAR sensor . . . . .	22
3.16	SONAR scan of two ships . . . . .	22
3.17	SONAR sensor . . . . .	22
3.18	Stereo vision system . . . . .	23
3.19	PR2 head capable of active stereo vision . . . . .	23
3.20	Stereo vision overview . . . . .	24
4.1	Localization system overview . . . . .	26
4.2	Laser scans assembled with tilting platform (red points) . . . . .	28
4.3	Voxel grid applied over trees point clouds . . . . .	29
4.4	Octree of a stag beetle . . . . .	29
4.5	2-d tree . . . . .	30

## LIST OF FIGURES

4.6	3-d tree . . . . .	30
4.7	Table point cloud before (left) and after (right) voxel grid downsampling . . . . .	31
4.8	Statistical outlier removal filter . . . . .	33
4.9	Surface smoothing using moving least squares algorithm . . . . .	34
4.10	Surface normals refinement using moving least squares algorithm . . . . .	34
4.11	Point neighborhood for normal estimation . . . . .	35
4.12	Point cloud registration with outlier detection . . . . .	37
5.1	Jarvis testing platform . . . . .	40
5.2	Guardian testing platform . . . . .	40
5.3	Guardian Gazebo simulation . . . . .	40
5.4	Jarvis tests environment . . . . .	41
5.5	Guardian testing environment . . . . .	42
5.6	Guardian cluttered (left) and dynamic (right) testing environment . . . . .	42
5.7	Interactive CAD of Guardian testing environment (.u3d file) . . . . .	43
5.8	Paths from ground truth (green), localization system (blue) and odometry (red) . .	45
5.9	Localization system translation error (left) and its statistical distributions (right) .	45
5.10	Localization system translation corrections (left) and its statistical distributions (right) . . . . .	45
5.11	Localization system translation error (left) and corrections (right) components . . .	46
5.12	Localization system rotation error (left) and its statistical distributions (right) . .	46
5.13	Localization system rotation corrections (left) and its statistical distributions (right) .	46
5.14	Odometry translation error (left) and its statistical distributions (right) . . . . .	46
5.15	Odometry rotation error (left) and its statistical distributions (right) . . . . .	47
5.16	Localization system inliers RMSE (left) and its statistical distributions (right) . .	47
5.17	Cloud registration outlier percentage (left) and inliers angular distribution (right) .	47
5.18	Localization system computation times . . . . .	47
5.19	Paths from ground truth (green), localization system (blue) and odometry (red) . .	48
5.20	Localization system translation error (left) and its statistical distributions (right) .	48
5.21	Localization system translation corrections (left) and its statistical distributions (right) . . . . .	48
5.22	Localization system translation error (left) and corrections (right) components . . .	49
5.23	Localization system rotation error (left) and its statistical distributions (right) . .	49
5.24	Localization system rotation corrections (left) and its statistical distributions (right) .	49
5.25	Odometry translation error (left) and its statistical distributions (right) . . . . .	49
5.26	Odometry rotation error (left) and its statistical distributions (right) . . . . .	50
5.27	Localization system inliers RMSE (left) and its statistical distributions (right) . .	50
5.28	Cloud registration outlier percentage (left) and inliers angular distribution (right) .	50
5.29	Localization system computation times . . . . .	50
5.30	Paths from ground truth (green), localization system (blue) and odometry (red) . .	51
5.31	Localization system translation error (left) and its statistical distributions (right) .	51
5.32	Localization system rotation error (left) and its statistical distributions (right) . .	51
5.33	Localization system translation (left) and rotation (right) corrections . . . . .	52
5.34	Odometry translation (left) and rotation (right) error . . . . .	52
5.35	Localization system inliers root mean square error (left) and outlier percentage (right) . . . . .	52
5.36	Cloud registration outlier percentage (left) and inliers angular distribution (right) .	52
5.37	Paths from ground truth (green), localization system (blue) and odometry (red) . .	53
5.38	Localization system translation error (left) and its statistical distributions (right) .	53

## LIST OF FIGURES

5.39 Localization system rotation error (left) and its statistical distributions (right) . . . . .	53
5.40 Localization system translation (left) and rotation (right) corrections . . . . .	54
5.41 Odometry translation (left) and rotation (right) error . . . . .	54
5.42 Localization system inliers root mean square error (left) and outlier percentage (right) . . . . .	54
5.43 Cloud registration outlier percentage (left) and inliers angular distribution (right)	54
5.44 Paths from ground truth (green), localization system (blue) and odometry (red) .	55
5.45 Localization system translation error (left) and its statistical distributions (right) .	55
5.46 Localization system rotation error (left) and its statistical distributions (right) . .	55
5.47 Localization system translation (left) and rotation (right) corrections . . . . .	56
5.48 Odometry translation (left) and rotation (right) error . . . . .	56
5.49 Localization system inliers root mean square error (left) and outlier percentage (right) . . . . .	56
5.50 Cloud registration outlier percentage (left) and inliers angular distribution (right)	56
5.51 Paths from ground truth (green), localization system (blue) and odometry (red) .	57
5.52 Localization system translation error (left) and its statistical distributions (right) .	57
5.53 Localization system rotation error (left) and its statistical distributions (right) . .	57
5.54 Localization system translation (left) and rotation (right) corrections . . . . .	58
5.55 Odometry translation (left) and rotation (right) error . . . . .	58
5.56 Localization system inliers root mean square error (left) and outlier percentage (right) . . . . .	58
5.57 Cloud registration outlier percentage (left) and inliers angular distribution (right)	58
5.58 Paths from ground truth (green), localization system (blue) and odometry (red) .	59
5.59 Localization system translation error (left) and its statistical distributions (right) .	59
5.60 Localization system rotation error (left) and its statistical distributions (right) . .	59
5.61 Localization system translation (left) and rotation (right) corrections . . . . .	60
5.62 Odometry translation (left) and rotation (right) error . . . . .	60
5.63 Localization system inliers root mean square error (left) and outlier percentage (right) . . . . .	60
5.64 Cloud registration outlier percentage (left) and inliers angular distribution (right)	60
5.65 Paths from ground truth (green), localization system (blue) and odometry (red) .	61
5.66 Localization system translation error (left) and its statistical distributions (right) .	61
5.67 Localization system rotation error (left) and its statistical distributions (right) . .	61
5.68 Localization system translation (left) and rotation (right) corrections . . . . .	62
5.69 Odometry translation (left) and rotation (right) error . . . . .	62
5.70 Localization system inliers root mean square error (left) and outlier percentage (right) . . . . .	62
5.71 Cloud registration outlier percentage (left) and inliers angular distribution (right)	62
5.72 Paths from ground truth (green), localization system (blue) and odometry (red) .	63
5.73 Localization system translation error (left) and its statistical distributions (right) .	63
5.74 Localization system rotation error (left) and its statistical distributions (right) . .	63
5.75 Localization system translation (left) and rotation (right) corrections . . . . .	64
5.76 Odometry translation (left) and rotation (right) error . . . . .	64
5.77 Localization system inliers root mean square error (left) and outlier percentage (right) . . . . .	64
5.78 Cloud registration outlier percentage (left) and inliers angular distribution (right)	64
5.79 Paths from ground truth (green), localization system (blue) and odometry (red) .	65
5.80 Localization system translation error (left) and its statistical distributions (right) .	65

## LIST OF FIGURES

5.81 Localization system rotation error (left) and its statistical distributions (right) . . . . .	<b>65</b>
5.82 Localization system translation (left) and rotation (right) corrections . . . . .	<b>66</b>
5.83 Odometry translation (left) and rotation (right) error . . . . .	<b>66</b>
5.84 Localization system inliers root mean square error (left) and outlier percentage (right) . . . . .	<b>66</b>
5.85 Cloud registration outlier percentage (left) and inliers angular distribution (right) . . . . .	<b>66</b>
5.86 Paths from ground truth (green), localization system (blue) and odometry (red) . . . . .	<b>67</b>
5.87 Localization system translation error (left) and its statistical distributions (right) . . . . .	<b>67</b>
5.88 Localization system rotation error (left) and its statistical distributions (right) . . . . .	<b>67</b>
5.89 Localization system translation (left) and rotation (right) corrections . . . . .	<b>68</b>
5.90 Odometry translation (left) and rotation (right) error . . . . .	<b>68</b>
5.91 Localization system inliers root mean square error (left) and outlier percentage (right) . . . . .	<b>68</b>
5.92 Cloud registration outlier percentage (left) and inliers angular distribution (right) . . . . .	<b>68</b>
5.93 Paths from ground truth (green), localization system (blue) and odometry (red) . . . . .	<b>69</b>
5.94 Localization system translation error (left) and its statistical distributions (right) . . . . .	<b>69</b>
5.95 Localization system rotation error (left) and its statistical distributions (right) . . . . .	<b>69</b>
5.96 Localization system translation (left) and rotation (right) corrections . . . . .	<b>70</b>
5.97 Odometry translation (left) and rotation (right) error . . . . .	<b>70</b>
5.98 Localization system inliers root mean square error (left) and outlier percentage (right) . . . . .	<b>70</b>
5.99 Cloud registration outlier percentage (left) and inliers angular distribution (right) . . . . .	<b>70</b>
5.100 Paths from ground truth (green), localization system (blue) and odometry (red) . . . . .	<b>71</b>
5.101 Localization system translation error (left) and its statistical distributions (right) . . . . .	<b>71</b>
5.102 Localization system rotation error (left) and its statistical distributions (right) . . . . .	<b>71</b>
5.103 Localization system translation (left) and rotation (right) corrections . . . . .	<b>72</b>
5.104 Odometry translation (left) and rotation (right) error . . . . .	<b>72</b>
5.105 Localization system inliers root mean square error (left) and outlier percentage (right) . . . . .	<b>72</b>
5.106 Cloud registration outlier percentage (left) and inliers angular distribution (right) . . . . .	<b>72</b>
5.107 Paths from ground truth (green), localization system (blue) and odometry (red) . . . . .	<b>73</b>
5.108 Localization system translation error (left) and its statistical distributions (right) . . . . .	<b>73</b>
5.109 Localization system rotation error (left) and its statistical distributions (right) . . . . .	<b>73</b>
5.110 Localization system translation (left) and rotation (right) corrections . . . . .	<b>74</b>
5.111 Odometry translation (left) and rotation (right) error . . . . .	<b>74</b>
5.112 Localization system inliers root mean square error (left) and outlier percentage (right) . . . . .	<b>74</b>
5.113 Cloud registration outlier percentage (left) and inliers angular distribution (right) . . . . .	<b>74</b>
5.114 Initial pose estimation using feature matching in Guardian static environment . . . . .	<b>75</b>
5.115 Initial pose estimation using feature matching in Jarvis environment . . . . .	<b>75</b>
5.116 Initial pose estimation distribution in Jarvis environment . . . . .	<b>75</b>

# List of Tables

2.1	Overview of self-localization approaches . . . . .	12
5.1	LIDARs hardware specifications . . . . .	41
5.2	3 DoF localization system results . . . . .	44

## LIST OF TABLES

# Abbreviations

**AGPS** Assisted Global Positioning System.

**API** Application Programming Interface.

**CAD** Computer Aided Design.

**CARLoS** Cooperative Autonomous Robot for Large Open Spaces.

**DoF** Degrees of Freedom.

**EKF** Extended Kalman Filter.

**ESF** Ensemble of Shape Functions.

**FPFH** Fast Point Feature Histogram.

**GLONASS** GLObalnaya NAVigatsionnaya Sputnikovaya Sistema.

**GNSS** Global Navigation Satellite System.

**GPS** Global Positioning System.

**GPU** Graphics Processing Unit.

**ICP** Iterative Closest Point.

**IP** Internet Protocol.

**ISS3D** 3D Intrinsic Shape Signatures.

**LIDAR** LIght Detection And Ranging.

**MCL** Monte Carlo Localization.

**NDT** Normal Distributions Transform.

**PCA** Principal Component Analysis.

**PCL** Point Cloud Library.

**PFH** Point Feature Histogram.

**RADAR** RAdio Detection And Ranging.

**RANSAC** Random Sample Consensus.

**ROS** Robot Operating System.

**SAC-IA** Sample Consensus Initial Alignment.

**SC3D** Shape Context 3D.

**SHOT** Signature of Histograms of Orientations.

**SIFT** Scale Invariant Feature Transform.

**SLAM** Simultaneous Localization And Mapping.

**SONAR** SOund Navigation And Ranging.

**TCP** Transmission Control Protocol.

**ToA** Time of Arrival.

**ToF** Time of Flight.

**TTFF** Time To First Fix.

**UDP** User Datagram Protocol.

**UKF** Unscented Kalman Filter.

**USC** Unique Shape Context.

**XML** Extensible Markup Language.

**XML-RPC** Extensible Markup Language Remote Procedure Call.

# Chapter 1

## <sup>2</sup> Introduction

- <sup>4</sup> This chapter provides an overview about the motivations and objectives of this dissertation along with its practical applications.

### <sup>6</sup> 1.1 Context

Humanity has sought a reliable method of navigation ever since it started to explore the world. It <sup>8</sup> began with simple landmark reference points for local travels, then perfected celestial navigation for global journeys, and when it finally conquered space, it deployed a global system for high <sup>10</sup> accuracy localization. Autonomous robots face the same problem, because in order to be able to navigate with precision, they first need to know their location.

<sup>12</sup> Over the years, several localization methods have been proposed and refined, according to the navigation environment and the accuracy requirements. Some are meant for high precision local <sup>14</sup> navigation, while others provide an approximate global position.

A robot capable of operating safely and accurately in a dynamic environment can have in-<sup>16</sup> numerous applications, ranging from simple delivery tasks to advanced assembly. Besides im-<sup>18</sup> proving productivity by performing repetitive tasks with precision and speed, robots can also act as coworkers, helping humans perform their jobs more efficiently and thus, reducing the overall production costs.

### <sup>20</sup> 1.2 Project

Cooperative Autonomous Robot for Large Open Spaces (CARLoS)<sup>1</sup> is a European research project <sup>22</sup> that aims to develop an autonomous robot capable of performing repetitive tasks alongside human co-workers in dynamic environments. The robot will operate in shipyards and is intended to per-<sup>24</sup> form fit-out operations, such as stud welding and projection mapping of Computer Aided Design

---

<sup>1</sup><http://carlosproject.eu/>

## Introduction

([CAD](#)) drawings. Stud welding is a repetitive task that provides structural support for other components, such as heat insulation layers or electrical systems. Projection mapping of [CAD](#) drawings or other important information will help human co-workers assemble components faster, because it will mark the exact position in which they must be installed.

2  
4

### 1.3 Motivation and objectives

With the increase of competitiveness in the current globalized trading markets, companies are trying to reduce production costs and improve the productivity of their assets. Robots can help achieve these goals by performing the simple and repetitive jobs while giving humans more free time to perform the complex and creative tasks.

6  
8

Mobile platforms equipped with robotic arms provide a flexible way to automate a wide range of tasks that must be performed over large areas. However, before performing the intended operations they first need to know where they are and how they can reach the desired location. Moreover, given their limited computational resources and energy storages, they require efficient, reliable and accurate control systems capable to operate in real time.

10  
12  
14

### 1.4 Contributions

This dissertation introduces an efficient, modular and extensible 3/6 [DoF](#) localization system for mobile robot platforms capable of operating accurately and reliably in dynamic environments. It is a multi-level registration pipeline that uses geometric features to estimate the initial position of a robot platform and point cloud registration algorithms to track its pose. The tracking subsystem can have two different configurations. One tuned for maximum efficiency used for the normal operation of the mobile platform and another for unlikely situations that may require more robust registration algorithms / configurations. It also supports incremental map update and can adjust its operation rate based on the estimated robot velocity. For critical operations, it provides a detailed analysis of the tracking quality and when initial pose estimation is required it gives the distribution of the acceptable poses, which can be very valuable information if there are several areas in the known map with very similar geometry.

16  
18  
20  
22  
24  
26

### 1.5 Dissertation outline

The remaining of this dissertation is split over 5 chapters. [Chapter 2](#) provides an overview of the main localization methods available for mobile robot platforms. [Chapter 3](#) introduces the main frameworks used to implement the self-localization system. [Chapter 4](#) details the architecture and [ROS](#) implementation of the proposed 3/6 [DoF](#) self-localization system. [Chapter 5](#) evaluates the results achieved with the localization system in several testing environments. Finally, [chapter 6](#) presents the conclusions of this dissertation and suggestions for future work.

28  
30  
32

# Chapter 2

## <sup>2</sup> Localization methods

- <sup>4</sup> Self-localization is critical to any autonomous robot that must navigate the environment and requires the calculation of a 3/6 DoF pose in a given world coordinate system.
  - <sup>6</sup> Over the years, several approaches were developed according to the precision requirements and the environment in which the robot is designed to operate. Some require support systems
  - <sup>8</sup> to calculate the position, while others are completely autonomous, allowing the robot to localize itself without any outside dependencies. Also, some systems have limited range while others can
  - <sup>10</sup> only be effective in open spaces. Moreover, several of these methods were designed to cope with errors in the localization sensors and tolerate temporary malfunctions.
- <sup>12</sup> The following sections will introduce some of the most used self-localization systems that can be employed in the estimation of a robot's pose.

### <sup>14</sup> 2.1 Proprioceptive methods

<sup>16</sup> Proprioceptive methods rely on internal information that the robot possesses about its own systems operation and movement in order to update the current pose estimation. As a result, they allow the robot to operate without an external support system.

<sup>18</sup> Since these methods don't correct their estimations based on environment observations, they are bound to have significant cumulative errors. As such, in order to maintain an accurate estimation of a robot's pose, they are usually combined with exteroceptive systems.

#### 2.1.1 Odometry

<sup>22</sup> Odometry estimates the current pose by integrating the velocity of the robot over time. This velocity is usually calculated by measuring the number of rotations of the wheels (using optical encoders like the ones shown in [figure 2.1](#)). This method can provide a viable approximated location, as can be seen in [[RKZ13](#)].

## Localization methods

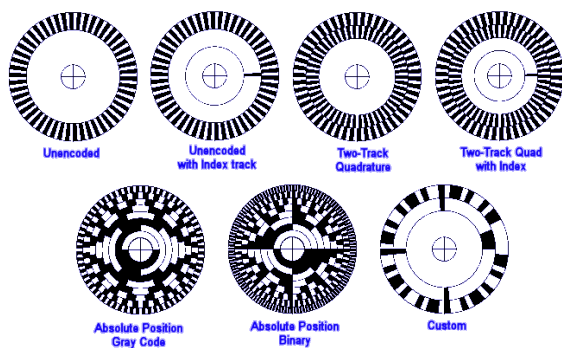


Figure 2.1: Different types of optical encoders used to measure distances<sup>1</sup>

### 2.1.2 Dead reckoning

Dead reckoning is an extension of the odometry method, in which the acceleration and angular velocity are used to improve the localization estimations. 2

Other sensors, such as accelerometers and gyroscopes, can also be used to improve the position estimation [Ibr10] and provide the robot orientation. 4

## 2.2 Exteroceptive methods

Exteroceptive methods use a range of sensors to analyze the environment and retrieve the necessary information to perform localization. 6 8

### 2.2.1 Trilateration methods

Trilateration is a geometric technique that can be employed in the calculation of absolute or relative positions using distances from known points. 10

For 3D localization, it usually involves the intersection of 4 or more spheres, in which their radius is the distance to known positions. 12

#### 2.2.1.1 Global Navigation Satellite System (GNSS)

Global Navigation Satellite System (GNSS) such as the Global Positioning System (GPS) or GLObalnaya NAvigatsionnaya Sputnikovaya Sistema (GLONASS), allow 3D positioning in the planet Earth using a trilateration method [DKU<sup>+07</sup>]. 14 16

In these systems, a constellation of satellites broadcasts a radio signal with information about its position along with the time of the message dispatch. Using this data and knowing the speed of the radio waves, the distances to the satellites can be computed. 18 20

With at least 3 satellites distances, the 3D position can be calculated, since the Earth can be used as the 4<sup>th</sup> sphere (figure 2.2 shows a visual representation of the trilateration technique used in a global localization system). 22

<sup>1</sup><http://www.mindspring.com/~tom2000/Delphi/Codewheel.html>

Given that the correct measurement of the distances to the satellites relies in the accurate

- 2 computation of the elapsed time between the message dispatch and its reception, it is critical that both the satellites and the receiver have synchronized clocks. This is achieved by using high
- 4 precision atomic clocks in the satellites and a clock reset technique in the receiver. This reset method relies on the fact that 3 satellite distances will only have a valid location if the clock of the
- 6 receiver is synchronized. With this knowledge, the receiver can compute the necessary corrections to reset its internal clock to match the satellites time.

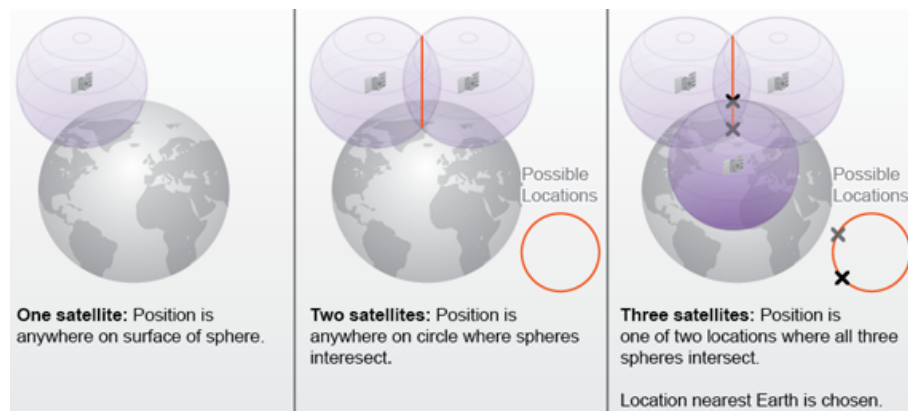


Figure 2.2: Trilateration technique in a global localization system<sup>2</sup>

### 8 2.2.1.2 Differential Global Positioning System (DGPS)

The accuracy of the **GPS** position can be increased with the help of local broadcast stations. These  
10 stations are fixed and provide information about the corrections that can be made to the satellite signals in order to improve the localization precision.

12 These corrections are useful to mitigate some of the ambient interference that the satellite signals face. These interferences can range from simple signal reflection in the environment landscape to the more complex interactions with the atmosphere, which can change the speed and path of the radio signals.

16 The computation of the corrections [KKOO07] is based on the fact that these stations are fixed, and as such, they can compare the location given by the satellite signals with their known location.  
18 With this position differential, the appropriate corrections can be calculated and broadcasted to the **GPS** receivers.

### 20 2.2.1.3 Assisted Global Positioning System (AGPS)

Assisted Global Positioning System (AGPS) systems are a common method used to speed up the  
22 Time To First Fix (TTFF) of a **GPS** receiver. They usually rely on the cellphone network to provide location estimation and signal corrections [R.48]. This information can greatly reduce the **TTFF**  
24 when there are few satellites visible or their signal is very weak and only temporary available.

<sup>2</sup><https://www.e-education.psu.edu/geog160/node/1923>

### 2.2.1.4 Signal strength geolocation methods

Signal strength geolocation [CK02], also known as fingerprinting localization [BOG<sup>+</sup>10], is an approximate method that can be used to calculate relative positions. 2

It relies on the analysis of the signal attenuation from a given access point (like a Wi-Fi router or cellphone tower), to estimate distances. With enough access points (usually 4), an approximate position can be computed. 4  
6

This type of distance estimation can be useful for indoor navigation, but requires a propagation model of the signal and the environment. If these models aren't accurate, then the localization precision of these methods will be very low. 8

Although this method is less accurate than the more recent global localization systems (such as **GPS**), it can be used without human made infrastructures, and as such, is a viable solution in case of temporary disruption of the **GPS** signal. 10  
12

## 2.2.2 Celestial navigation

Celestial navigation [YXL11] relies on the observation of stars, planets or other reference objects, to calculate the latitude and longitude. 14

The calculation of the position on the surface of the Earth using celestial navigation is similar to trilateration, but in this case, angles are used instead of distances. These angles (delta), are measured between the Earth horizon and the center of the celestial object. 16  
18

Having the delta, and knowing the relative position of the Earth to the reference object, along with the Greenwich hour time, it is possible to calculate a circle of position (as shown in [figure 2.3](#)). 20

Having at least 3 circles of position, the latitude and longitude can be computed.

Although this method is less accurate than the more recent global localization systems (such as **GPS**), it can be used without human made infrastructures, and as such, is a viable solution in case of temporary disruption of the **GPS** signal. 22  
24

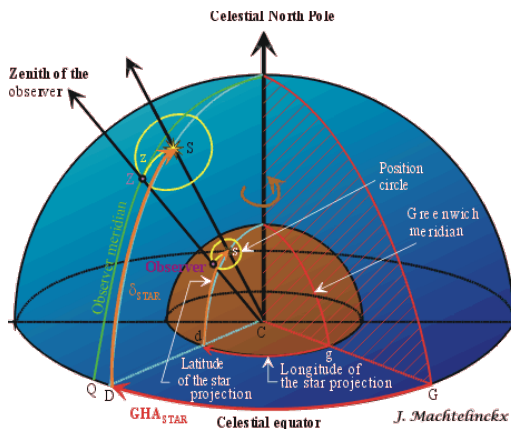


Figure 2.3: Circle of position in celestial navigation<sup>3</sup>

<sup>3</sup><http://onboardintelligence.com/CelestialNav/Celnav2.aspx>

### 2.2.3 Landmark methods

- 2 Landmark methods [LKP06] can be used to perform relative localization, and are very useful to reduce the required information for navigation.
- 4 In these methods a database of markers / environment geometry is stored along with its location, and when the robot recognizes one of these markers, it corrects its proprioceptive methods
- 6 measures.
- 8 It is a simplification of the method that will be presented in the next section, and it is useful for environments that have unique geometry in key positions of the navigation map.

### 2.2.4 Point cloud methods

- 10 Point cloud localization methods can be used to perform relative localization by finding the best point cloud match between the environment and the known map (figure 2.4 shows its application to small objects).
- 12 These methods require a 2D or 3D representation of the environment and tend to be used in conjunction with proprioceptive methods (to have an estimation of movement), and
- 14 also with probabilistic methods (when the point cloud acquisition location is not known).

One of the most used algorithms for 3D point cloud matching is the **Iterative Closest Point (ICP)** [BM92, Jez08, Zha94, BTP13, CSSK02, DZA<sup>+</sup>13, ZL11]. It is an iterative algorithm that finds the translation and rotation transformation that minimizes the distances of the corresponding points on both clouds. It finishes when the matching error is below a given threshold or when the maximum allowed iterations is reached.

20 There are several variants that optimize different parts of the algorithm [RL01].

The main steps for each iteration of the **ICP** algorithm are presented below.

- 22 1. Selection of points in one or both point clouds (source and reference clouds)
- 24 2. Matching / pairing source points to reference points
- 26 3. Weighting the corresponding pairs
- 4. Rejecting low quality matches (outliers)
- 5. Assigning an error metric based on the point pairs
  - (a) Usually mean square error based on points distance

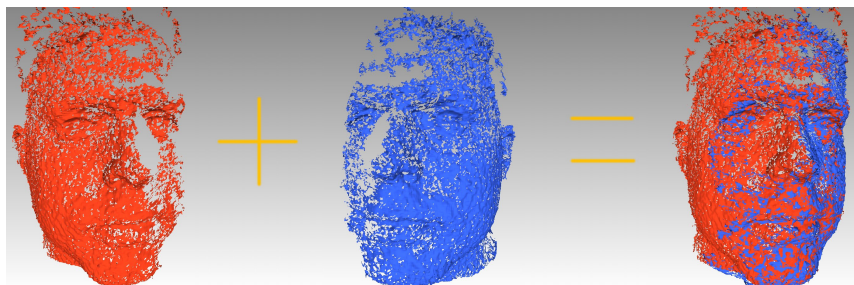


Figure 2.4: ICP point cloud matching<sup>4</sup>

---

<sup>4</sup><http://dynface4d.isr.uc.pt/database.php>

## 2.2.5 Probabilistic methods

Probabilistic methods aim to reduce the impact of sensor accumulated errors or even temporary malfunctions by using Bayesian estimations and Markov processes.

### 2.2.5.1 Monte Carlo Localization (MCL)

**Monte Carlo Localization (MCL)** (also known as particle filter), is a global localization algorithm that estimates the position and orientation of a robot by analyzing and adjusting the distribution and weights of state particles on a given environment [BOG<sup>+</sup>10, AMGC02, BGFM10, Che03, FBDT99, SS09].

It starts by randomly distributing the state particles on the map, and over time it changes their position and weight according to new sensor readings. The probable location of the robot will be in the area of the map that has the largest cluster of state particles. The figures below show the evolution of the state particles distribution during the robot movement in the environment, and illustrates how the new sensor readings changed the particles clusters<sup>5</sup>.

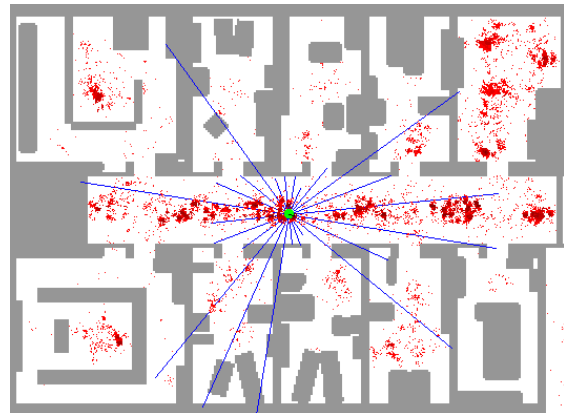


Figure 2.5: MCL particle distribution animation

Figure 2.6: MCL redistribution of particles

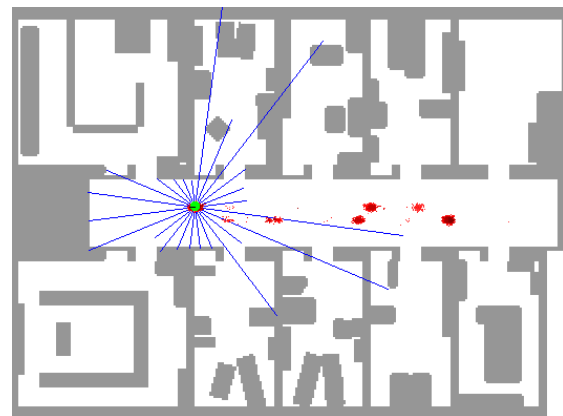


Figure 2.7: MCL position refinement

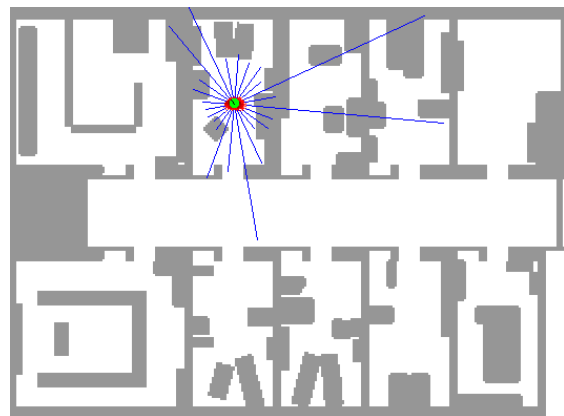


Figure 2.8: MCL position estimation

<sup>5</sup><http://www.cs.washington.edu/robotics/mcl/>

### 2.2.5.2 Kalman filters

- 2 Kalman filters [Kal60] are probabilistic algorithms that estimate a given system state even when it is affected by noise or other errors. They perform linear quadratic estimations to achieve optimal  
 4 results and can be efficiently implemented to be used in real time systems. They are recursive  
 6 algorithms based on Marcov processes, and as a result, they only need to know the current system  
 8 state in order to perform measurement corrections.

The Extended Kalman Filter (EKF) [EW99, Rib04, IKP10, LYL11] is a variant of the Kalman  
 8 filter, designed to handle non-linear systems by performing linear approximations to the state  
 10 variables. These approximations may lead to divergence in the estimations, and as such, the EKF  
 12 can't guarantee optimal results.

The Unscented Kalman Filter (UKF) [JU97, WM00] is another variant of the Kalman filter  
 12 that was designed for highly non-linear systems. It usually achieves better results than EKF due  
 14 to its unscented transform.

16 For the particular case of localization, these algorithms start with an initial estimation of the  
 18 system state, and for each new position (computed from the sensors data), they predict the esti-  
 mated robot location (according to the Bayes estimation model and the Gaussian distribution of  
 errors), and then update their internal model of the system (mean and covariance) to incorporate  
 the system evolution.

In figure 2.9 can be seen that the UKF estimated position (red) is closer to the real position  
 20 (blue) than the raw sensor measurements (green).

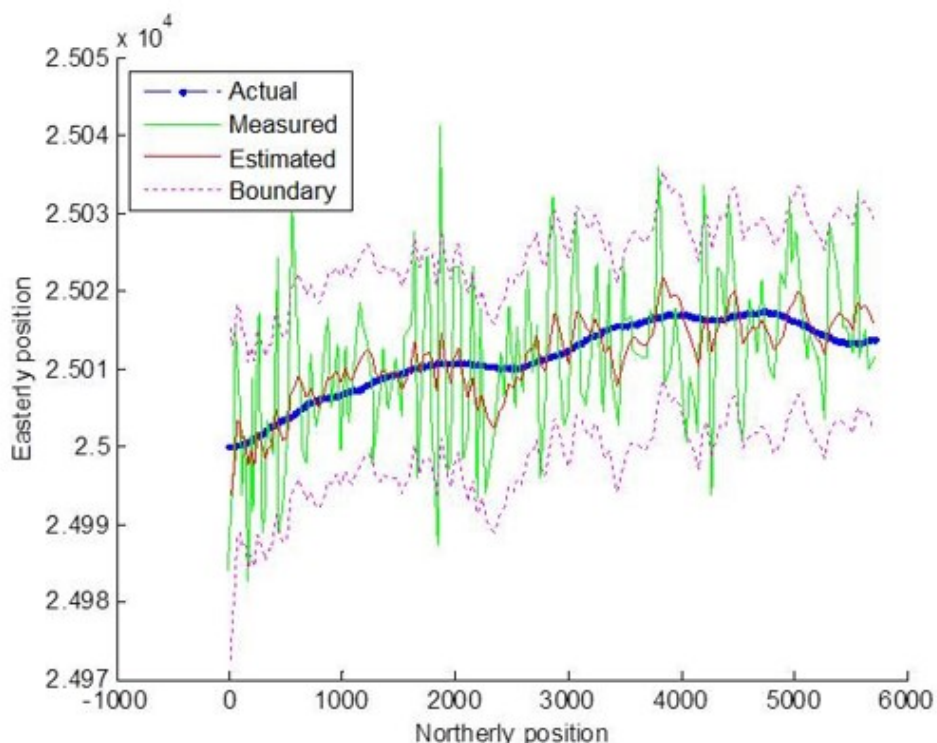


Figure 2.9: Unscented Kalman Filter<sup>6</sup>

### 2.2.5.3 Perfect Match

The Perfect Match [LLRM06, PM63] is an efficient self-localization algorithm that is largely used in the Robocup Robotic Soccer Mid Size League. Its main goal is to minimize the localization error by carefully analyzing the known map and selecting the most probable current position using a gradient descent approach. To improve tracking accuracy, the algorithm also uses a stochastic weighted approach.

With the proper configuration, it can achieve a localization accuracy similar to the particle filter, while using about ten times less computations.

An example of the position estimation can be seen in the figures below. Figure 2.10 shows the probable locations when the robot detects a line on the floor, and figure 2.11 illustrates their associated errors (brighter areas indicate smaller error). By using a gradient descent, the most probable location was selected (black circle).

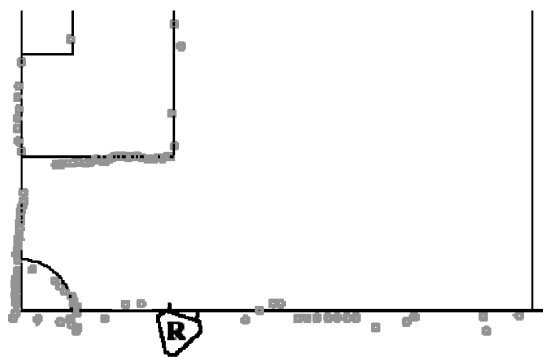


Figure 2.10: Position estimates

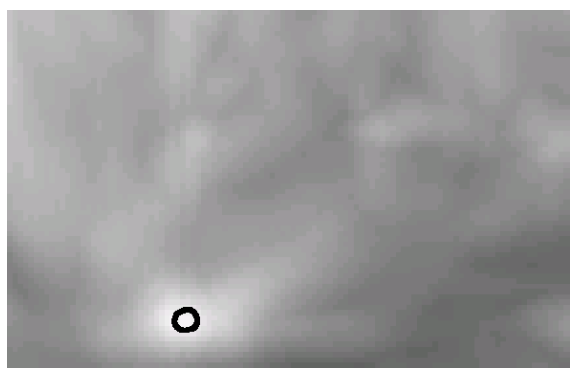


Figure 2.11: Positions associated error

### 2.2.6 Simultaneous Localization And Mapping (SLAM)

**Simultaneous Localization And Mapping (SLAM)** [Thr02] is a very effective approach to either explore unknown environments or update a known map. It relies on both proprioceptive and exteroceptive methods to perform localization and mapping. It is also very useful to make the robot navigation more robust in dynamic environments, in which the topology of the world may change considerably over time.

There are numerous approaches to perform **SLAM** [TGCV12]. Some optimized for exploration and others for map improvement. For the exploration tasks, proprioceptive methods play a critical role, and are usually paired with probabilistic methods, such as Kalman filters, in order to reliably map the environment. For map correction and improvement, several probabilistic methods can be employed according to the precision required. For high accuracy 3D mapping, the **ICP** algorithm can be used to build accurate point clouds of the environment.

---

<sup>6</sup><http://www.lzcheng.com/courseworks/kalmanfilter>

## 2.3 Summary

- 2 This chapter introduced several localization systems that can be used in different types of environments and with different degrees of accuracy. It started with the simple proprioceptive methods
- 4 and then moved on to the more robust exteroceptive approaches.

Some techniques can be combined to improve the pose estimate or to make the localization  
6 more efficient to a particular type of environment.

For outside tasks, a **GNSS** approach can give accurate localization estimations with very little  
8 computation cost. On the other hand, indoor localization requires more advanced techniques in  
order to infer the current position based on the analysis of the robot surroundings. These tech-  
10 niques usually start with an estimation of the robot movement and then refine it with probabilistic  
or geometric methods.

12 [Table 2.1](#) presents an overview of the mentioned localization techniques.

## Localization methods

Table 2.1: Overview of self-localization approaches

<i>Method</i>	<i>Ideal environment</i>	<i>Accuracy</i>	<i>Operational cost</i>	<i>Computational cost</i>	<i>Notes</i>
Odometry	Any	Low	Low	Low	Position estimation is affected by cumulative errors
	Any	Low	Low	Low	Pose estimation is affected by cumulative errors
	Outside	Medium	Low	Low	Requires a clear line of sight to at least 3 satellites
<b>GNSS</b>	Any	Low	Low	Low	Requires an accurate model for the signal attenuation
Signal strength	Any	Low	Low	Low	Requires an accurate model for the signal attenuation
Celestial	Outside	Low	Low	Low	Requires a clear view of the celestial objects and a nautical almanac
Landmark	Any	Medium	Low	Medium	Requires a database of landmarks
<b>ICP</b>	Indoors	High	Medium	High	Requires a detailed 3D representation of the environment
<b>MCL</b>	Indoors	Medium	Medium	Medium	Inefficient for large areas
Kalman filters	Any	Medium	Low	Low	Useful to improve estimations of other methods
Perfect Match	Any	Medium	Low	Low	Not ideal for large or dynamic environments
<b>SLAM</b>	Indoors	Medium	Medium	High	Adapts well to dynamic environments

# Chapter 3

## 2 Relevant software / hardware technologies

4

Robot self-localization in complex environments is a multidisciplinary problem that requires advanced computer software systems. In order to speed up the implementation and deployment of the localization system, several frameworks and libraries were used. Among the most important were ROS for the system architecture, Point Cloud Library (PCL) for the point cloud processing and Gazebo for simulation and testing.

### 10 3.1 ROS

ROS<sup>1</sup> [QCG<sup>+</sup>09] is a software framework designed to ease the development of robot systems. It provides seamless integration between hardware drivers and software modules, allowing a fast transition between simulation and deployment.

It's an open source project that offers a distributed computing framework with several core libraries and development tools that aims to speedup software prototyping, testing and deployment.

#### 18 3.1.1 Architecture

The ROS architecture was designed from the beginning to be a distributed peer-to-peer software framework that could be deployed in several operating systems and implemented in a range of different programming languages. However, given that most of the ROS community prefers open source software, the Ubuntu<sup>2</sup>] operating system is the main developing and testing environment, and as such, the recommended choice for ROS developers. Moreover, considering that robotics



Figure 3.1: ROS logo

---

<sup>1</sup><http://www.ros.org/>

<sup>2</sup><http://www.ubuntu.com/>

research requires software with both performance and maintainability at its core, the C++<sup>3</sup> programming language is used in most of the available packages, along with Python<sup>4</sup> and Java<sup>5</sup>. 2

Being a distributed computing framework, ROS relies in network connections and exchange of messages to perform the intended tasks. As such, its architecture was developed to follow a publish / subscribe pattern (ROS topics<sup>6</sup>) and request and reply communication paradigm (ROS services<sup>7</sup> and actions<sup>8</sup>). This allows ROS nodes<sup>9</sup> (operating system processes) to be deployed in different computing platforms with ease and simplifies testing and exchange of software modules. 4  
6

The next sections provide a more detailed description of the main ROS architecture concepts. 8

### 3.1.1.1 Nodes

ROS nodes are operating system processes that are part of the peer-to-peer communication graph. They are the fundamental building blocks of any ROS system and can be spread among several computing platforms. 10  
12

In order to manage the communications between nodes, the ROS framework provides a master node (roscore<sup>10</sup>) that uses Extensible Markup Language Remote Procedure Call (XML-RPC) to maintain a communication graph of the system. This allows nodes to be started without knowing the location (Internet Protocol (IP) address and port) of the other nodes in the network and greatly simplifies their integration and exchange. Also, by using ROS launch files<sup>11</sup> (Extensible Markup Language (XML) configuration files), the specification of a system communication data flow and configuration can be easily altered. 14  
16  
18

Besides handling communications, the master node also manages system configurations through the parameter server. This allows nodes to share and change the system configuration at runtime. However, given that the parameter server is usually queried only when a node starts up, the dynamic reconfigure<sup>12</sup> Application Programming Interface (API) can be used instead, if it is necessary to change the configuration of a node when it is already running. This is achieved by providing a callback that is asynchronously called when a configuration change is requested. 20  
22  
24

The flexibility provided by ROS in both module integration and exchange can greatly speedup testing and deployment and the possibility of changing the configuration of the system at runtime and restart software modules individually (nodes) is very useful when implementing system supervisors and recovery behaviors. 26  
28

---

<sup>3</sup><http://www.cplusplus.com/>

<sup>4</sup><https://www.python.org/>

<sup>5</sup><https://www.java.com>

<sup>6</sup><http://wiki.ros.org/Topics>

<sup>7</sup><http://wiki.ros.org/Services>

<sup>8</sup><http://wiki.ros.org/actionlib>

<sup>9</sup><http://wiki.ros.org/Nodes>

<sup>10</sup><http://wiki.ros.org/roscore>

<sup>11</sup><http://wiki.ros.org/roslaunch>

<sup>12</sup>[http://wiki.ros.org/dynamic\\_reconfigure](http://wiki.ros.org/dynamic_reconfigure)

### 3.1.1.2 Nodelets

- 2 A nodelet<sup>13</sup> is a special kind of node that aims to reduce the overhead of message exchange. This overhead can be significant when messages are very large, such as point clouds or video.
- 4 To mitigate this problem, the nodelets exchange pointers to shared memory regions, instead of sending the entire messages between nodes.
- 6 To achieve this overhead reduction, some architecture changes are required. The most important being the use of threads instead of processes, and the creation of a superclass that all nodelets
- 8 must inherit. This leads to the creation of plugin libraries for each nodelet instead of an executable for each node.
- 10 Another important change is the introduction of nodelet managers to allow loading and setup of nodelets in different threads inside the same process.
- 12 In terms of implementation, the transition from nodes to nodelets requires few code changes and can lead to a significant improvement of the overall system performance.

### 14 3.1.1.3 Topics

15 **ROS** topics are named communication buses that follow the publish / subscribe pattern. They  
 16 provide a simple method for exchanging messages between nodes and allow the decoupling of  
 18 information production and consumption. This is useful when there are multiple sources of the  
 20 same information or there are multiple consumers that are interested in processing the same data  
 for different purposes. Moreover, this communication architecture allows to log and replay the  
 exchanged messages, which can be helpful to test different algorithms with the same data.

22 Currently, topics can use either the **Transmission Control Protocol (TCP)** or **User Datagram  
 24 Protocol (UDP)** protocols to exchange messages. The **TCP** implementation is used by default  
 and creates a bidirectional channel between each producer and subscriber while guaranteeing the  
 delivery of all messages. The **UDP** implementation uses an unreliable and stateless transport  
 approach, in which a subscriber listens to a given broadcast address, and has no guarantee that  
 will receive all messages. As such, **TCP** should be used when all messages must be processed,  
 and **UDP** should be considered when the latency and the **TCP** overhead are important issues.

### 28 3.1.1.4 Services

30 **ROS** services are named communication buses that follow the request and reply paradigm, in  
 32 which a node asks for a given service and receives a response according to the data that was sent  
 in the request message and the state of the service node. They are useful to query other nodes state  
 or to request the execution of some behavior / action.

---

<sup>13</sup><http://wiki.ros.org/nodelet>

### 3.1.1.5 Actions

**ROS** actions are a special kind of service in which the progress of the request can be queried.  
They are very useful when the request might take a long time, and gives the caller the necessary  
information to supervise the execution of the request and if necessary, terminate its execution.

2

4

### 3.1.2 Build system

The latest **ROS** build system is named catkin<sup>14</sup>, and is the successor of the original rosbuild<sup>15</sup>  
system. It combines CMake<sup>16</sup> macros and Python scripts to allow building multiple dependent  
projects at the same time. It is a cross-platform build system, organized in packages and meta-  
packages (group of packages). Each package is a software module that can produce libraries or  
binaries from source code.

6

8

10

Catkin was designed to deal with complex build configurations, which in the case of **ROS**  
packages involves a considerable amount of build dependencies for each project. As such, catkin  
provides a build system that can easily find, build and link both **ROS** and system dependencies.  
Moreover, it provides install targets to allow faster code releases and simplifies builds from source  
for the final users.

12

14

Other useful features of the catkin build system are the concepts of workspace and overlays.  
Catkin uses a workspace with out-of-source builds to keep the source code separate from the build  
files. This allows the code directory structure to be clean of compiler generated files that are  
platform dependent. Moreover, it simplifies the concurrent usage of packages (overlay), because  
catkin gives priority to workspace packages (in relation to system packages). This is particularly  
useful when it is necessary to modify and test some package that has been released and is installed  
in the system (without having to uninstall the stable release of that package).

16

18

20

22

Finally, catkin is a cross-platform build system that can be used to build other projects that use  
CMake and are not related to **ROS**.

24

### 3.1.3 Development tools

**ROS** provides several development tools that allow introspection and visualization of the system  
state. They are very useful for testing, debugging and profiling.

26

The next sections give an overview of the most important **ROS** tools that are currently available.

28

#### 3.1.3.1 Graphical User Interface tools

30

The **ROS** development tools that have graphical user interfaces are aggregated in the rqt framework<sup>17</sup>, and are loaded as plugins at runtime (some can be started as standalone applications).

32

<sup>14</sup><http://wiki.ros.org/catkin>

<sup>15</sup><http://wiki.ros.org/rosbuild>

<sup>16</sup><http://www.cmake.org/>

<sup>17</sup><http://wiki.ros.org/rqt>

Currently there are plugins to visualize sensor data (rviz<sup>18</sup>); introspect the contents of topics; log

- 2 and replay ROS messages (rosbag<sup>19</sup>); display node, package and coordinate systems graphs; list
- 4 and filter debug messages; change configuration of running nodes (dynamic reconfigure); monitor
- nodes memory and processor usage and much more.

### 3.1.3.2 Command line tools

- 6 The ROS command line tools<sup>20</sup> are split across several executables and can be used for advanced
- 8 introspection (rosnode, rostopic and rosservice), system configuration (rosparam), package build-
- ing and management (catkin, rosdep and rosinstall) and also to search ROS message types docu-
- mentation (rosmsg and rossrv).
- 10 Finally, it is available a diagnostics tool (roswtf), that can detect packages / dependencies
- issues and configuration problems.

## 12 3.2 PCL

The PCL<sup>21</sup> [RC11] is an open source project that provides algorithms  
14 for processing point clouds. These algorithms can be used to filter and  
register point clouds as well as perform object segmentation, recogni-  
16 tion and tracking.

Figure 3.3 gives an overview of the main modules currently avail-  
18 able in PCL.



Figure 3.2: PCL logo

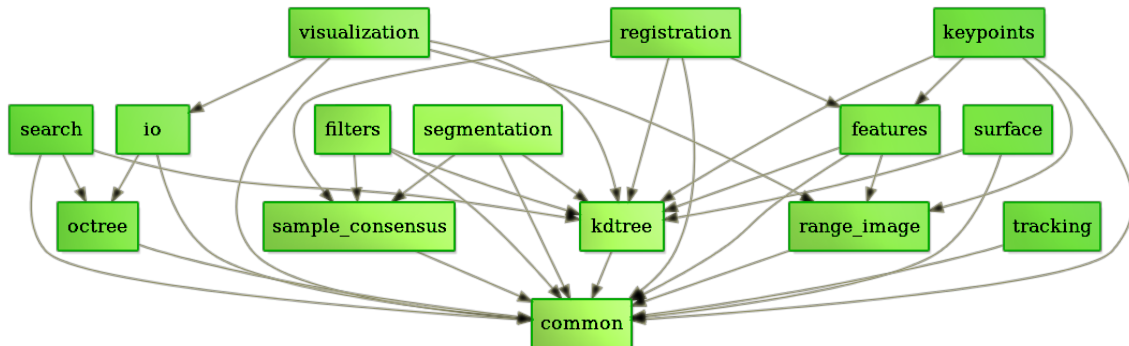


Figure 3.3: Point Cloud Library<sup>22</sup>

<sup>18</sup><http://wiki.ros.org/rviz>

<sup>19</sup><http://wiki.ros.org/rosbag>

<sup>20</sup><http://wiki.ros.org/ROS/CommandLineTools>

<sup>21</sup><http://pointclouds.org/>

<sup>22</sup><http://pointclouds.org/about/>

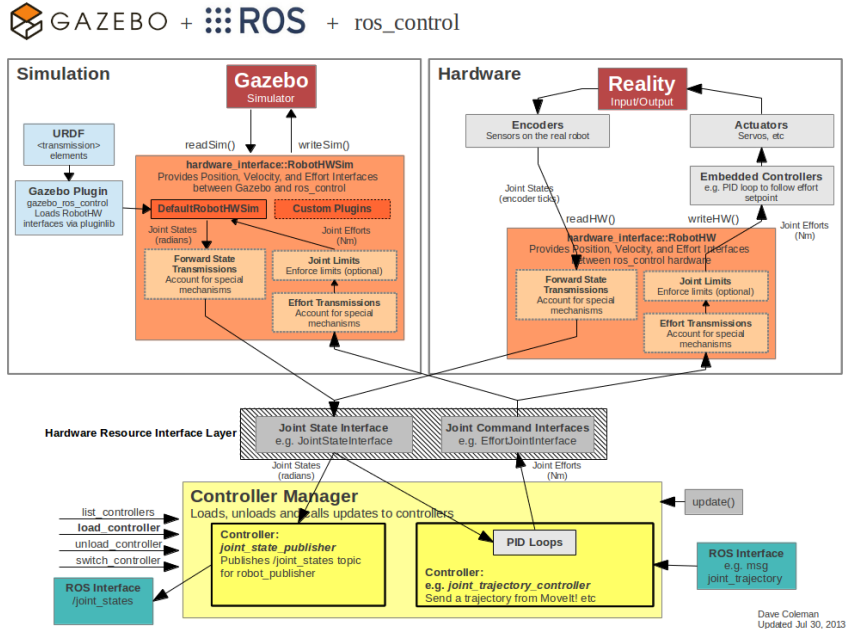
### 3.3 Gazebo

Gazebo<sup>23</sup> is a 3D multi-robot simulator capable of generating hardware sensor data for different kinds of robots while providing a realistic environment with physics simulation and 3D visualization. It is very useful to speedup testing of algorithms with different types of robots and environments.

Figure 3.5 shows how Gazebo can be used instead of a real robot, without requiring any implementation code modification (because it implements the same ROS interfaces that the hardware drivers use).



Figure 3.4: Gazebo logo


 Figure 3.5: Integration of ROS and Gazebo<sup>24</sup>

<sup>23</sup><http://gazebosim.org/>

<sup>24</sup>[http://gazebosim.org/tutorials?tut=ros\\_control](http://gazebosim.org/tutorials?tut=ros_control)

### 3.4 Point cloud acquisition

- 2 Point clouds can be retrieved with a wide range of sensors with varying levels of precision and assembly time [STD09]. The next sections provide a brief overview of the three main groups of methods capable of generating point clouds.

#### 3.4.1 Structured light methods

- 6 Structured light methods can retrieve 3D geometry from images by projecting a known pattern into the environment and analyzing its deformation (example in Figure 3.6). They can achieve
- 8 sample rates of 30 Hz, and besides 3D geometry they can also retrieve color information.

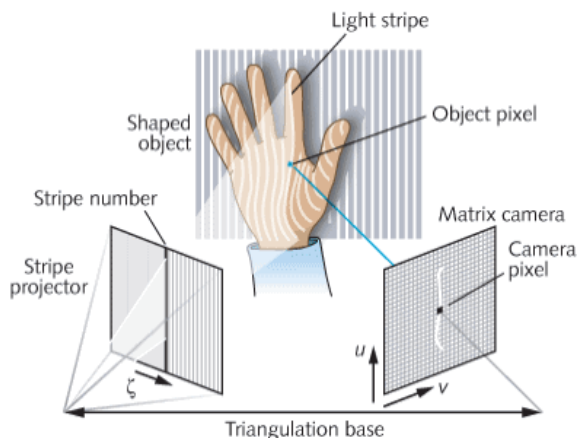


Figure 3.6: Structured light system diagram<sup>25</sup>

The Kinect 2<sup>26</sup> (seen in figure 3.7) is an example of a structured light system and can achieve  
10 measurements with millimeter accuracy for objects close to the sensor. Another similar sensor is Structure IO<sup>27</sup> which is intended for mobile devices and can be seen in figure 3.8.



Figure 3.7: Kinect 2 sensor<sup>28</sup>



Figure 3.8: Structure IO sensor<sup>29</sup>

---

<sup>25</sup><http://www.laserfocusworld.com/articles/2011/01/lasers-bring-gesture-recognition-to-the-home.html>

<sup>26</sup><http://www.microsoft.com/en-us/kinectforwindows/>

<sup>27</sup><http://structure.io/>

<sup>28</sup><https://www.ifixit.com/Teardown/Xbox+One+Kinect+Teardown/19725>

<sup>29</sup><http://structure.io/press>

### 3.4.2 Time of Flight methods

Time of Flight (ToF) or Time of Arrival (ToA) methods can be used to calculate distances based on the amount of time that a given wave takes from the moment it is created to the moment it is received. By assembling a large amount of sensor readings a 3D representation of the environment can be achieved.

Since these systems rely on active interaction with the environment, they can be used without being affected by lighting interferences. Nevertheless, they should take in consideration the conditions in which the waves propagate and also the geometry of the environment, because it can affect the path that the waves take, and as a result, can lead to the decrease of precision in the measurements.

#### 3.4.2.1 Light waves

Light waves generated with lasers can estimate distances with millimeter accuracy at long ranges (system operation overview in [figure 3.10](#)) and their sensors usually have a low sample rate (below 20 Hz). Systems like LIDAR (2D sensor example in [figure 3.12](#) and for 3D in [figure 3.13](#)) take advantage of this fact and can be used to obtain a very detailed 3D point cloud of the environment (like the one showed in [figure 3.9](#)). Moreover, some LIDARs can also capture the environment reflectivity / intensity besides their 3D geometry. On the other hand, ToF cameras (example in [figure 3.11](#)) have a very high sample rate (30 Hz or even higher), but have much more measurement error (greater than 1 cm). However, these methods allow the mapping of the environment with low latency, which can be a critical requirement in robots that must react very fast to changes in their surroundings, such as autonomous cars [[MCB10](#)].

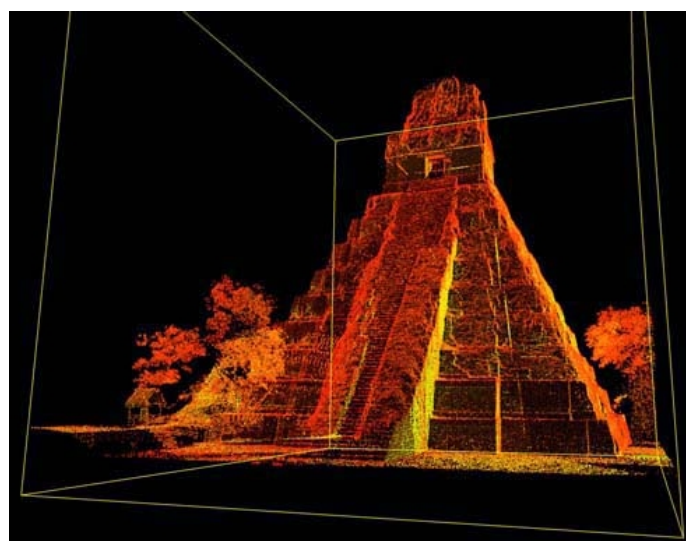


Figure 3.9: LIDAR scan<sup>30</sup>

---

<sup>30</sup><http://blogs.scientificamerican.com/cocktail-party-physics/2012/03/12/1-is-for-lidar/>

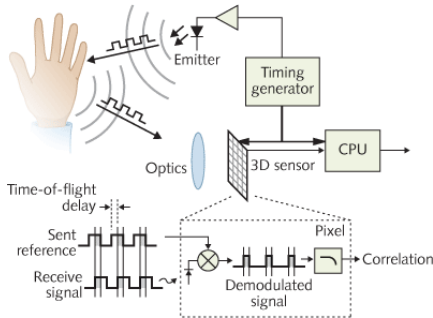


Figure 3.10: Time of Flight system diagram<sup>31</sup>

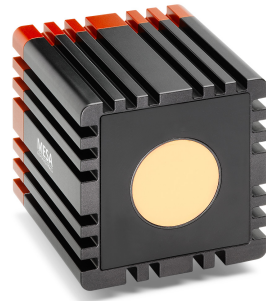


Figure 3.11: Mesa SR4000 sensor<sup>32</sup>



Figure 3.12: 2D SICK NAV 350 sensor<sup>33</sup>

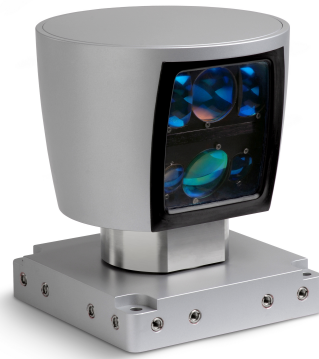


Figure 3.13: 3D Velodyne HDL-64E sensor<sup>34</sup>

### 3.4.2.2 Radio waves

- 2 Similar to **LIDAR**, radio waves can be used to calculate distances using the **ToF** technique. Systems like **RADAR** provide an effective way to calculate the
- 4 distance, altitude, direction and speed of objects that can be used as landmarks in navigation.

Like any electromagnetic wave localization method, it must take in consideration ambient interferences and even jamming, in order to validate the obtained measures. Moreover, some types of materials with a given geometric configuration might be invisible to **RADAR**, and as such, critical localization systems might have to employ some additional techniques to ensure the correct mapping of the robot surroundings.

- 10 Since **RADAR** has a less focused beam than **LIDAR**, it can have considerable less accuracy, as can be seen in figure 3.14. Nevertheless, it can be an effective method to avoid obstacles [WY07].

---

<sup>31</sup><http://www.laserfocusworld.com/articles/2011/01/lasers-bring-gesture-recognition-to-the-home.html>

<sup>32</sup><http://www.mesa-imaging.ch/products/product-overview/>

<sup>33</sup><https://www.sick.com/de/en/detection-and-ranging-solutions/2d-laser-scanners/nav/nav350-3232/p/p256041>

<sup>34</sup><http://www.velodynelidar.com/lidar/hdlproducts/hdl64e.aspx>

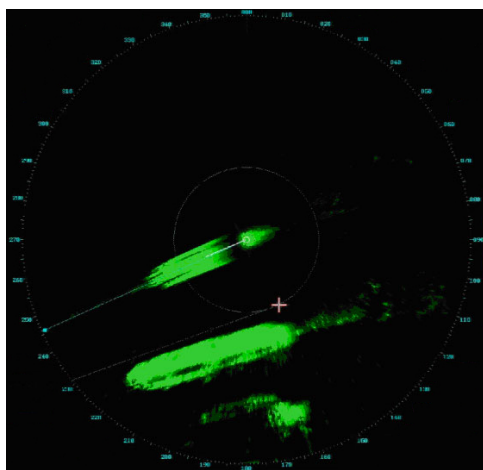


Figure 3.14: RADAR scan of two ships<sup>35</sup>



Figure 3.15: QT50R-AFH RADAR sensor<sup>36</sup>

### 3.4.2.3 Sound waves

Another type of 3D sensor that can be used to map underwater environments relies in the acoustic analysis of the reflections of sounds in the surrounding objects. Like the previous methods, **SOund Navigation And Ranging (SONAR)** can actively scan the environment to calculate the locations of the objects using a **ToF** technique (as can be seen in figure 3.16). Although this method is usually applied to underwater mapping, it can also be used in other sound propagation environments, such as air [GWG13].

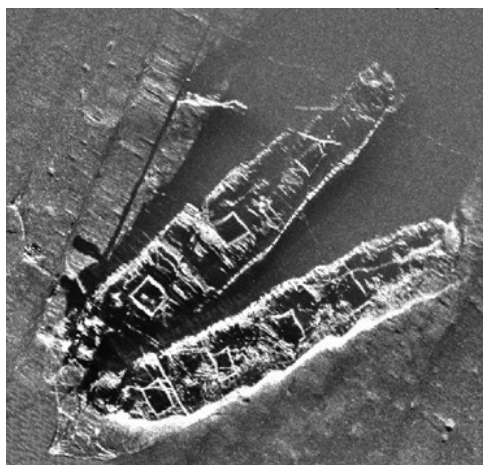


Figure 3.16: SONAR scan of two ships<sup>37</sup>



Figure 3.17: SONAR sensor<sup>38</sup>

<sup>35</sup><http://www.sintef.no/Projectweb/STSOps/News/Operational-Aspects-on-Decision-making-in-STS-Lightering>

<sup>36</sup><http://www.bannerengineering.com/en-US/products/8/Sensors/658/Radar-Sensors/617/>

R-GAGE-QT50R-AFH-Adjustable-Field%2C-High-Sensitivity-Sensor/

<sup>37</sup><http://stellwagen.noaa.gov/maritime/palmercracy.html>

<sup>38</sup><http://www.parallax.com/product/28015>

### 3.4.3 Stereo vision

- 2 Stereo vision systems (example in [figure 3.18](#)) can generate 3D representations of the environment by comparing the displacement of corresponding points in the two ambient images ([figure 3.20](#) gives an overview of such a system). This can be achieved because the relative position of the cameras is known. As such, points farther away will have smaller displacement between images
- 4
- 6
- 8 Given that the accuracy of the disparity image relies heavily in the correct matching of points between the left and right image, some stereo vision systems employ active observation by projecting a pattern into the environment in order to refine the point matching (example of hardware setup in [figure 3.19](#)). This can significantly improve the accuracy if the environment has a lot of
- 10
- 12 smooth surfaces with homogeneous colors.



Figure 3.18: Stereo vision system [[Kac13](#)]



Figure 3.19: PR2 head capable of active stereo vision<sup>39</sup>

---

<sup>39</sup><https://www.willowgarage.com/pages/pr2/overview>

## Relevant software / hardware technologies

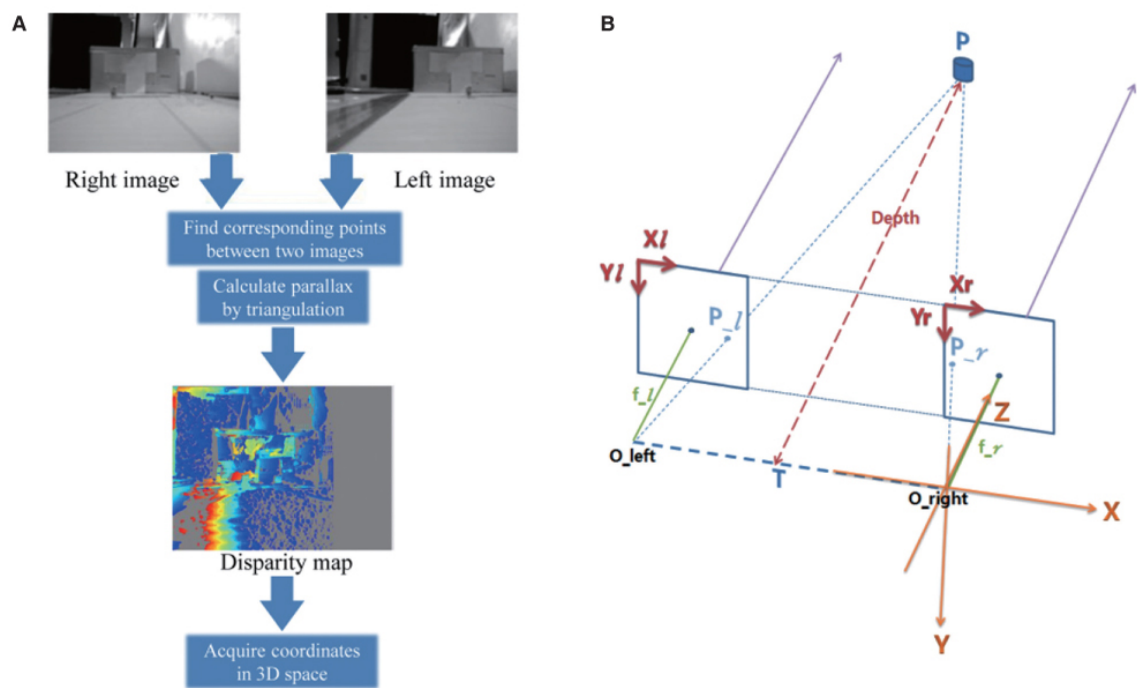


Figure 3.20: Stereo vision overview [YPH<sup>+</sup>14]

# Chapter 4

## **2 Localization system**

- 4** This chapter details the **ROS** implementation of the proposed 3/6 **DoF** self-localization system<sup>1</sup>. It starts with an overview of the main processing stages and then details the control flow and **6** algorithms within the localization pipeline.

### **4.1 Overview**

- 8** The self-localization system was implemented as a **ROS** package and provides 3/6 **DoF** localization by publishing *geometry\_msgs::PoseStamped*<sup>2</sup> and *geometry\_msgs::TransformStamped*<sup>3</sup> **10** messages along with a detailed analysis of the pose estimation and registered point cloud (split into inliers and outliers). Moreover, it also gives detailed analysis of the computation runtime of each **12** of its modules in order to pinpoint which algorithms are using more computation resources, which is very useful information when configuring or upgrading the system.
- 14** The **ROS** implementation can receive sensor data through *sensor\_msgs::PointCloud2*<sup>4</sup> messages and as a result it can directly use data from RGB-D and **ToF** cameras. To use **LIDARs** **16** it provides an assembler that can produce point clouds by merging measurements from several **18** sensor scans using spherical interpolation. As such, if the **LIDAR** sensors are mounted on tilting platforms, they can emulate a 3D sensor and retrieve a very detailed view of the environment.

The self-localization system has a modular software architecture and was implemented as **20** several C++ templated shared libraries that can be easily used for other applications besides robot self-localization. As can be seen in [figure 4.1](#), it is an extensible and flexible system able to fit **22** the needs of a wide range of mobile platforms. It can be configured as a tracking system, with or without pose recovery and can also have initial pose estimation using feature detection and **24** matching. Moreover, it can dynamically create and update the map if necessary.

---

<sup>1</sup>[https://github.com/carlosmccosta/dynamic\\_robot\\_localization](https://github.com/carlosmccosta/dynamic_robot_localization)

<sup>2</sup>[http://docs.ros.org/api/geometry\\_msgs/html/msg/PoseStamped.html](http://docs.ros.org/api/geometry_msgs/html/msg/PoseStamped.html)

<sup>3</sup>[http://docs.ros.org/api/geometry\\_msgs/html/msg/TransformStamped.html](http://docs.ros.org/api/geometry_msgs/html/msg/TransformStamped.html)

<sup>4</sup>[http://docs.ros.org/api/sensor\\_msgs/html/msg/PointCloud2.html](http://docs.ros.org/api/sensor_msgs/html/msg/PointCloud2.html)

## Localization system

It supports two configurable processing pipelines in order to allow fast deployment of robots in large environments. One to process new reference maps and another to localize a mobile robot platform using ambient point clouds. This enables the loading of either processed or unprocessed referenced point clouds and allows a navigation supervisor to dynamically provide the relevant map sections based on the robot position (in order to reduce the computation resources needed).

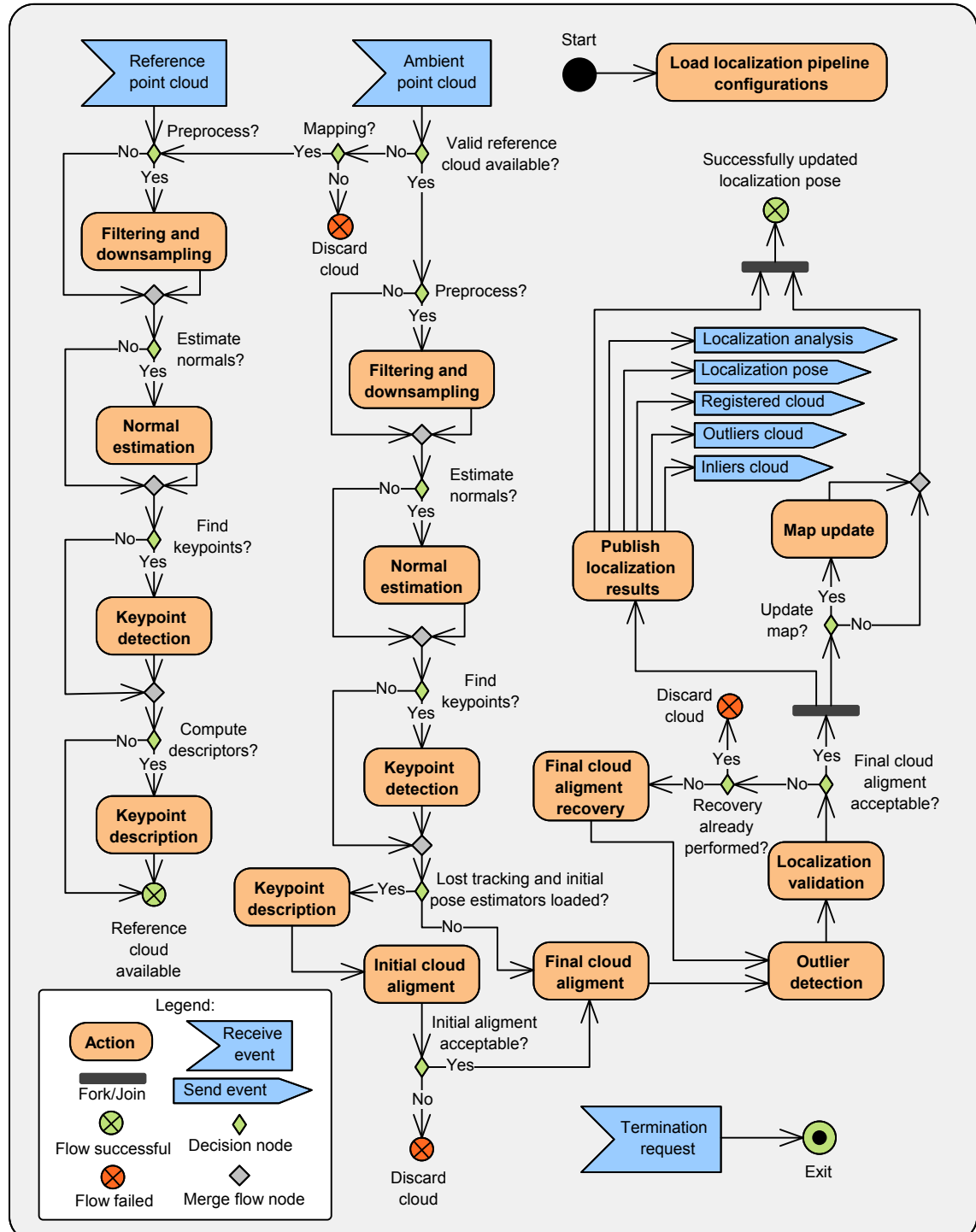


Figure 4.1: Localization system overview

## 4.2 Pipeline configuration

2 The self-localization system was designed to allow fast reconfiguration<sup>5</sup> and parameterization  
 4 through the use of yaml<sup>6</sup> files and the ROS parameter server<sup>7</sup>. This gives the possibility to quickly  
 6 tune the localization system to the specific needs of a given mobile platform moving in a particu-  
 lar environment, in order to use the least amount of computational resources possible and without  
 8 requiring any reprogramming or source code modification. Nevertheless, the system can use a  
 generic configuration if hardware resources are not a concern.

10 In a typical configuration (following the Yes paths of the activity diagram in figure 4.1), the first  
 12 time the localization system is used, it receives a raw reference point cloud that is preprocessed  
 14 and saved to long term memory along with its associated keypoints and keypoint descriptors. This  
 16 allows a much faster startup the next time the localization system is initialized. After having a ref-  
 18 erence point cloud, the localization system will estimate the robot pose periodically by analyzing  
 20 the ambient point cloud sensor data. This data can be preprocessed with several filters and can be  
 22 associated with computed surface normals. The robot pose estimation is performed by applying a  
 24 matrix transformation correction to the current robot pose and is based on the registration of the  
 ambient point cloud with the know map. This registration can use a tracking algorithm configura-  
 tion tuned for efficiency and a second configuration for tracking recovery purposes. These tracking  
 algorithms require a initial pose estimation, and as such, if one isn't available, a third configura-  
 tion can be employed to estimate the global position of the robot based on geometric features of the en-  
 vironment. The switch between these configuration is based on the analysis of the registered cloud  
 metrics, such as outlier percentage, inliers root mean square error, inliers angular distribution and  
 26 the registration corrections performed on the ambient point cloud. After successfully performing  
 28 the robot pose estimation, the map can be updated by either integrating the full registered point  
 cloud, its inliers or its outliers. Finally, like most ROS nodes, the localization system will stop its  
 execution when it receives a termination signal request.

26 The next sections explain in detail the architecture and algorithms used in each of the process-  
 28 ing modules present in figure 4.1.

## 28 4.3 Reference map

The reference point cloud can be loaded from a CAD file, point cloud file or dynamically arrive  
 30 trough a ROS topic as either a 3 DoF nav\_msgs::OccupancyGrid<sup>8</sup> or 6 DoF sensor\_msgs::PointCloud2<sup>9</sup>.  
 This allows a localization supervisor to give only sections of a global map in order to use the least  
 32 amount of memory and processing power (very large maps have deeper search structures, such as  
 kd-trees, and should be avoided in order to improve the system efficiency).

---

<sup>5</sup>[https://github.com/carlosmccosta/dynamic\\_robot\\_localization/blob/hydro-devel/yaml/schema/drl\\_configs.yaml](https://github.com/carlosmccosta/dynamic_robot_localization/blob/hydro-devel/yaml/schema/drl_configs.yaml)

<sup>6</sup><http://yaml.org/>

<sup>7</sup><http://wiki.ros.org/Parameter%20Server>

<sup>8</sup>[http://docs.ros.org/api/nav\\_msgs/html/msg/OccupancyGrid.html](http://docs.ros.org/api/nav_msgs/html/msg/OccupancyGrid.html)

<sup>9</sup>[http://docs.ros.org/api/sensor\\_msgs/html/msg/PointCloud2.html](http://docs.ros.org/api/sensor_msgs/html/msg/PointCloud2.html)

## 4.4 Point cloud assembly

The self-localization system can use any sensor that provides point clouds, namely RGB-D / ToF cameras, LIDARs and stereo vision systems. Each of these types of sensors have very different operation rates and measurement accuracy. As such, the localization system allows the assembly of several ambient scans using a circular buffer in order to reduce the impact of sensor noise.

For LIDARs, the system provides a *sensor\_msgs::LaserScan*<sup>10</sup> assembler<sup>11</sup> that converts laser measurements in polar coordinates into Cartesian coordinates and projects the points using spherical interpolation (in order to account for laser scan deformation that occurs when the robot is moving and rotating). It can merge scans from several lasers sensors and it will publish the final point cloud after assembling a given number of scans or periodically after a specified duration. These assembly configurations can be changed at runtime based on the robot velocity (for example, when the robots moves slower, more laser scans are assembled for each published point cloud) or through the use of the ROS dynamic reconfigure API, which allows a navigation supervisor to control the rate at which the localization system operates.

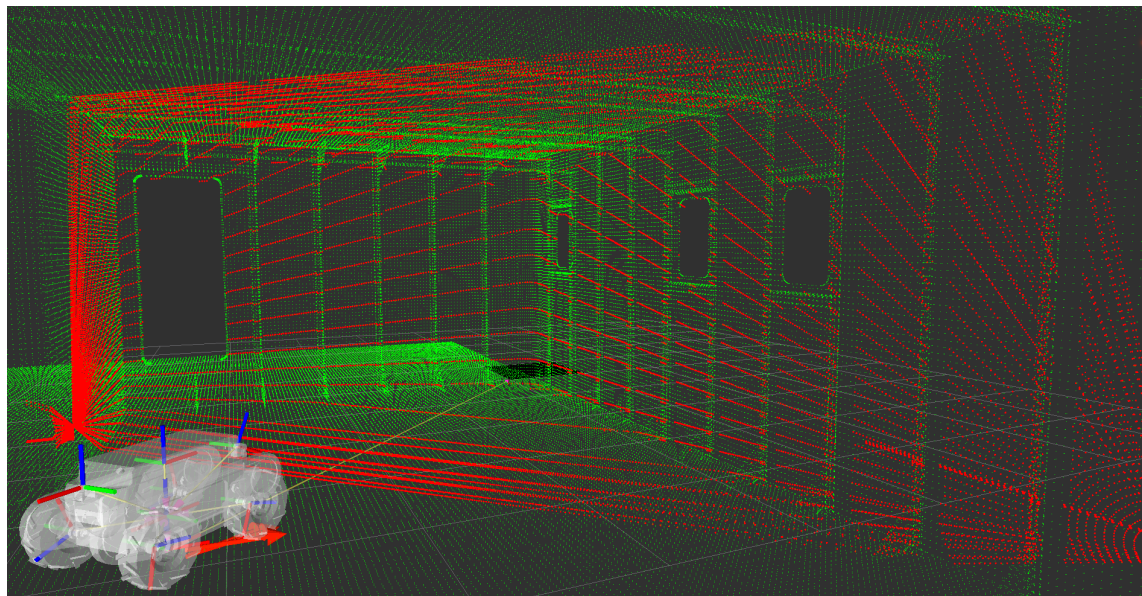


Figure 4.2: Laser scans assembled with tilting platform (red points)

## 4.5 Point cloud search data structures

Most of the point cloud algorithms use neighbor searches to analyze the surroundings of a given point. As such, efficient data structures are needed to speedup these operations, in order to execute the algorithms efficiently.

<sup>10</sup>[http://docs.ros.org/api/sensor\\_msgs/html/msg/LaserScan.html](http://docs.ros.org/api/sensor_msgs/html/msg/LaserScan.html)

<sup>11</sup>[https://github.com/carlosmccosta/laserscan\\_to\\_pointcloud](https://github.com/carlosmccosta/laserscan_to_pointcloud)

#### 4.5.1 Voxel grids

- 2 A voxel grid is a three dimensional space partition data structure that splits the Euclidean space into regular voxels (volume pixel). It can be built very fast but is not very efficient for sparse point clouds. [Figure 4.3](#) shows voxel grids with different voxel size.

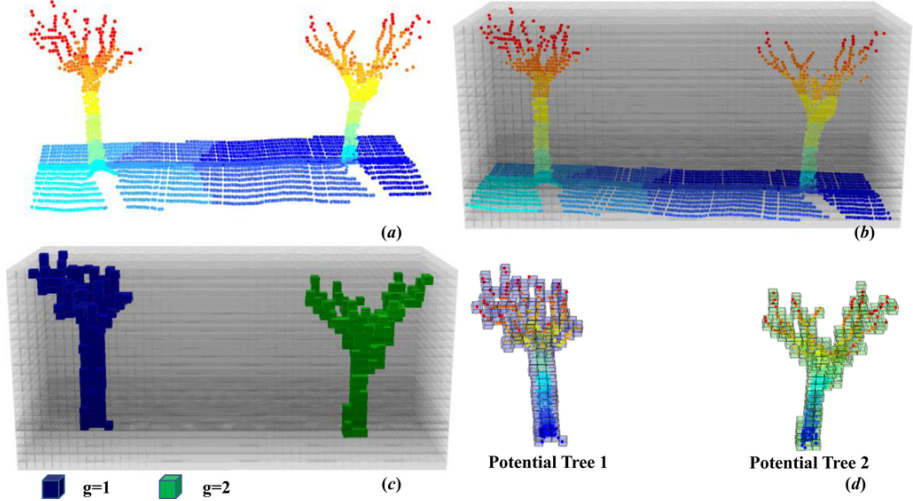


Figure 4.3: Voxel grid applied over trees point clouds [[WYY<sup>+</sup>13](#)]

#### 4.5.2 Octrees

- 6 An octree is a hierarchical space partition technique that adapts its tree data structure to the distribution of points in the cloud. It accomplishes this by recursively dividing each voxel in 8  
8 octants until the tree depth is reached or when there is no more points in that region of space. This  
10 can be seen in [figure 4.4](#) in which areas with no points have large voxels while areas with high point density have much smaller voxels.

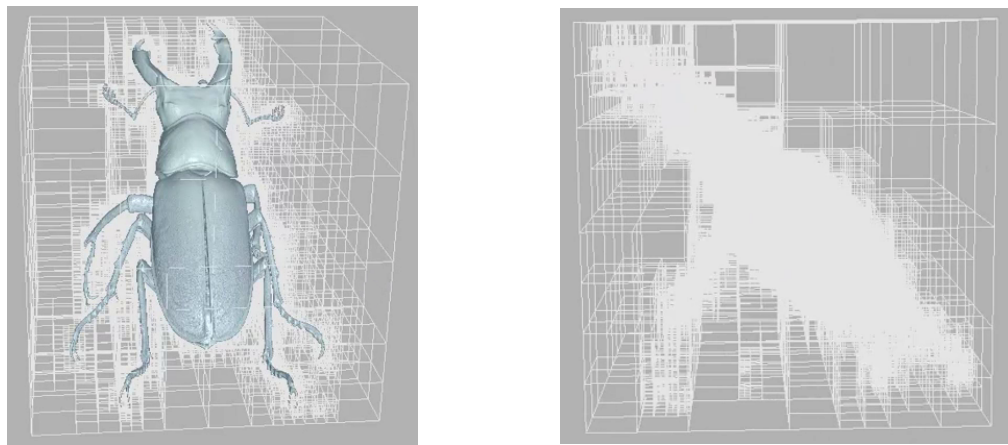


Figure 4.4: Octree of a stag beetle<sup>12</sup>

---

<sup>12</sup><http://blog.mpanknin.de/?p=753>

### 4.5.3 k-d trees

A k dimensional tree is a space partition technique that can organize points with k dimensions. It is a generic data structure that can be used for 2D and 3D points (examples in [figure 4.5](#) and [figure 4.6](#)) as well as any other types of data that have an arbitrary number of dimensions (such as point cloud feature descriptors).

The binary k-d tree is built by successively selecting the median point in each axis until all points are inserted in the tree (the selection of the next axis is performed in a circular way, which in the case of three dimensional data, means that after processing the z axis, the x axis would be selected).

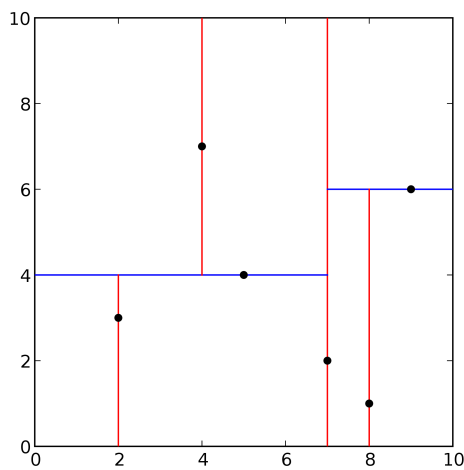


Figure 4.5: 2-d tree<sup>13</sup>

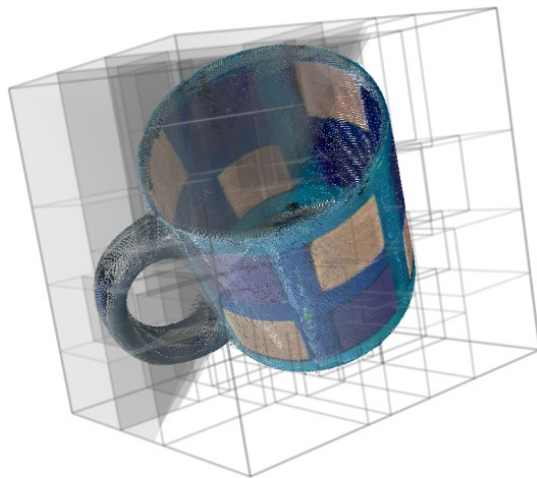


Figure 4.6: 3-d tree<sup>14</sup>

## 4.6 Filtering and down sampling

The time it takes to perform cloud registration is proportional to the amount of points in the ambient point cloud and in the reference map. As such, adjusting the level of detail of the point clouds by using voxel grids gives some control over the desired localization accuracy and the computational resources that will be required. This stage is also useful to mitigate the measurement errors of the depth sensors, since the centroid of a voxel that contains points from several scans will be closer to the real surface (if the voxels have dimensions slightly larger than the expected measurement errors).

The localization system allows the application of several preprocessing algorithms (algorithm type / configuration and execution order customizable). The next sections detail some of these methods that can be used to filter and downsample point clouds.

<sup>13</sup>[http://en.wikipedia.org/wiki/K-d\\_tree](http://en.wikipedia.org/wiki/K-d_tree)

<sup>14</sup>[http://docs.pointclouds.org/trunk/group\\_\\_kdtree.html](http://docs.pointclouds.org/trunk/group__kdtree.html)

#### 4.6.1 Point cloud downsampling

- 2   Downsampling methods aim to reduce the number of points while maintaining the surface structure of a given point cloud. They can be used to adjust the level of detail according to the point  
 4   cloud registration precision required.

##### 4.6.1.1 Voxel grid sampling

- 6   A voxel grid is a uniform space partition technique that can be used to cluster points according to their Euclidean coordinates. As can be seen in [figure 4.7](#), it is a very effective method to control  
 8   the level of detail of a point cloud because it gives the ability to specify the maximum number of points that a region of space should have.

10   The point cloud downsampling is achieved by replacing each voxel cluster with a single point. The selection of this point can be very fast if the voxel center is used, but computing the centroid  
 12   of the cluster yields better results because it represents the underlying surface with more accuracy and it attenuates errors in the sensors measurements.

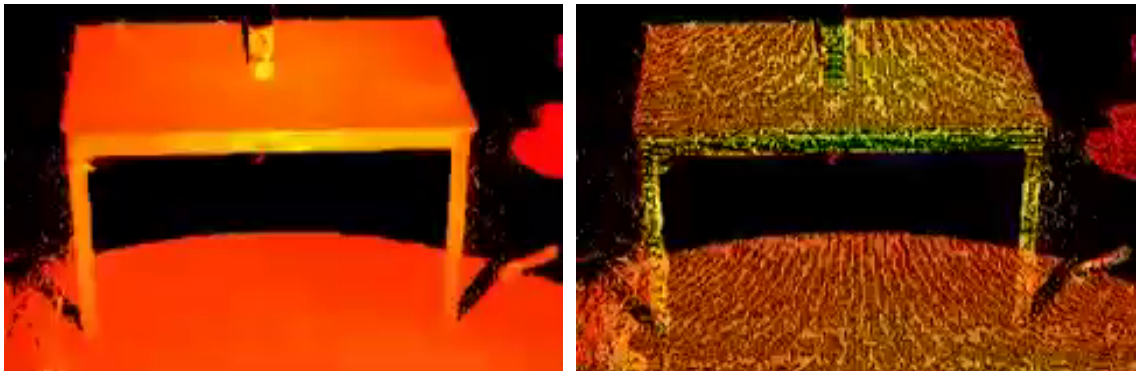


Figure 4.7: Table point cloud before (left) and after (right) voxel grid downsampling<sup>15</sup>

14   

#### 4.6.1.2 Random sampling

Random sampling [[Vit84](#)] is a fast downsampling method that randomly selects points from the  
 16   input cloud until the specified number of samples is reached. This has the advantage of using real  
 measures instead of downsampled approximations, but also means it is more sensible to sensor  
 18   measurements noise. However, for outdoor environments or very complex scenes, using the real  
 measurements can be preferable than using cluster centroids because the voxels may not have the  
 20   necessary resolution or may have a prohibitive computational cost.

##### 4.6.1.3 Covariance sampling

- 22   Covariance sampling [[GIRL03](#)] is a subsampling method that aims to create a stable downsampled point cloud to be registered with [ICP](#) algorithms. It incrementally builds the downsampled point

---

<sup>15</sup>[http://pointclouds.org/documentation/tutorials/voxel\\_grid.php](http://pointclouds.org/documentation/tutorials/voxel_grid.php)

cloud while trying to keep the 6 eigenvalues of the covariance matrix as close to each other as possible.

The resultant point cloud has the desired number of points and is stable enough to be matched with ICP point to plane algorithms.

#### 4.6.2 Outlier removal

Some depth sensors can perform measurements with high accuracy, but they have some limitations that can lead to the creation of outliers [Sot06].

One of those limitations can produce shadow points around objects boundaries. This is due to the fact that a portion of the laser beam may hit the object boundary and other part may hit other areas in the object background. And given that most laser range finders use a weighted sum of several beams, this can yield measurements that are not associated with any real object (outliers). Figure 4.7 shows a considerable amount of these shadow points close to the front table legs. Another issue is related to the angle in which the depth sensor sees the objects areas. If the incidence angle is very low, then it may be difficult to compute its distance and detect if the beam had ambient reflections. This can significant increase the measurements noise or even lead to the creation of outliers. Other common problem is associated with the material properties of the surfaces. For example, objects with very high or very low reflectance, such as metals or glass, can increase the measurements noise. Moreover depending on the combination of surface geometry, material and incidence angle, some objects may even be undetectable by depth sensors.

Given the negative effect that outliers have in surface normal computation and registration algorithms, they should be removed in a preprocessing stage. There are several approaches to perform outlier detection and removal [ZMH10], ranging from simple distance thresholds to more robust statistical analysis. The next sections present some of then that can be useful in a localization system.

##### 4.6.2.1 Distance filter

Given that depth sensors have a maximum recommended distance for their measurements, it is wise to remove points that are close or beyond this limit. Moreover, it may be useful to remove points that are too close to the sensor, because they may belong to the robot itself and not the environment.

This can be achieved by applying a minimum and maximum threshold to the distances returned by the depth sensor.

##### 4.6.2.2 Passthrough filter

A passthrough filter can select or remove points according to their properties.

For outlier removal, it can be used to select points that are within a given bounding box (useful when we already know what area of the environment we want to analyze) or remove points that don't have the appropriate intensity or color.

#### 4.6.2.3 Radius outlier removal filter

- <sup>2</sup> The radius outlier removal filter deletes points that don't have a minimum number of neighbors within a specified radius distance. It can be useful when the point density is known and is very effective in removing isolated points.

#### 4.6.2.4 Statistical outlier removal filter

- <sup>6</sup> The statistical outlier removal filter [Rus10] performs a global analysis of the distances between points and discards the ones that don't follow the global distance distribution.
- <sup>8</sup> It is a robust filter that adapts itself to the point cloud density and is very effective in removing shadow points. To do so, it computes the mean distance that each point has to a given number of <sup>10</sup> neighbors and builds a global distance distribution (example in figure 4.8). Then, assuming that the distribution is Gaussian, it discards the points that have a distance higher than a given threshold <sup>12</sup> (that is a percentage of the standard deviation of the distance distribution).

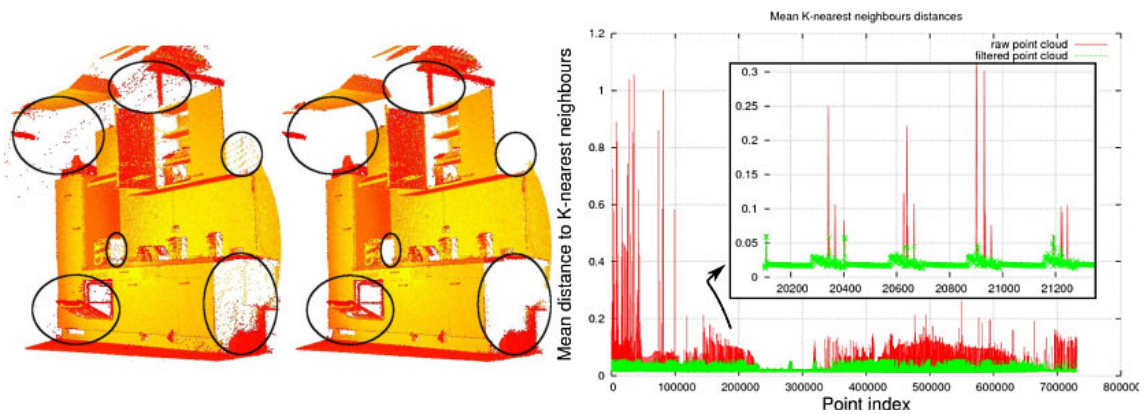


Figure 4.8: Statistical outlier removal filter<sup>16</sup>

#### 4.6.3 Surface and object reconstruction and resampling

- <sup>14</sup> Depending on the level of sensor noise and amount of outliers present in a given point cloud, it may be necessary to employ surface reconstruction techniques to fill gaps in sensor data or correct <sup>16</sup> measurements errors.

Moving least squares [ABCO<sup>+</sup>03] is a surface reconstruction algorithm that uses higher order <sup>18</sup> bivariate polynomials to fit surfaces to a given set of points. It can be used to fill possible gaps in sensor data, smooth the point cloud (shown in figure 4.9), refine surface normals (shown in <sup>20</sup> figure 4.10) and perform downsampling or upsampling.

Surface reconstruction can also be useful when the point cloud is built from several ambient <sup>22</sup> scans with different origins and registered with some alignment errors. In figure 4.10 can be seen that the normal estimation is not very accurate in the overlapping regions between different scans.

<sup>16</sup>[http://pointclouds.org/documentation/tutorials/statistical\\_outlier.php](http://pointclouds.org/documentation/tutorials/statistical_outlier.php)

This can be solved by estimating the normals using the surfaces computed by the moving least squares algorithm instead of using the point's neighbors.

2

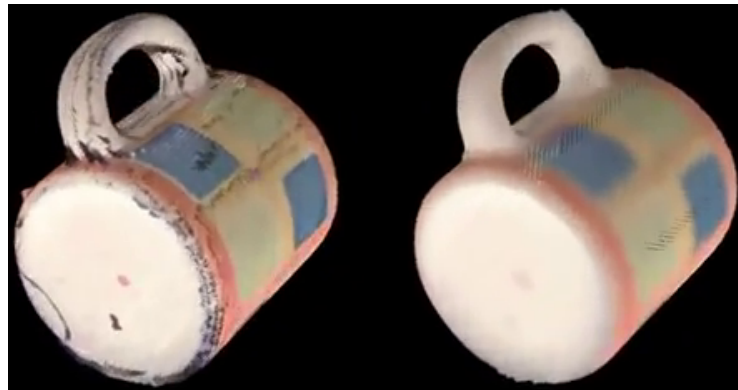


Figure 4.9: Surface smoothing using moving least squares algorithm<sup>17</sup>

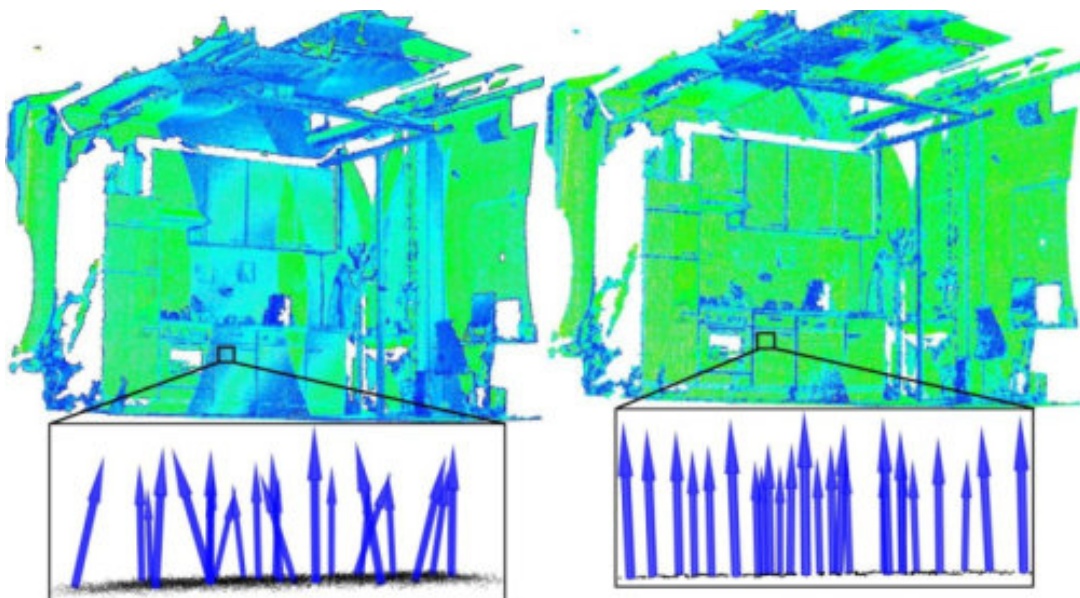


Figure 4.10: Surface normals refinement using moving least squares algorithm [Rus10]

## 4.7 Normal estimation

Most of feature detection, description and matching algorithms along with some registration methods rely on the point's surface normal and curvature. These algorithms analyze the neighborhood of a given point in order to compute the line / surface normal, and as such, the correct specification of what points should be included in the estimation is crucial to achieve accurate results. This depends on the environment geometry and the level of detail that is required, and is usually done

4

6

8

---

<sup>17</sup><http://pointclouds.org/documentation/tutorials/resampling.php>

by specifying a radius distance (example in [figure 4.11](#)) or by limiting the number of neighboring points to use.

The next sections describe some of the methods that are supported for 3/6 DoF sensor data.

#### **4.7.1 Line normal estimation**

Line normals give information about the spatial disposition and orientation of a given cluster of collinear points. They can be computed using [Random Sample Consensus \(RANSAC\)](#) methods [[FB81](#)] and their orientation can be corrected using the sensor's origin.

#### **4.7.2 Surface normal estimation**

Surface normals provide information about the orientation of the underlying geometry of a given point cluster. They can be computed using plane fitting methods or using more advanced techniques such as [Principal Component Analysis \(PCA\)](#) [[Jol02](#)] or the one presented in [section 4.6.3](#).

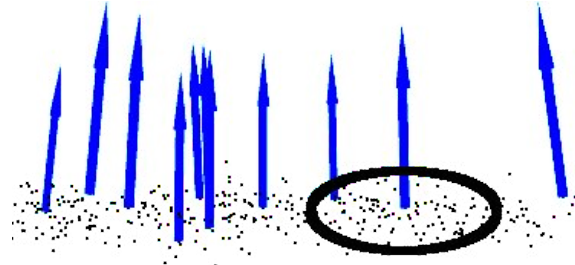


Figure 4.11: Point neighborhood for normal estimation [[Rus10](#)]

## **4.8 Keypoint detection**

Aligning two point clouds with overlapping views of the environment requires the establishment of point correspondences. If both point clouds have similar sensor origins, these can be determined with nearest neighbor's searches and filtered with correspondence rejectors (using other point properties such as reflectance and color). But if they were acquired in two very different positions, then more advanced techniques must be employed.

One of those techniques uses histograms to describe the geometric properties of the environment around a given point. This allows points to be matched even if they have completely different Euclidean coordinates. Also, by using histograms and sampling techniques, these descriptors are much more robust against sensor noise and varying level of point density. However, these advantages come with a heavy computational cost, and as such, point descriptors should only be computed on the most descriptive areas of the environment.

Identifying these environment points is known as feature / keypoint detection [[FA14](#)], and usually involves finding interesting points, such as corners and edges. Besides uniqueness, these points must also be repeatable. This means that the detection algorithms should be able to find the same points even if they are present in different point clouds with sensor noise and varying point

density. This is of the utmost importance, because if the same keypoints are not identified on both clouds, then matching the point descriptors will likely fail.

Currently, the localization system can use the [Scale Invariant Feature Transform \(SIFT\)](#) [KL04] algorithm on the point's curvature or the [3D Intrinsic Shape Signatures \(ISS3D\)](#) [Yu09] keypoint detector on the point's normals.

## 4.9 Keypoint description

Describing a keypoint usually involves analyzing its neighboring points and computing a given metric or histogram that quantifies the neighbor's relative distribution, their normals angular relation, associated geometry or other metrics that are deemed useful. Several approaches were suggested over the years according to different recognition needs and they are the basis of feature matching algorithms used in the initial pose estimation.

The localization system can use most of the keypoint descriptors available in [PCL](#), namely the [Point Feature Histogram \(PFH\)](#) [RBMB08], the [Fast Point Feature Histogram \(FPFH\)](#) [RBB09], the [Signature of Histograms of Orientations \(SHOT\)](#) [TSD11], the [Shape Context 3D \(SC3D\)](#) [FKH<sup>+</sup>04], the [Unique Shape Context \(USC\)](#) [TSD10] and the [Ensemble of Shape Functions \(ESF\)](#) [WV11].

## 4.10 Cloud registration

Point cloud registration is the process of finding the transformation matrix (usually translation and rotation only) that when applied to a given ambient cloud will minimize an error metric (such as the mean square error of the ambient point cloud in relation to a given reference point cloud). Several approaches were suggested over the years and they can be categorized as point or feature cloud registration.

### 4.10.1 Initial alignment with keypoints descriptor matching

Feature registration is the process of matching keypoint descriptors in order to find an initial alignment between two point clouds. The proposed localization system uses a feature registration method similar to the [Sample Consensus Initial Alignment \(SAC-IA\)](#) algorithm presented in [RBB09]. It uses a [RANSAC](#) approach to select the best registration transformation after a given number of iterations. In each iteration a subsample of randomly selected descriptors from the ambient cloud is retrieved. Then for each of these descriptors,  $k$  best matching descriptors in the reference point cloud are searched (using a kd-tree) and one of them is chosen randomly (this improves robustness against noise in the sensor data and changes in the environment that are not yet integrated into the map). Later after having filtered these correspondences between ambient and reference descriptors, the registration matrix is computed. If this registration matrix results in a point cloud overlap that has a minimum of inliers percentage (a point in the ambient cloud is an

inlier if it has a point in the reference cloud closer than a given distance), then it is considered an acceptable initial pose and is saved (to allow a localization supervisor to analyze the distribution of the acceptable initial poses). In the end of all iterations, the best initial pose (if found) is refined with a point cloud registration algorithm.

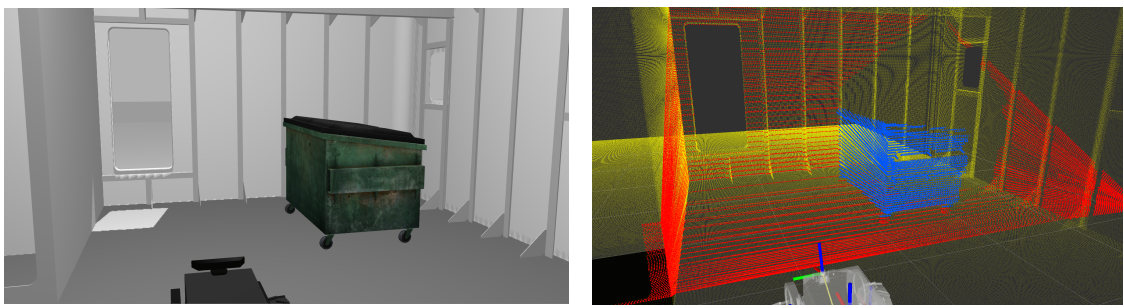
#### 4.10.2 Final alignment with point cloud error minimization

Point cloud registration algorithms (introduced in section 2.2.4) such as ICP [BM92] (with its several known variations [RL01, Pom13] like ICP point-to-point, ICP point-to-point non-linear, ICP point-to-plane and generalized ICP [SHT09]) and the Normal Distributions Transform (NDT) [Mag09] are among the most popular algorithms to register point clouds. They can achieve very accurate cloud registration but they require an approximate initial pose for the registration to successfully converge to a correct solution (otherwise they may achieve only partial cloud overlap or even fail to converge to a valid solution).

### 4.11 Outlier detection

Detecting which points of the environment are not part of the reference point cloud can be very useful to evaluate the quality of point cloud registration as well as to analyze the presence of previously unknown objects. Its computation splits the ambient cloud into two point sets. One containing inliers (points correctly registered and present in the reference point cloud) and the other having the outliers (points that are either incorrectly registered or not present in the reference cloud).

A given ambient point can be classified as outlier if the corresponding closest point in the reference cloud is farther way than a given distance threshold. These calculation can be done efficiently by using the reference point cloud kd-tree. In figure 4.12 is an example of a ambient point cloud retrieved with a tilting laser and registered with an indoor map (yellow points). After registration, the ambient point cloud was split into inliers (red points) and outliers (blue points).



(a) Gazebo overview

(b) RViz overview

Figure 4.12: Point cloud registration with outlier detection

## 4.12 Localization validation

After a point cloud is registered by the localization system, several metrics are calculated in order to evaluate if a valid pose can be retrieved using the registration matrix.

The first computed metrics are the percentage of inliers and the [Root Mean Square Error \(RMSE\)](#) of these inliers. If a minimum number of points was registered and the inlier percentage and root mean square error are acceptable, then the registration is considered successful. However, these registered points can be agglomerated in a small area and may not be representative of the robot location. As such, a second metric is computed that takes into account the angular distribution of these inliers. This metric gives a measurement of how reliable is this registration and is based on the fact that there is high confidence in a given pose estimation when there are correctly registered points all around the robot.

The last metrics are the corrections that the registration matrix introduced. Given that the localization system will be in tracking mode most of the time, it is possible to define how far a new pose can be in relation to the previous accepted location and discard new poses that exceed a given threshold. This is useful to discard pose corrections that are very unlikely to happen, such as the robot moving half a meter between poses when it is expected to move only at 30 cm/s. These situations can happen when there is a sudden decrease in the field of view (that can occur due to sensor occlusion or malfunction) or when large unknown objects very similar to sections of the map appear into the field of view of the robot.

If all these metrics are within acceptable thresholds, then the robot pose can be computed by applying the matrix correction to the initial pose associated with the ambient sensor data. If any of these metrics are not acceptable, then the system can be configured to simply discard this pose estimation and try to estimate the pose in the next sensor data update or it can apply a tracking recovery attempt with a different registration algorithm (or the same algorithm with different parameters). If several consecutive pose estimations are discarded, the system can have a second level of recovery that can be configured to use the initial pose estimation algorithms in order to finally estimate the robot pose and reset the tracking state.

## 4.13 Dynamic map update

After performing a successful pose estimation, the localization system can update the localization map by either integrating only the unknown objects or the full registered point cloud (it can also be used in conjunction with OctoMap [[HWB<sup>+</sup>13](#)] to perform probabilistic map updates). Integrating only the unknown objects is the recommended approach when there is a known map and the environment is expected to change gradually. This is also more efficient as only the points that need to be integrated are processed and ray traced in OctoMap. On the other hand, integrating the full registered cloud can be desirable if the map of the environment is very incomplete, very outdated or expected to change considerably during the operation of the robot.

# Chapter 5

## **Localization system evaluation**

- 4 This chapter presents several test scenarios that were devised to evaluate the implemented local-  
5 ization system. They aim to test the accuracy and robustness of the implementation under different  
6 environmental conditions and hardware configurations.

### **5.1 Testing platforms**

- 8 The localization system was tested on laser sensor data retrieved from two different robots and  
9 executed on the same computer in order to allow a direct comparison of computation time. This  
10 computer was a Clevo P370EM3 laptop (with a Intel Core i7 3630QM CPU at 2.4GHz, 16 GB of  
11 RAM DDR3, Nvidia GTX680M graphics card and a Samsung 840 Pro SSD) and it was running  
12 Ubuntu 12.04 along with ROS Hydro, PCL 1.7 and Gazebo 1.9.

13 The sensor data was recorded into rosbags, and is publicly available at<sup>1</sup> along with all the de-  
14 tailed results and experiments videos, in order to allow future comparisons with other localization  
15 systems. The hardware specifications of the LIDARs used is presented in [table 5.1](#) and the laser  
16 points after downsampling and registration can be seen on the movement paths figures as green  
circles (inliers) and red circles (outliers).

18 **5.1.1 Jarvis platform**

19 The Jarvis platform is an autonomous ground vehicle equipped with a SICK NAV 350 laser for  
20 self-localization (mounted about 2 meters from the floor) and a SICK S3000 laser for collision  
21 avoidance (mounted about 0.20 meters from the floor). It uses a tricycle locomotion system with  
22 two back wheels and a steerable wheel at the front. In [figure 5.1](#) the robot is performing a delivery  
23 task with the package on top of a moving support. The 3 DoF ground truth is provided by the SICK  
24 NAV350 system, uses 6 laser reflectors with 9 cm of diameter (shown as blue circles in [figures 5.8](#)  
and [5.19](#)) and is certified for robot docking operations with precision up to 4 millimeters.

---

<sup>1</sup>[https://github.com/carlosmccosta/dynamic\\_robot\\_localization\\_tests](https://github.com/carlosmccosta/dynamic_robot_localization_tests)



Figure 5.1: Jarvis testing platform

### 5.1.2 Guardian platform

The Guardian platform is an autonomous mobile manipulator equipped with a Hokuyo URG-04LX laser in the front and a Hokuyo URG-04LX\_UG01 laser in the back (both mounted about 0.37 meters from the ground). The front laser had a tilting platform which allows 3D mapping of the environment. The arm is a SCHUNK Powerball LWA 4P and in [figure 5.2](#) it is attached to a stud welding machine (in simulation it is attached to a video projector). It uses a differential drive locomotion system and can be moved with wheels or with tracks. This platform didn't have a certified ground truth and as such, the results of the performed tests could not be quantified with an external localization system (the results performed with the Gazebo simulator will be presented instead - robot model shown in [figure 5.3](#)).



Figure 5.2: Guardian testing platform



Figure 5.3: Guardian Gazebo simulation

Table 5.1: LIDARs hardware specifications

<i>Laser model</i>	<i>Range (meters)</i>	<i>Field of view (degrees)</i>	<i>Scanning frequency (Hz)</i>	<i>Angular resolution (degrees)</i>	<i>Statistical error (millimeters)</i>
SICK NAV350	[0.5..250]	360	8	0.25	15
SICK S3000	[0.1..49]	190	8	0.25	150
Hokuyo URG-04LX	[0.06..4.095]	240	10	0.36	10
Hokuyo URG-04LX_UG01	[0.02..4]	240	10	0.36	30

## 5.2 Testing environments

- 2 The localization system was tested using the Jarvis platform in a large room with a RoboCup field and the Guardian platform in a simulated indoor environment with different internal layout  
 4 variations.

### 5.2.1 Jarvis in RoboCup field

- 6 The RoboCup field (shown in [figure 5.4](#)) occupies half of a large room (with 20.5 meters of length  
 8 and 7.7 meters of depth). It has two doors, several small windows and two large glass openings into  
 the hallway. Several tests were performed with the robot at different speeds in this environment  
 10 but the ground truth provided by the SICK NAV 350 was only reliable at low paces. As such,  
 12 only the results of the robot moving at 5 cm/s will be show (along with the tests performed in the  
 Stage simulator<sup>2</sup>). These tests were performed with two different movement paths. The first is a  
 simple rounded path (shown in [figure 5.8](#)) that aimed to test the robot in the region of space that  
 had better ground truth (due to its position in relation to the laser reflectors) and the second path  
 14 was more complex and contained several sub paths with different velocities and shapes (shown in  
[figure 5.19](#)).

---

<sup>2</sup><http://rtv.github.io/Stage/>



Figure 5.4: Jarvis tests environment

### 5.2.2 Guardian in structured environment

The structured environment simulated in Gazebo is a large room with 12.4 meters of length and 8.4 meters of depth. It has 4 doors, several small windows and the walls have small ledges at regular intervals (as can be seen from [figures 5.5 to 5.7](#)). 2  
4

Given that the Guardian mobile manipulator is expected to work on the walls of this environment, several tests were devised with a path following the lower and right wall of the environment (shown in [??](#)). The first test was done in a static environment clear of unknown objects and was meant to evaluate the best precision that the localization system could achieve. The second test was done in a cluttered environment and was designed to test the robustness of the localization system against static unknown objects, that were placed in the middle of the environment and close to the walls (to block sensor data from reaching known positions and analyze the robustness of matching unknown points that are close to known areas). The last test added a moving car to the scene and aimed to assess the impact of dynamic objects on the point cloud registration algorithms. 6  
8  
10  
12

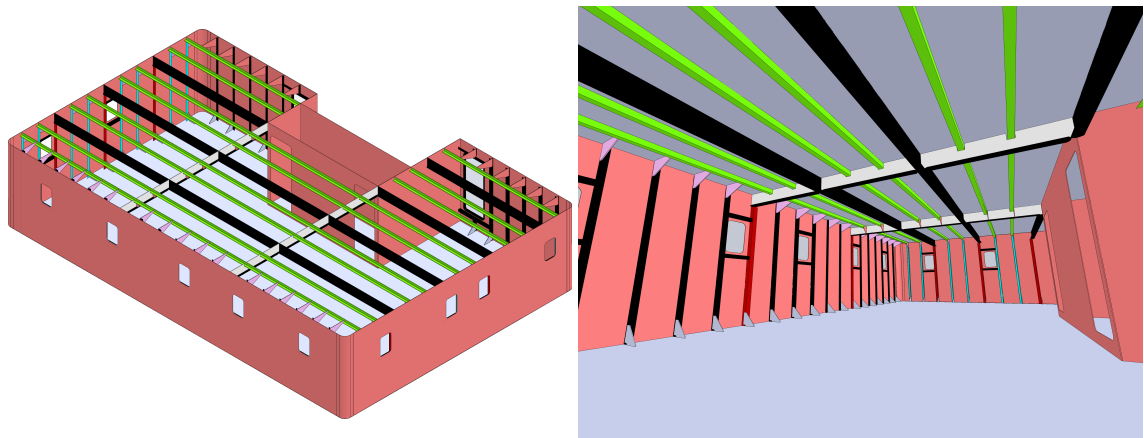


Figure 5.5: Guardian testing environment

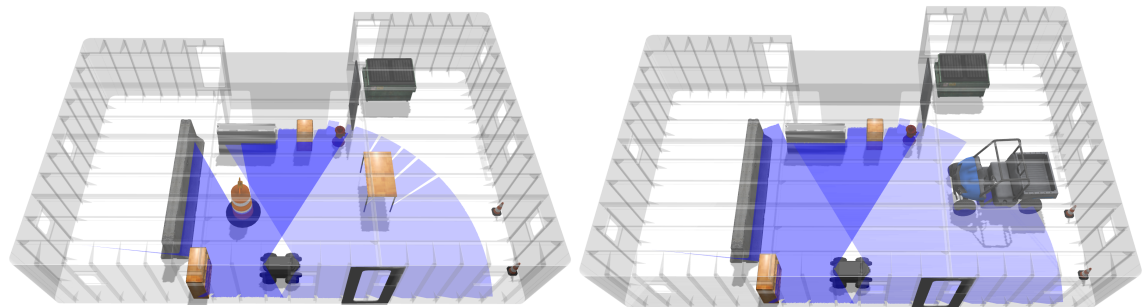


Figure 5.6: Guardian cluttered (left) and dynamic (right) testing environment

Figure 5.7: Interactive CAD of Guardian testing environment (.u3d file)

### 5.3 3 DoF localization system tests

#### 2 5.3.1 Overview

The main results of the 3 DoF tests performed with the localization system are presented in table 5.2. It summarizes each test by fitting a normal distribution for each evaluation metric. They were retrieved with a known initial pose using ICP point-to-point as tracking algorithm and ICP point-to-plane as tracking recovery method. The Jarvis tests had a map built using the localization system in SLAM mode and were manually corrected to achieve a resolution of 10 mm. The Guardian tests relied on a map built from the CAD model with resolution of 2 mm. A voxel grid of 75 mm was applied to the assembled laser scans in the Jarvis experiments while in the Guardian tests it was used a voxel grid of 25 mm. The initial pose estimation subsystem used SIFT for keypoint selection, FPFH for keypoint description and the feature matching algorithm described in section 4.10.1 to estimate the initial position and orientation of the robot (figure 5.114 shows the accepted initial poses when the robot was in the lower right corner of the Guardian test environment).

The next sections contain the main 3 DoF results of the localization system. To avoid cluttering the next subsections with too many graphs, only the tests with the physical robot platforms will have a detailed analysis (the tests on simulators will only have the movement paths and localization error). In <sup>3</sup> is available the full test results along with videos and the configurations used.

The robot movement paths present in the next sections illustrate the synchronized poses from the localization system (blue arrows), ground truth (green arrows) and odometry (red arrows). A regular grid with one meter spacing was applied on top of the figures to ease their analysis.

---

<sup>3</sup>[https://github.com/carlosmccosta/dynamic\\_robot\\_localization\\_tests](https://github.com/carlosmccosta/dynamic_robot_localization_tests)

## Localization system evaluation

**Table 5.2: 3 DoF localization system results**

Platform	Ambient	Test conditions		$\frac{\text{N}^{\text{o}} \text{ scans}}{\text{N}^{\text{o}} \text{ lasers}}$	Translation error (millimeters)		Rotation error (degrees)		Outliers percentage [0..100]		Global computation time (milliseconds)		
		Path shape	Path velocities		Mean	Standard deviation	Mean	Standard deviation	Mean	Standard deviation	Mean	Standard deviation	
					Cluttered	Rounded	Cluttered	Rounded	Cluttered	Rounded	Cluttered	Rounded	
Jarvis robot	Cluttered dynamic	Complex	5 cm/s	2/1	6.235	3.242	0.529	0.157	20.16	5.87	7.827	7.990	
Jarvis simulator (Stage)	Rounded	100 cm/s	5 cm/s	2/1	2.817	1.551	0.038	0.026	16.11	0.93	12.600	12.459	
Jarvis simulator (Gazebo)	Cluttered	50-30-20 cm/s	5 cm/s	2/1	4.479	3.769	0.106	0.137	15.82	1.14	24.500	13.592	
Guardian simulator (Gazebo)	Static	30 cm/s	5 cm/s	2/2	4.710	2.788	0.135	0.134	16.13	0.92	16.432	12.291	
Cluttered dynamic		5 cm/s	5 cm/s	2/2	2.476	1.370	0.017	0.017	17.00	0.92	10.374	12.138	
					3.557	1.800	0.033	0.040	17.61	1.33	14.863	15.898	
					2/1	4.199	2.596	0.048	0.110	17.84	1.23	13.150	14.351
					2/2	2.642	0.463	0.016	0.023	0.0	0.0	5.723	1.868
					2/2	4.961	3.953	0.032	0.084	0.0	0.0	6.365	2.906
					2/2	2.912	0.856	0.020	0.026	25.05	13.30	11.889	9.084
					2/2	6.713	6.380	0.141	0.203	30.39	14.66	25.367	35.724
					2/2	4.593	3.802	0.069	0.072	33.33	9.88	22.217	32.408
					2/2	5.847	5.585	0.105	0.125	34.20	16.64	26.892	35.630

### 5.3.2 Jarvis robot tests

#### 2 5.3.2.1 Rounded path using Jarvis robot at 5 cm/s

Figures 5.8 to 5.18 show the detailed results of the Jarvis robot in the RoboCup field following a rounded path and moving at 5 cm/s.

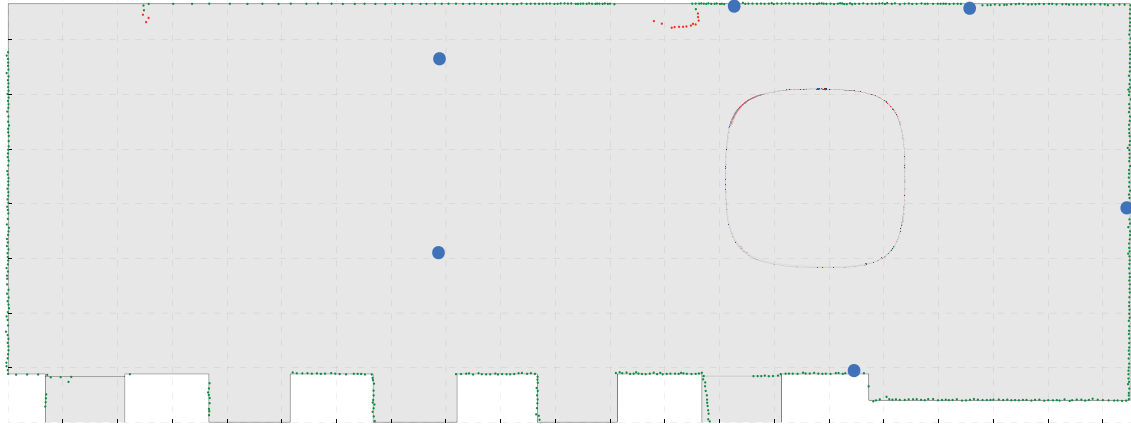


Figure 5.8: Paths from ground truth (green), localization system (blue) and odometry (red)

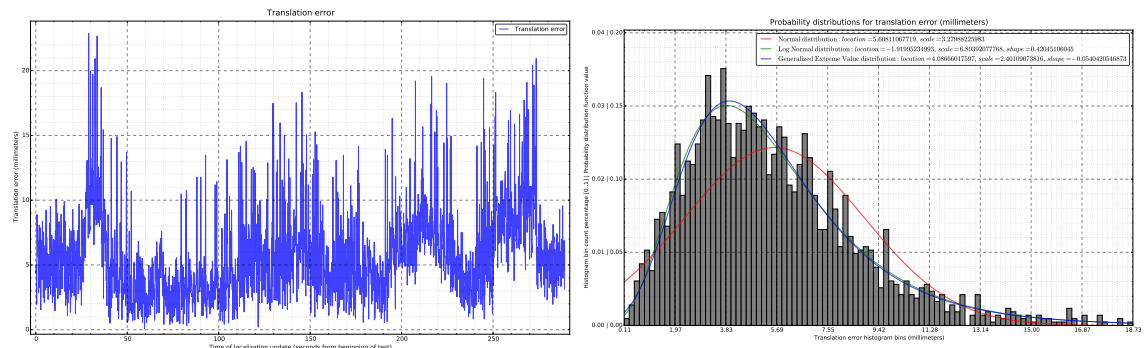


Figure 5.9: Localization system translation error (left) and its statistical distributions (right)

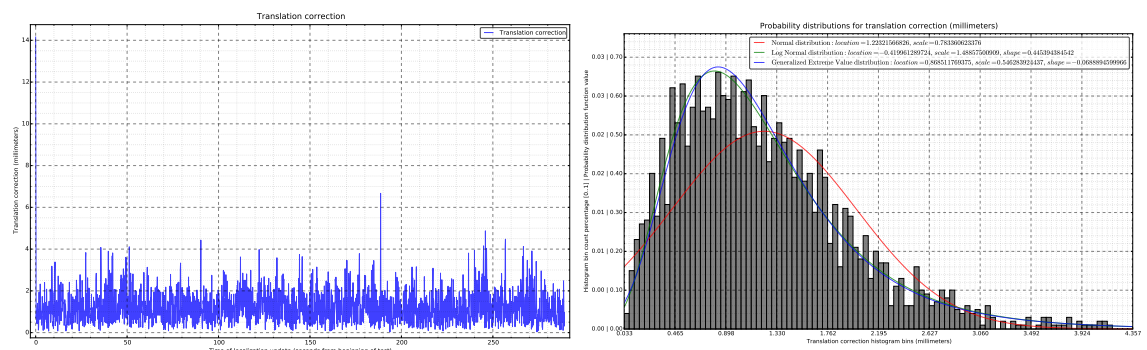


Figure 5.10: Localization system translation corrections (left) and its statistical distributions (right)

## Localization system evaluation

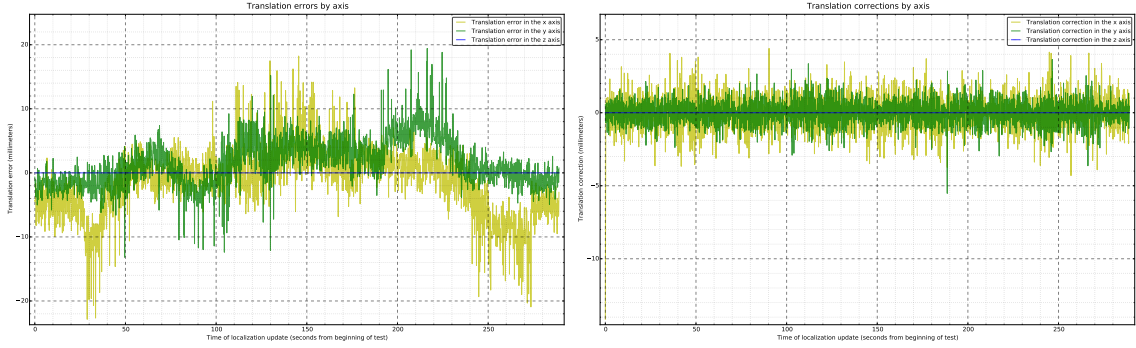


Figure 5.11: Localization system translation error (left) and corrections (right) components

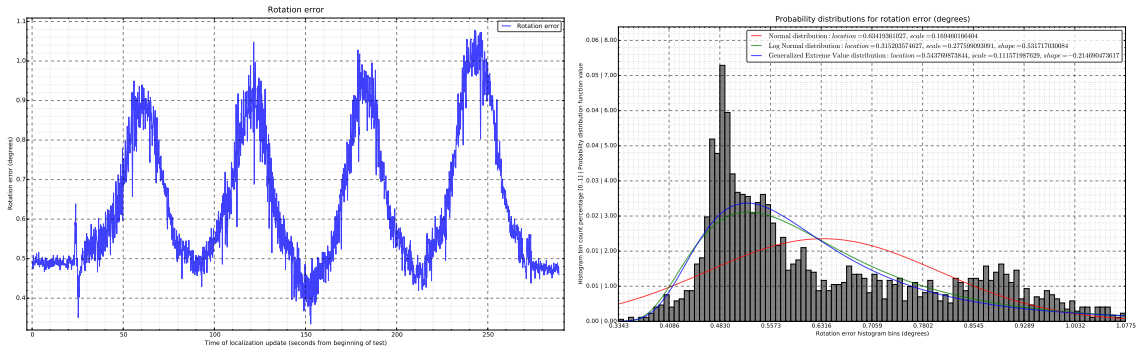


Figure 5.12: Localization system rotation error (left) and its statistical distributions (right)

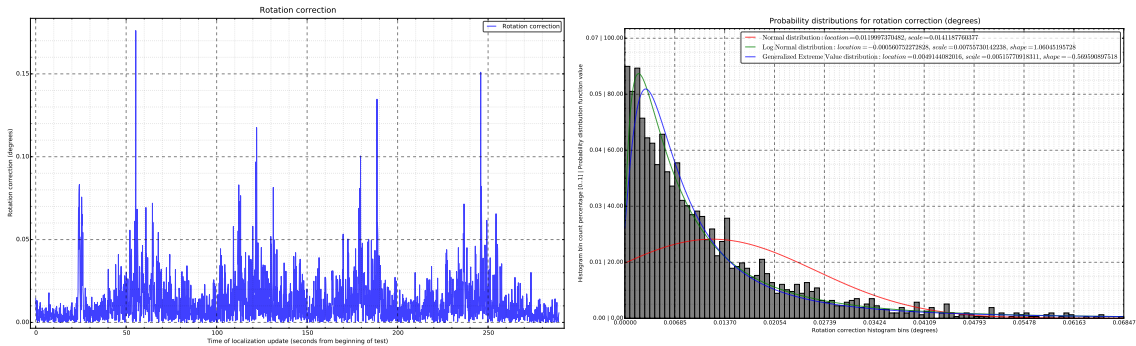


Figure 5.13: Localization system rotation corrections (left) and its statistical distributions (right)

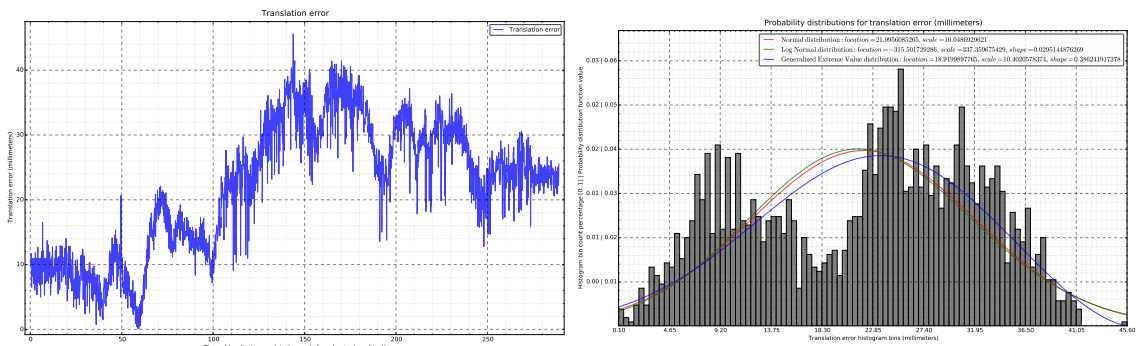


Figure 5.14: Odometry translation error (left) and its statistical distributions (right)

## Localization system evaluation

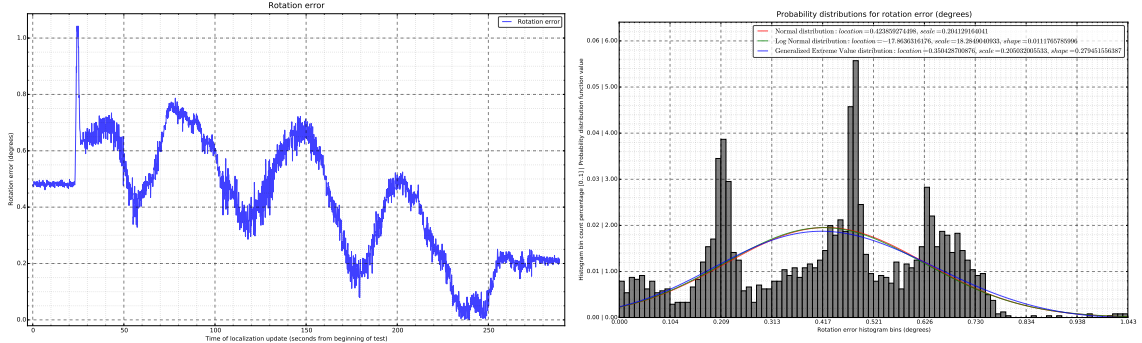


Figure 5.15: Odometry rotation error (left) and its statistical distributions (right)

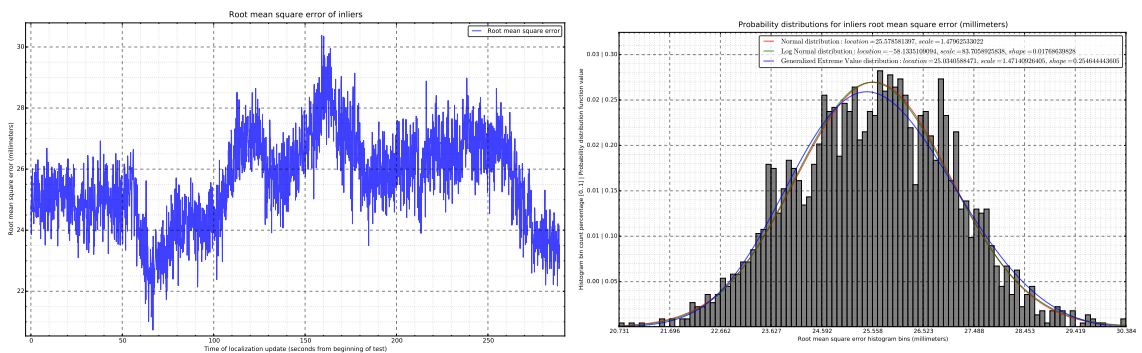


Figure 5.16: Localization system inliers RMSE (left) and its statistical distributions (right)

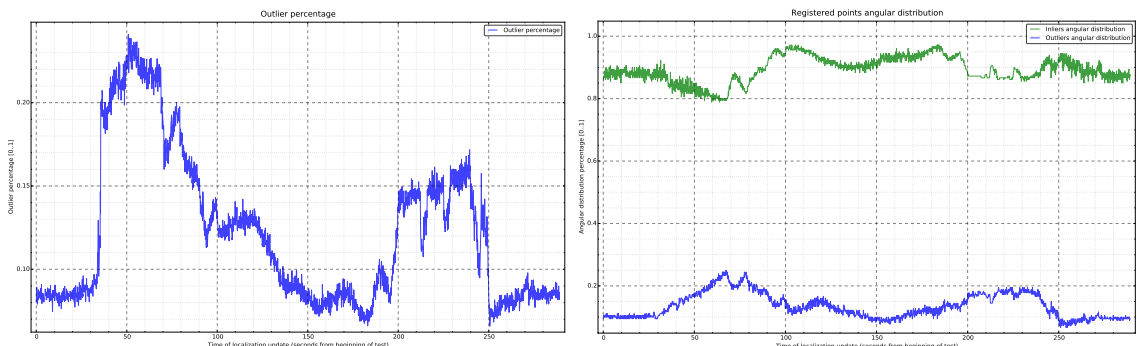


Figure 5.17: Cloud registration outlier percentage (left) and inliers angular distribution (right)

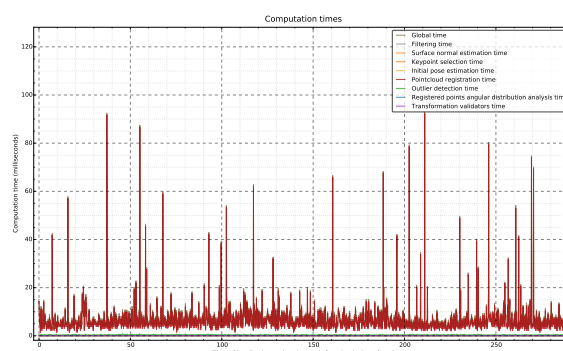


Figure 5.18: Localization system computation times

## Localization system evaluation

### 5.3.2.2 Complex path using Jarvis robot at 5 cm/s

Figures 5.19 to 5.29 show the detailed results of the Jarvis robot in the RoboCup field following a complex path and moving at 5 cm/s.

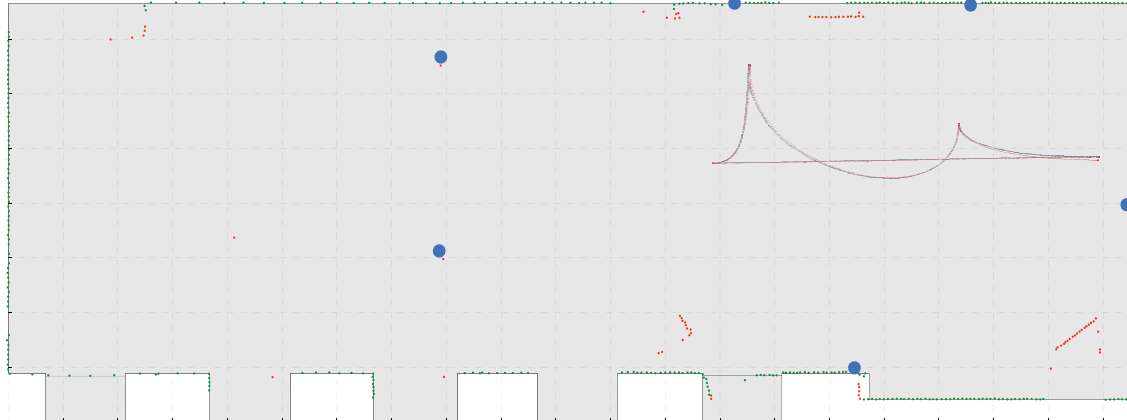


Figure 5.19: Paths from ground truth (green), localization system (blue) and odometry (red)

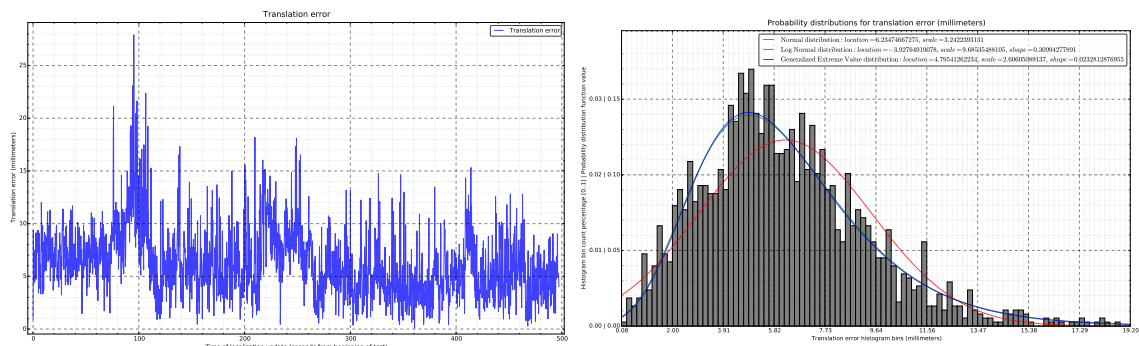


Figure 5.20: Localization system translation error (left) and its statistical distributions (right)

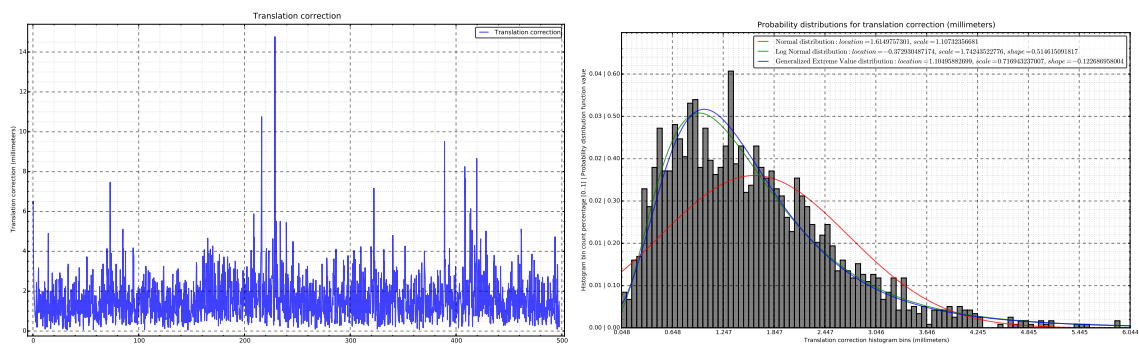


Figure 5.21: Localization system translation corrections (left) and its statistical distributions (right)

## Localization system evaluation

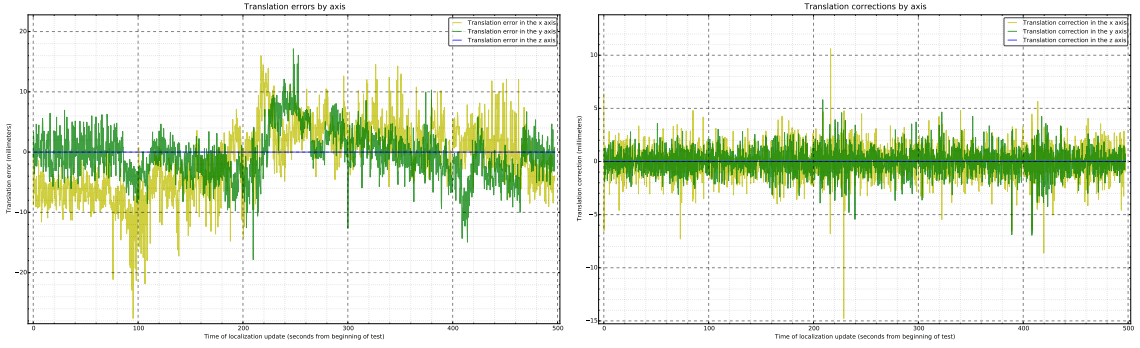


Figure 5.22: Localization system translation error (left) and corrections (right) components

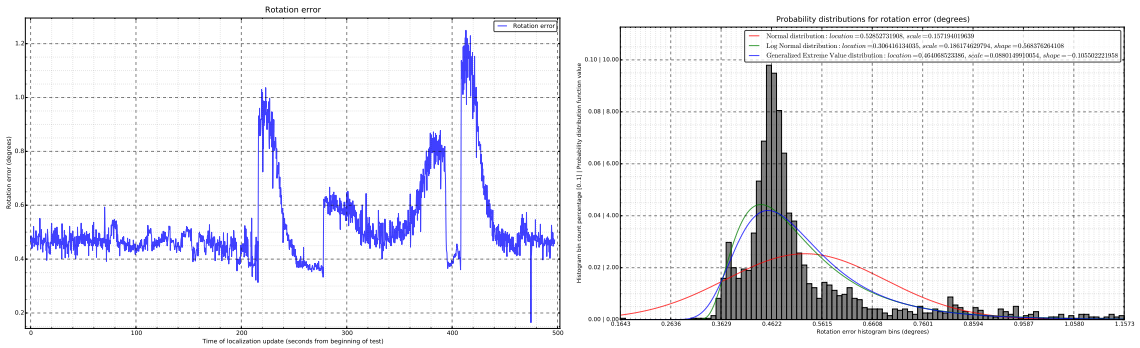


Figure 5.23: Localization system rotation error (left) and its statistical distributions (right)

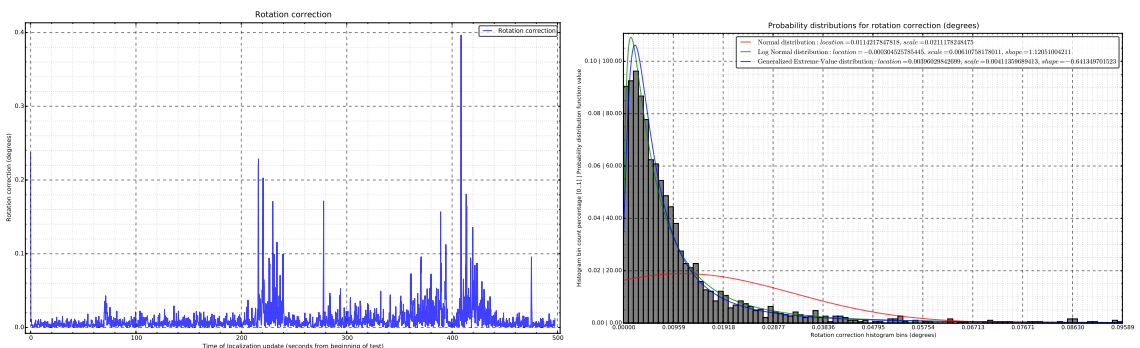


Figure 5.24: Localization system rotation corrections (left) and its statistical distributions (right)

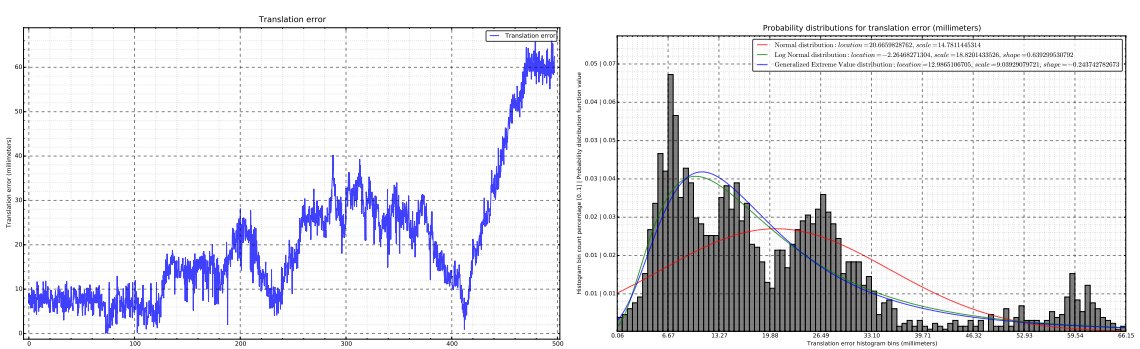


Figure 5.25: Odometry translation error (left) and its statistical distributions (right)

## Localization system evaluation

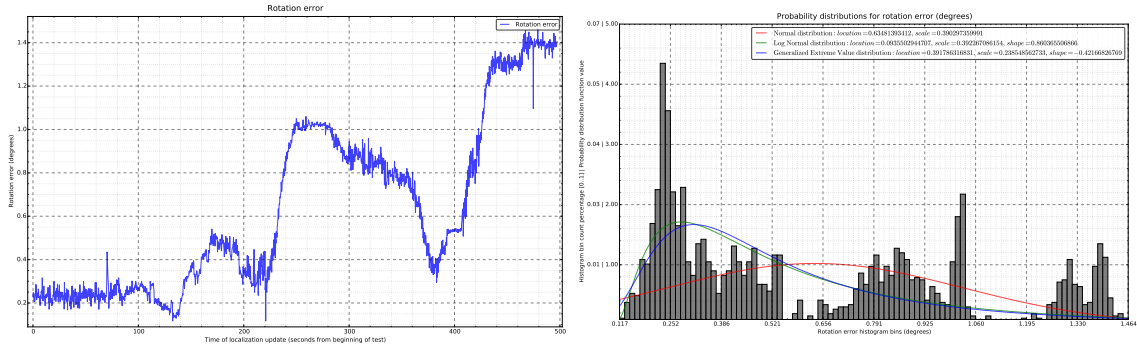


Figure 5.26: Odometry rotation error (left) and its statistical distributions (right)

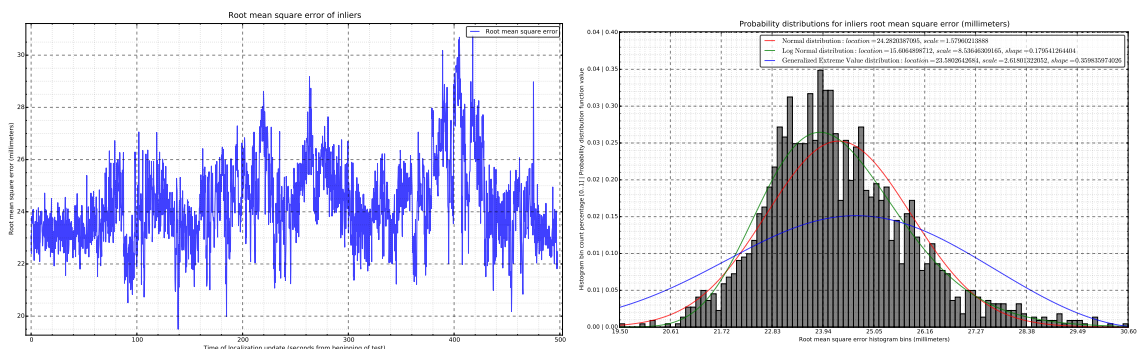


Figure 5.27: Localization system inliers RMSE (left) and its statistical distributions (right)

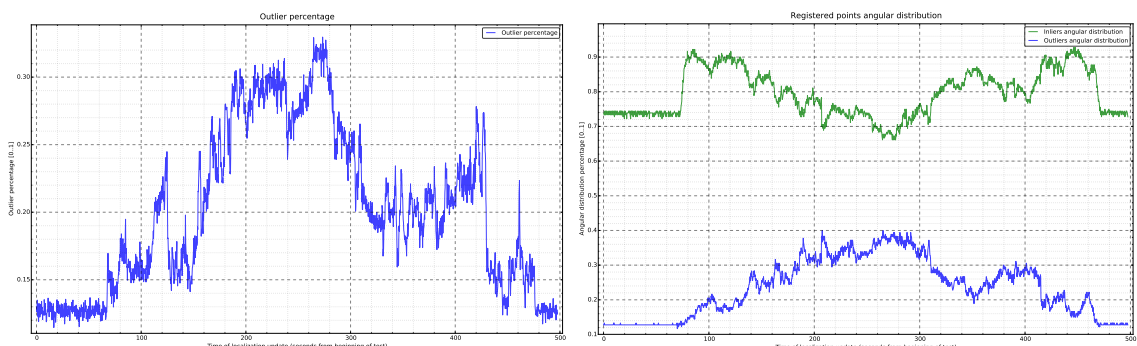


Figure 5.28: Cloud registration outlier percentage (left) and inliers angular distribution (right)

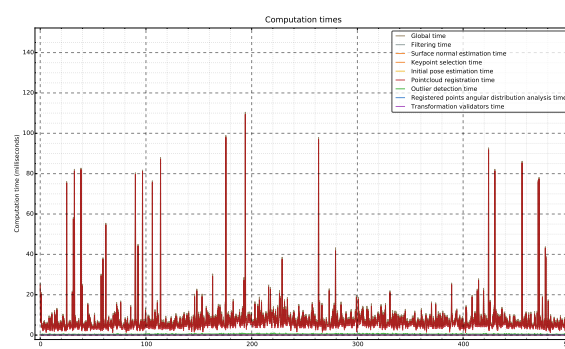


Figure 5.29: Localization system computation times

### 5.3.3 Jarvis simulator tests

#### 2 5.3.3.1 Rounded path using Jarvis simulator at 5 cm/s

Figures 5.30 to 5.36 show the results of the Jarvis platform using the Stage simulator in the RoboCup field map following a rounded path and moving at 5 cm/s.

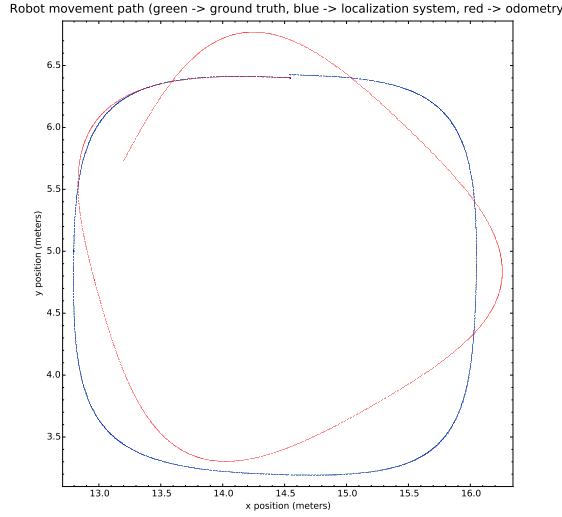


Figure 5.30: Paths from ground truth (green), localization system (blue) and odometry (red)

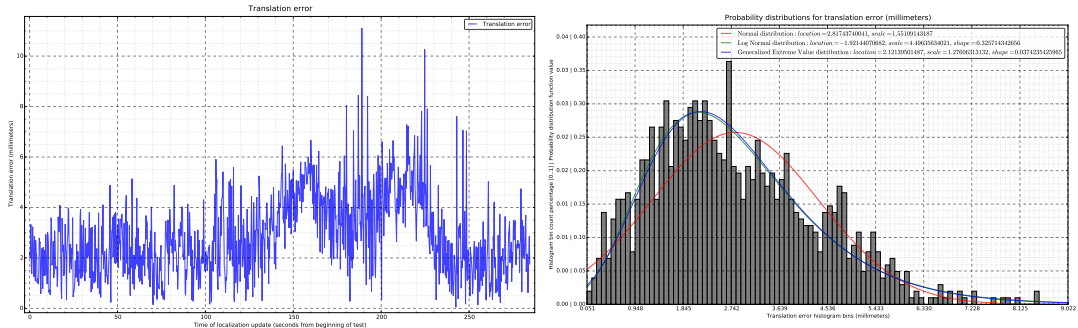


Figure 5.31: Localization system translation error (left) and its statistical distributions (right)

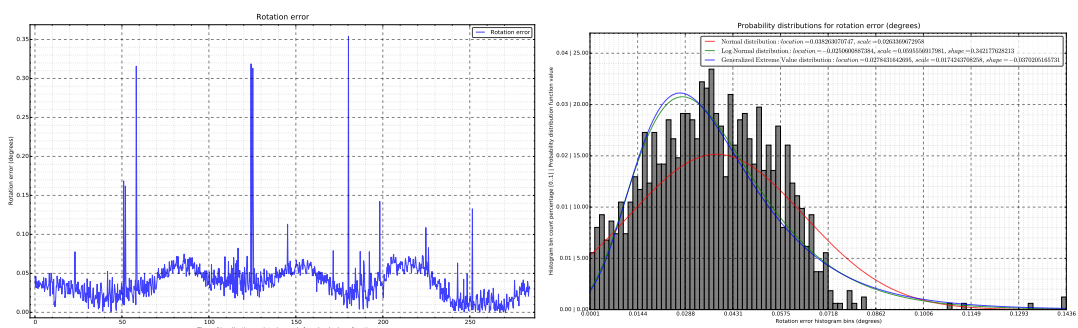


Figure 5.32: Localization system rotation error (left) and its statistical distributions (right)

## Localization system evaluation

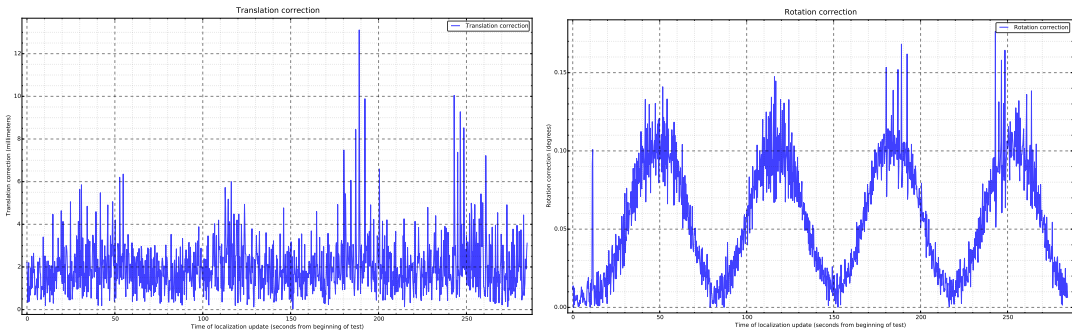


Figure 5.33: Localization system translation (left) and rotation (right) corrections

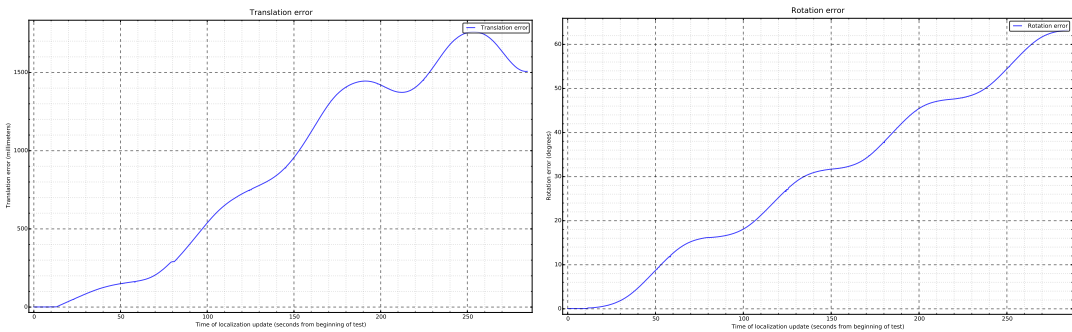


Figure 5.34: Odometry translation (left) and rotation (right) error

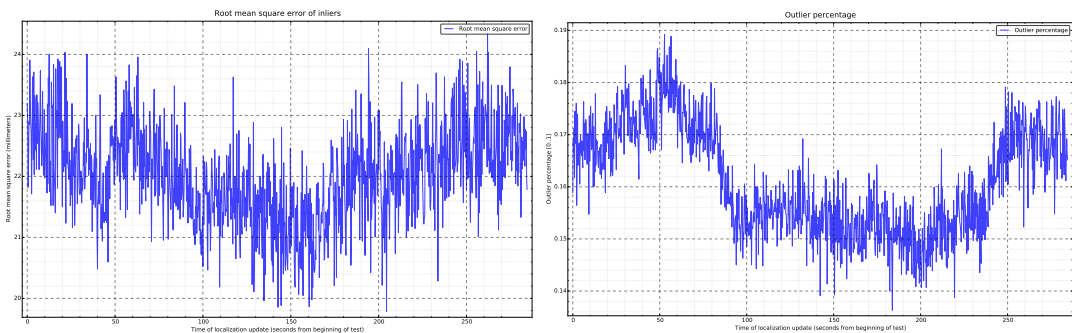


Figure 5.35: Localization system inliers root mean square error (left) and outlier percentage (right)

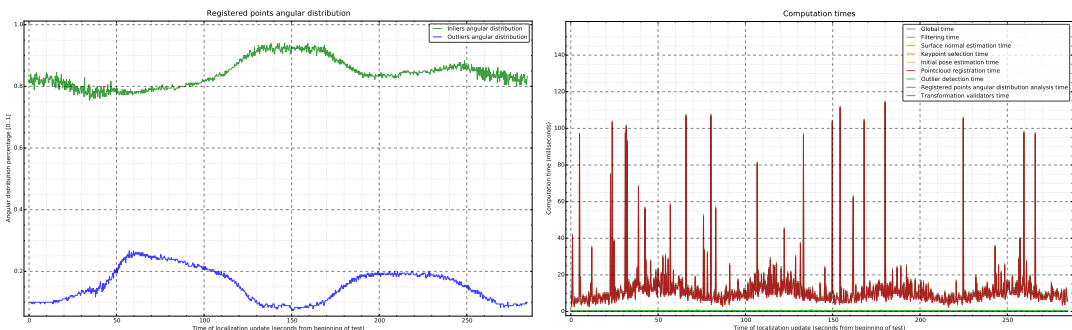


Figure 5.36: Cloud registration outlier percentage (left) and inliers angular distribution (right)

### 5.3.3.2 Rounded path using Jarvis simulator at 50 cm/s

- 2 Figures 5.37 to 5.43 show the results of the Jarvis platform using the Stage simulator in the RoboCup field map following a rounded path and moving at 50 cm/s.

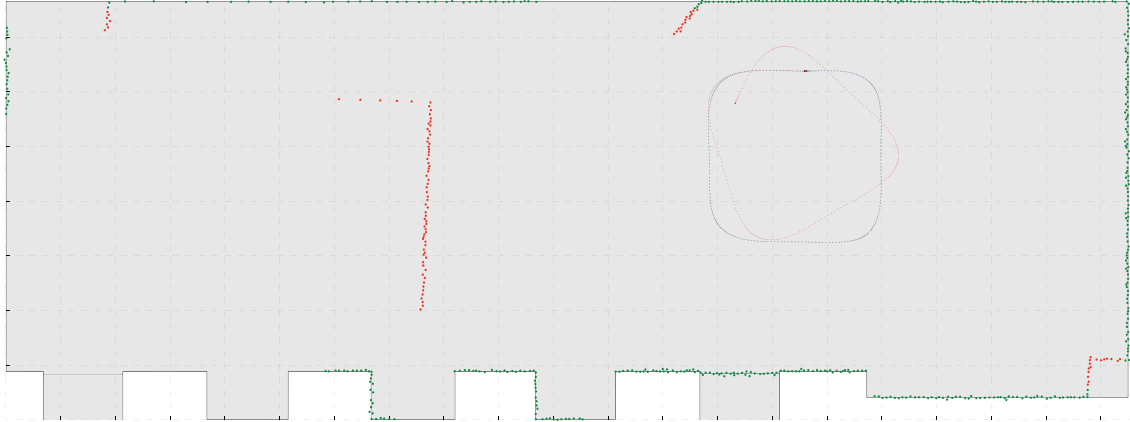


Figure 5.37: Paths from ground truth (green), localization system (blue) and odometry (red)

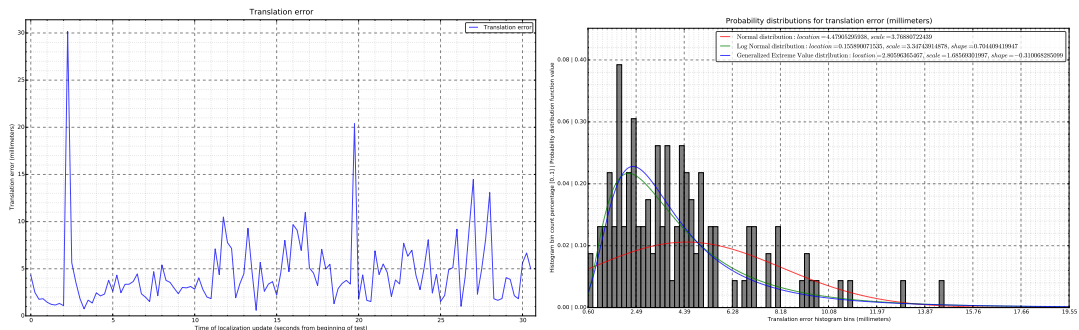


Figure 5.38: Localization system translation error (left) and its statistical distributions (right)

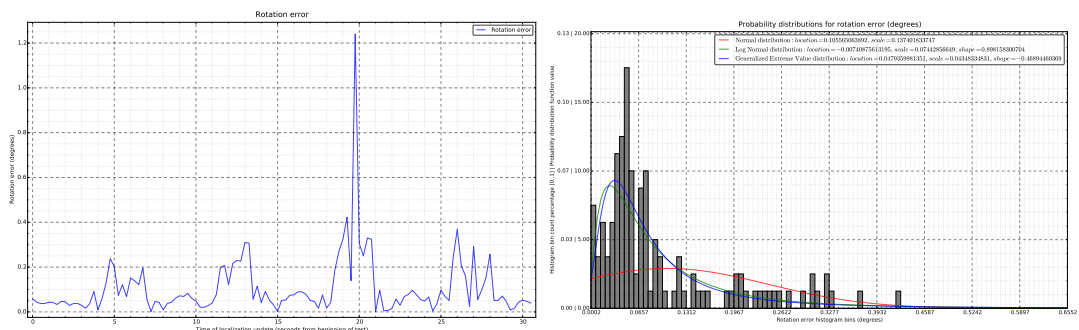


Figure 5.39: Localization system rotation error (left) and its statistical distributions (right)

## Localization system evaluation

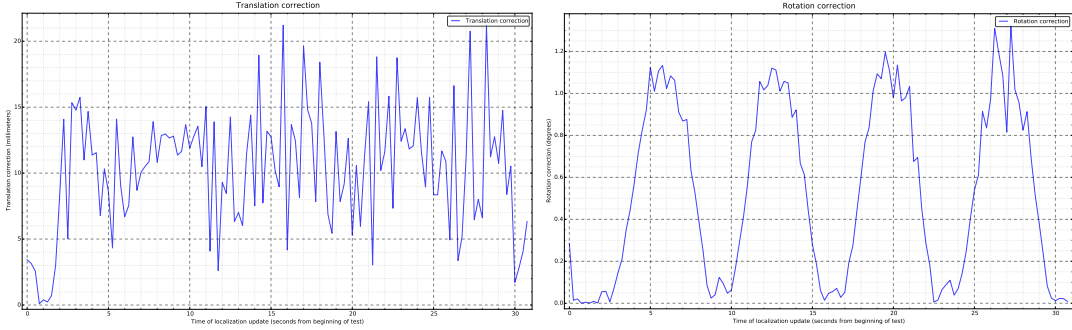


Figure 5.40: Localization system translation (left) and rotation (right) corrections

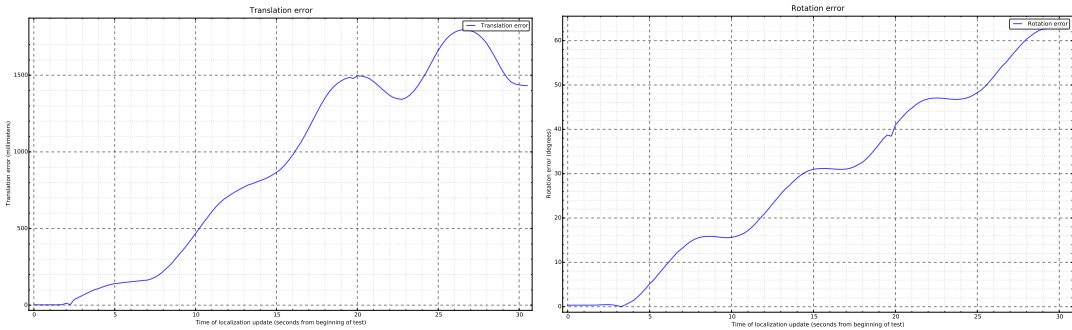


Figure 5.41: Odometry translation (left) and rotation (right) error

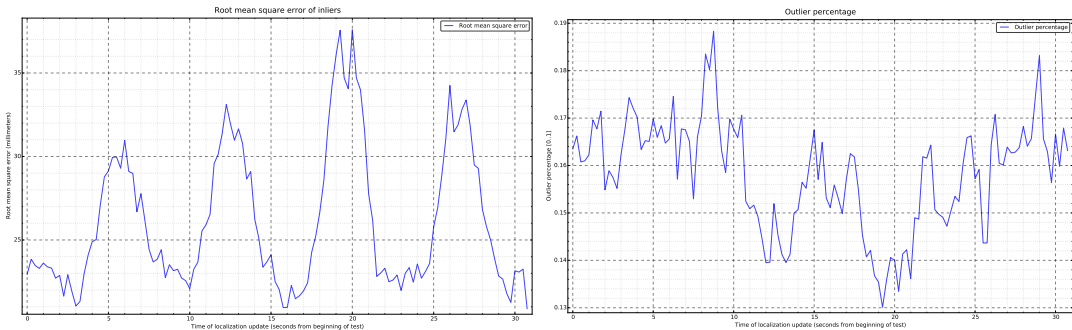


Figure 5.42: Localization system inliers root mean square error (left) and outlier percentage (right)

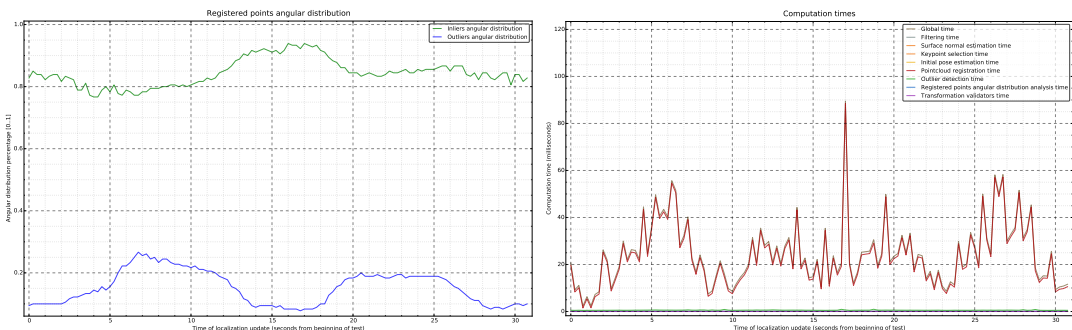


Figure 5.43: Cloud registration outlier percentage (left) and inliers angular distribution (right)

### 5.3.3.3 Rounded path using Jarvis simulator at 100 cm/s

- 2 Figures 5.44 to 5.50 show the results of the Jarvis platform using the Stage simulator in the RoboCup field map following a rounded path and moving at 100 cm/s.

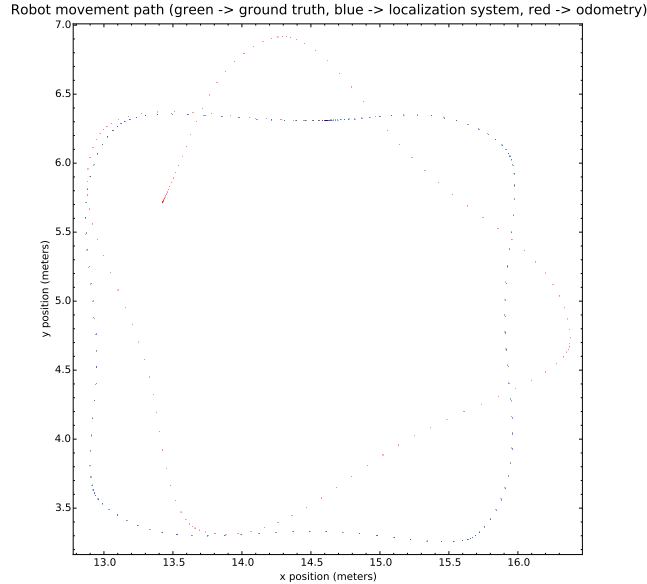


Figure 5.44: Paths from ground truth (green), localization system (blue) and odometry (red)

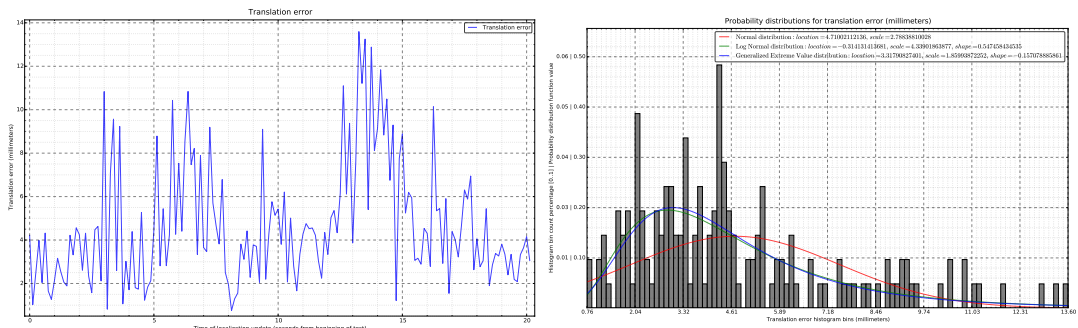


Figure 5.45: Localization system translation error (left) and its statistical distributions (right)

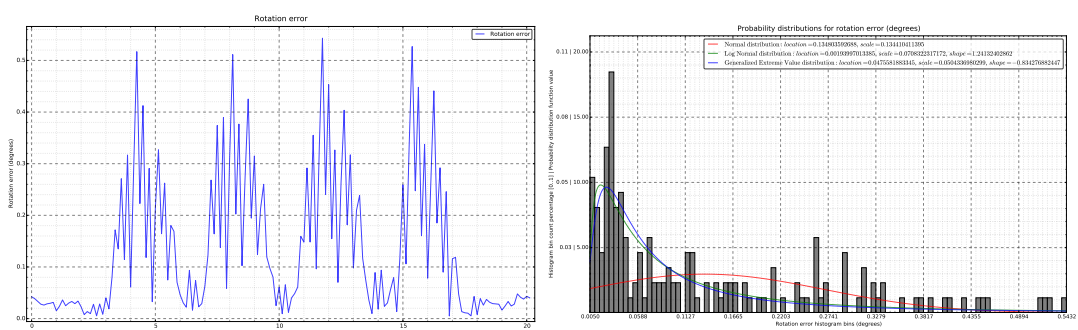


Figure 5.46: Localization system rotation error (left) and its statistical distributions (right)

## Localization system evaluation

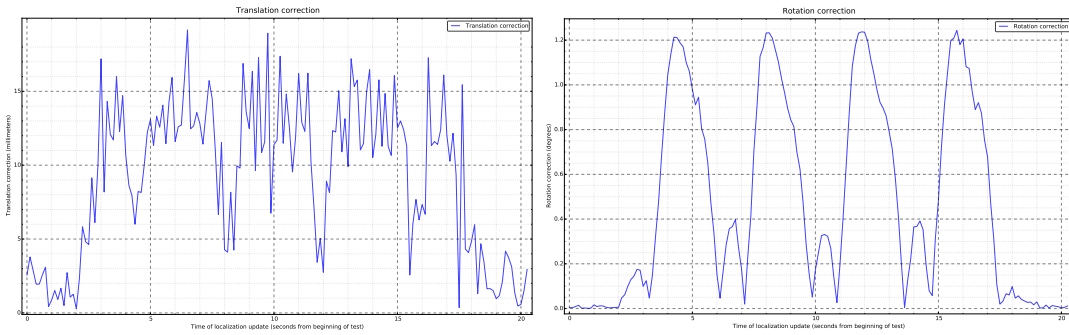


Figure 5.47: Localization system translation (left) and rotation (right) corrections

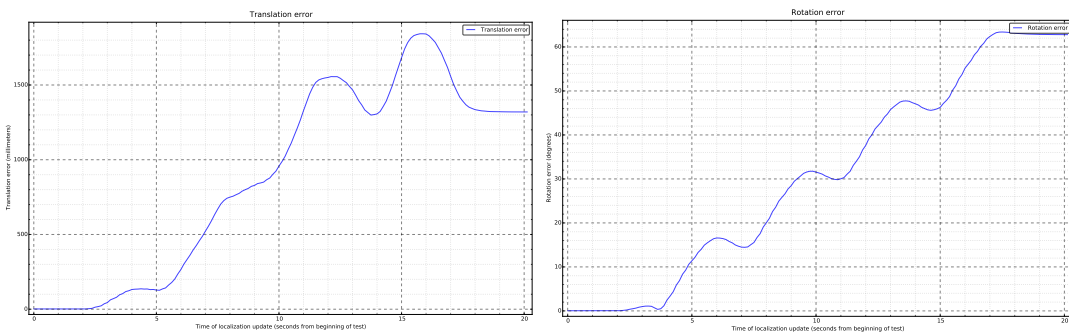


Figure 5.48: Odometry translation (left) and rotation (right) error

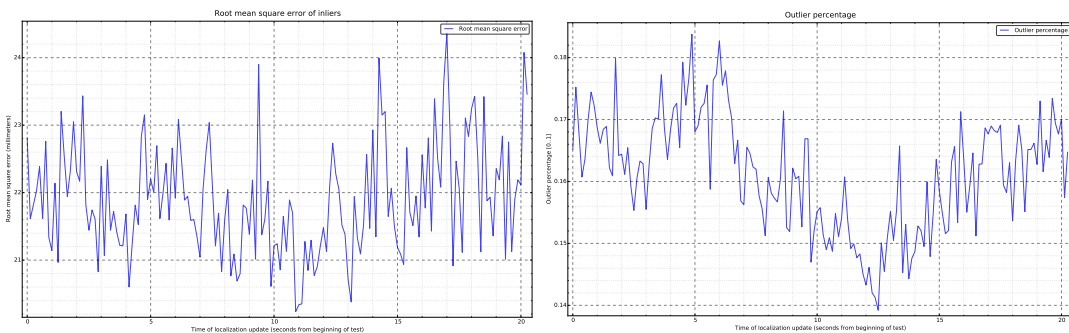


Figure 5.49: Localization system inliers root mean square error (left) and outlier percentage (right)

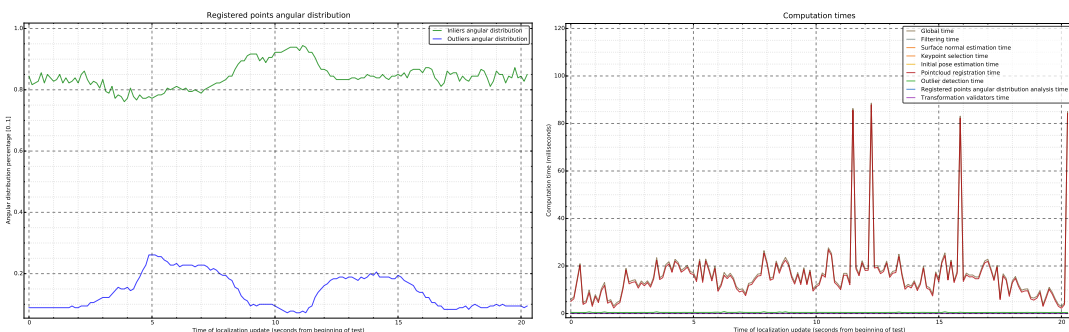


Figure 5.50: Cloud registration outlier percentage (left) and inliers angular distribution (right)

## Localization system evaluation

### 5.3.3.4 Complex path using Jarvis simulator at 5 cm/s

- 2 Figures 5.51 to 5.57 show the results of the Jarvis platform using the Stage simulator in the RoboCup field map following a complex path and moving at 5 cm/s.

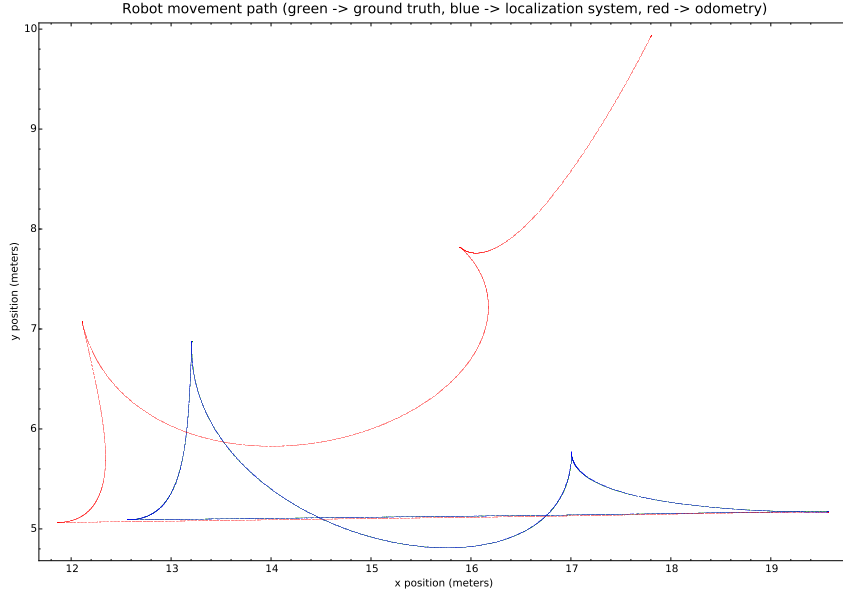


Figure 5.51: Paths from ground truth (green), localization system (blue) and odometry (red)

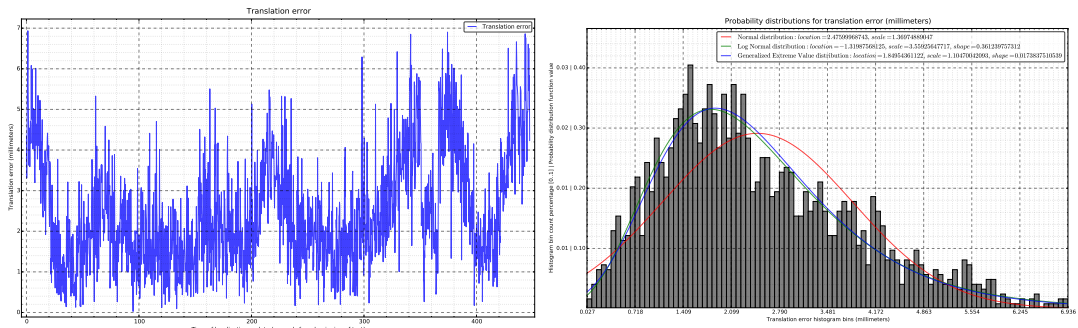


Figure 5.52: Localization system translation error (left) and its statistical distributions (right)

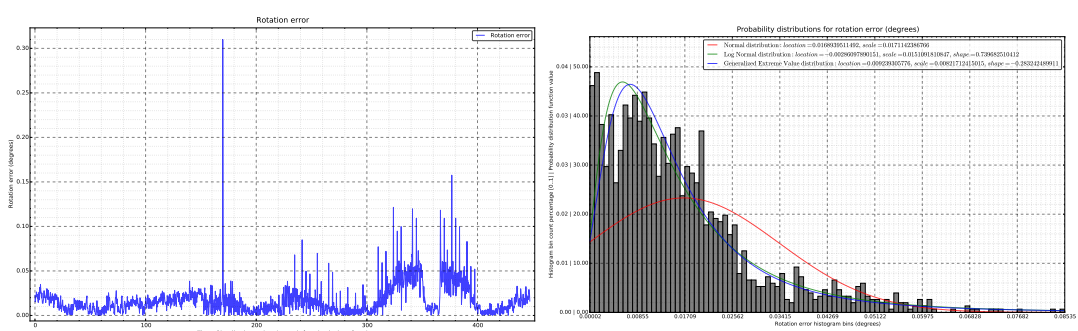


Figure 5.53: Localization system rotation error (left) and its statistical distributions (right)

## Localization system evaluation

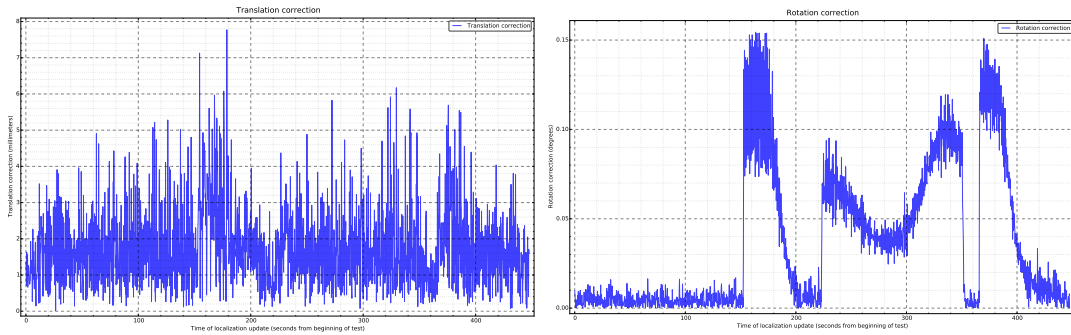


Figure 5.54: Localization system translation (left) and rotation (right) corrections

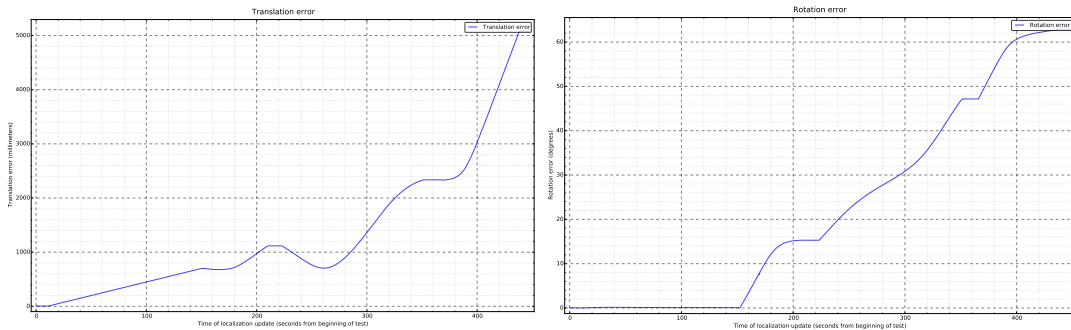


Figure 5.55: Odometry translation (left) and rotation (right) error

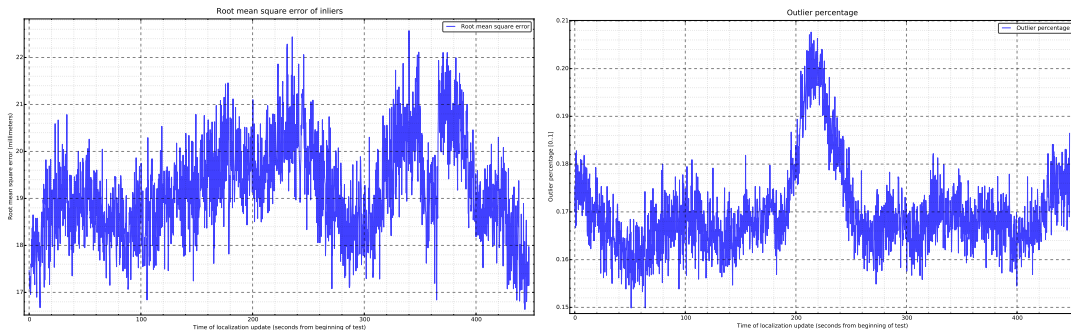


Figure 5.56: Localization system inliers root mean square error (left) and outlier percentage (right)

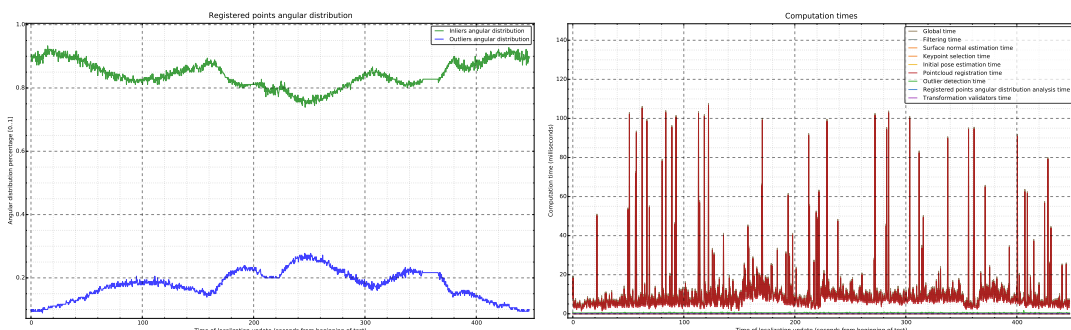


Figure 5.57: Cloud registration outlier percentage (left) and inliers angular distribution (right)

## Localization system evaluation

### 5.3.3.5 Complex path using Jarvis simulator at 50-30-50-20 cm/s

- 2 Figures 5.58 to 5.64 show the results of the Jarvis platform using the Stage simulator in the RoboCup field map following a complex path and moving at 50-30-50-20 cm/s.

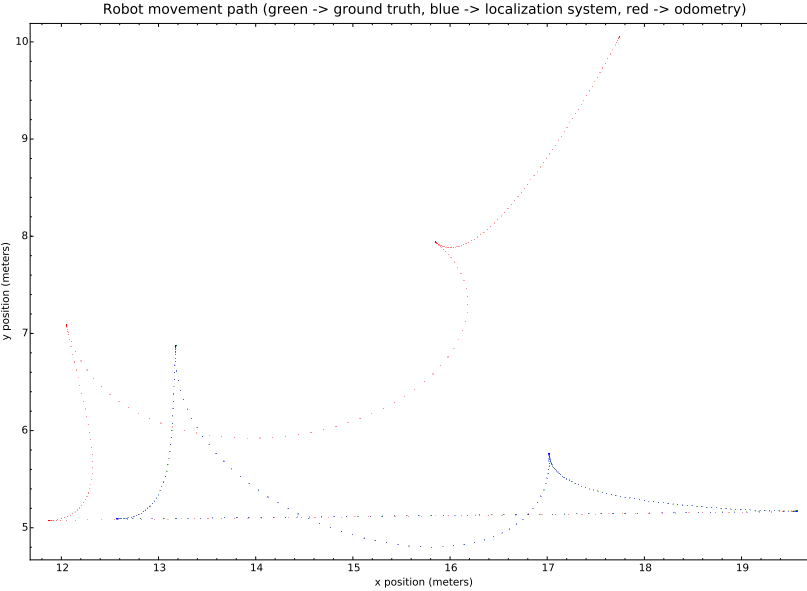


Figure 5.58: Paths from ground truth (green), localization system (blue) and odometry (red)

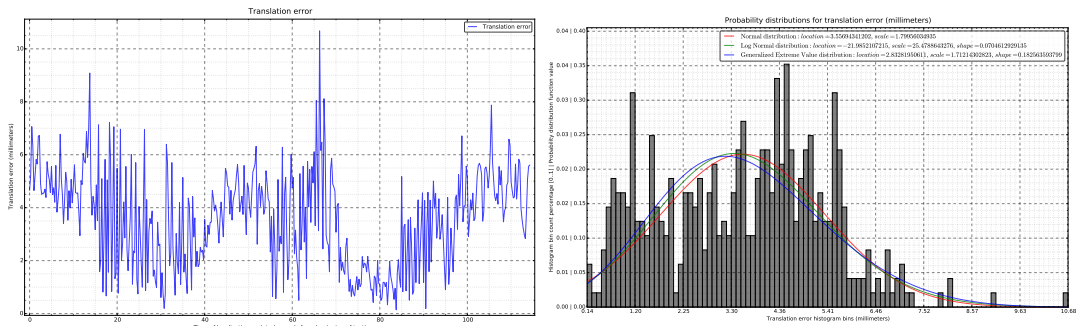


Figure 5.59: Localization system translation error (left) and its statistical distributions (right)

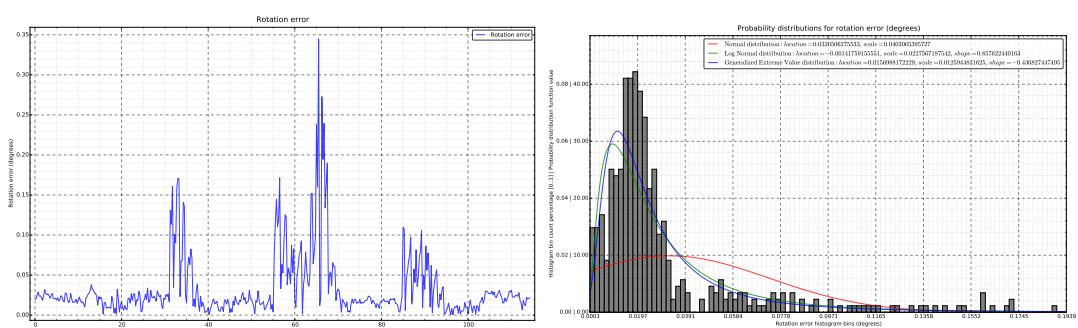


Figure 5.60: Localization system rotation error (left) and its statistical distributions (right)

## Localization system evaluation

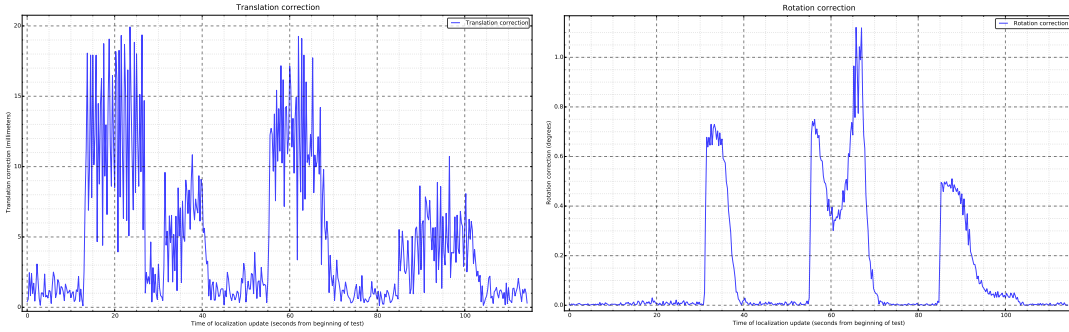


Figure 5.61: Localization system translation (left) and rotation (right) corrections

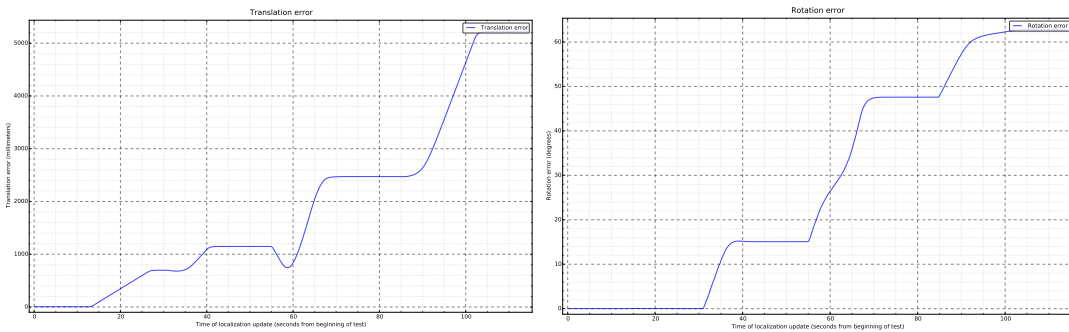


Figure 5.62: Odometry translation (left) and rotation (right) error

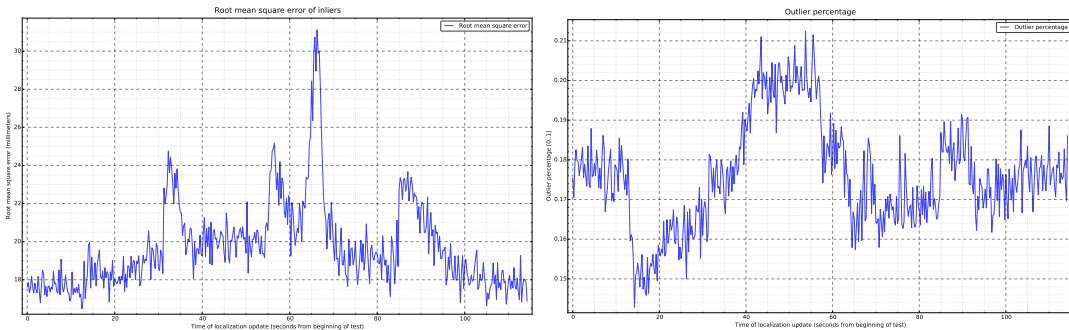


Figure 5.63: Localization system inliers root mean square error (left) and outlier percentage (right)

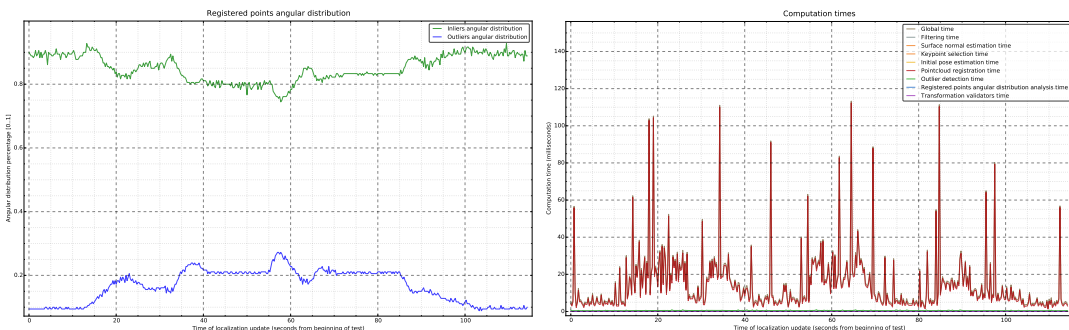


Figure 5.64: Cloud registration outlier percentage (left) and inliers angular distribution (right)

### 5.3.3.6 Complex path using Jarvis simulator at 200-30-200-30 cm/s

- 2 Figures 5.65 to 5.71 show the results of the Jarvis platform using the Stage simulator in the RoboCup field map following a complex path and moving at 200-30-200-30 cm/s.

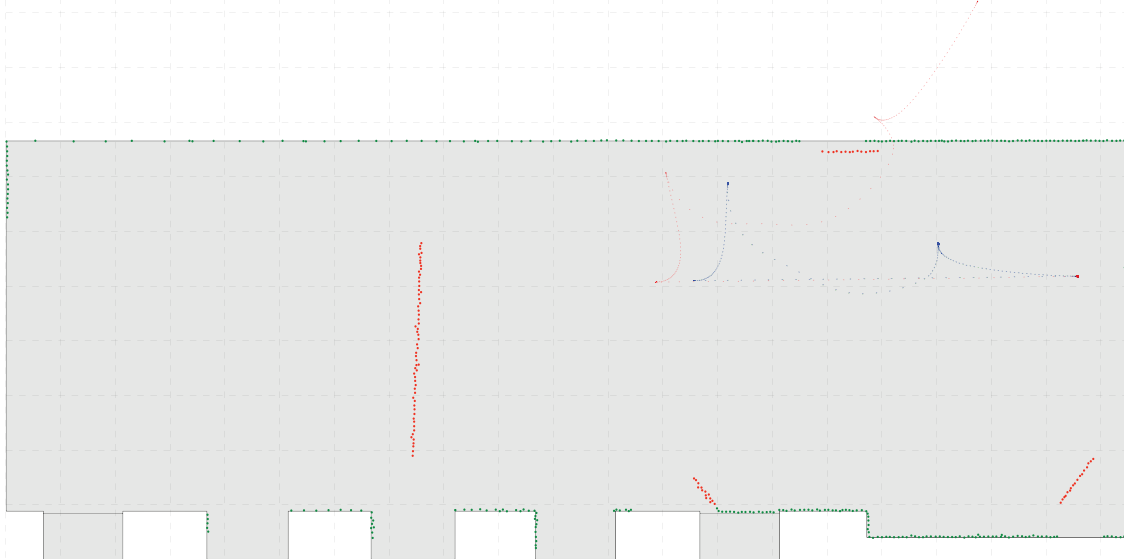


Figure 5.65: Paths from ground truth (green), localization system (blue) and odometry (red)

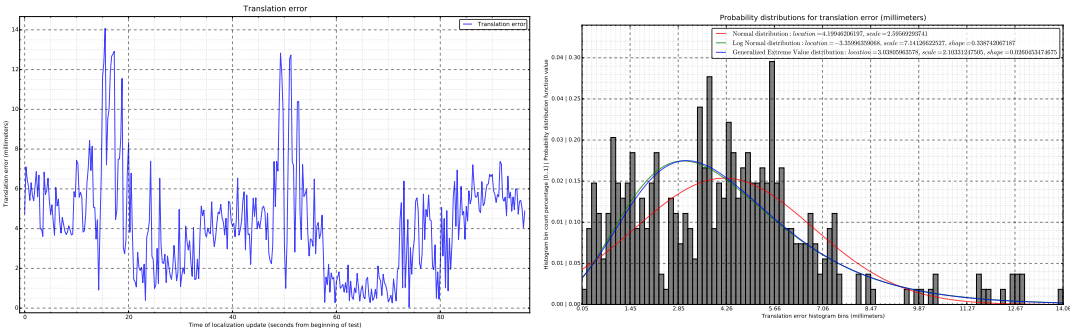


Figure 5.66: Localization system translation error (left) and its statistical distributions (right)

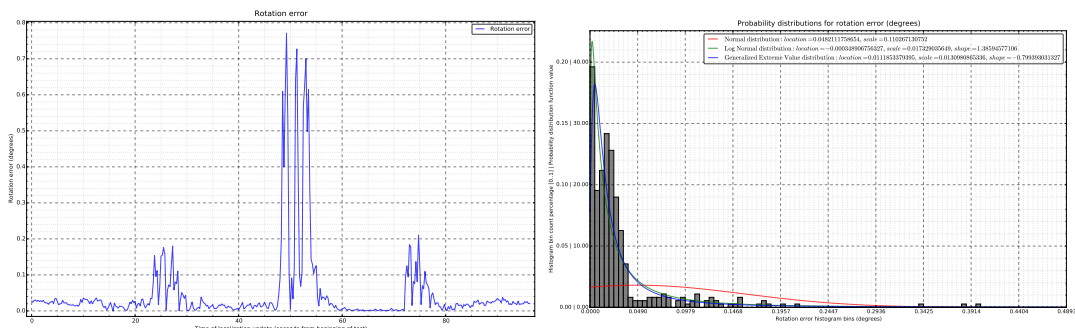


Figure 5.67: Localization system rotation error (left) and its statistical distributions (right)

## Localization system evaluation

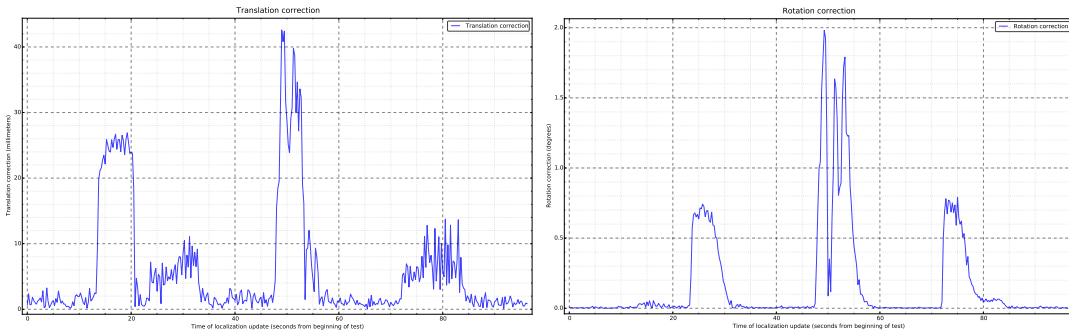


Figure 5.68: Localization system translation (left) and rotation (right) corrections

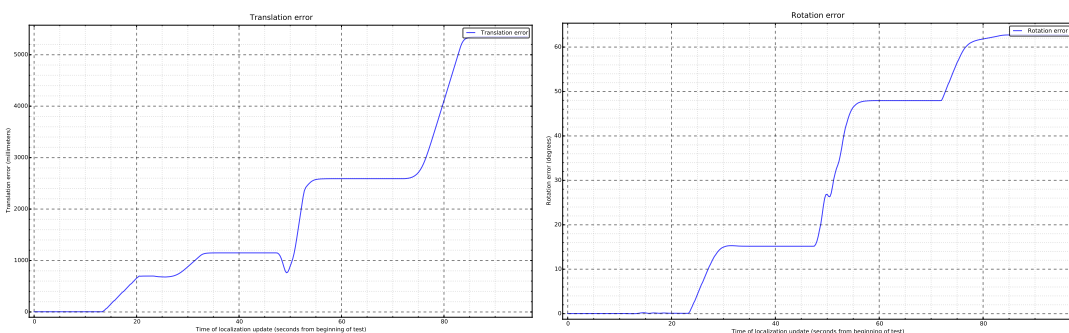


Figure 5.69: Odometry translation (left) and rotation (right) error

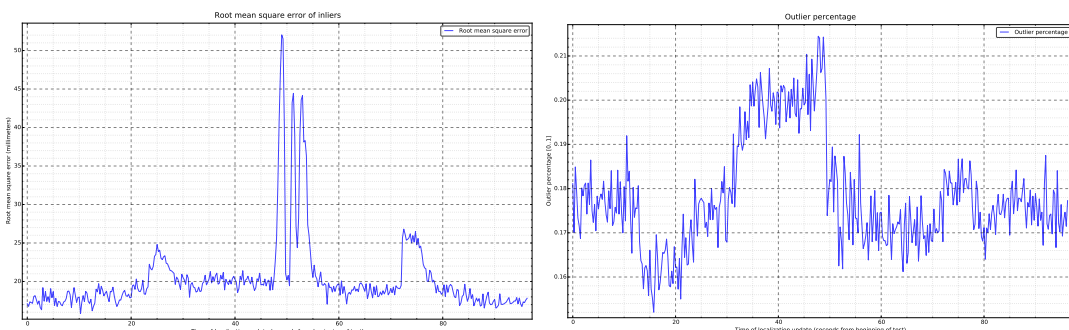


Figure 5.70: Localization system inliers root mean square error (left) and outlier percentage (right)

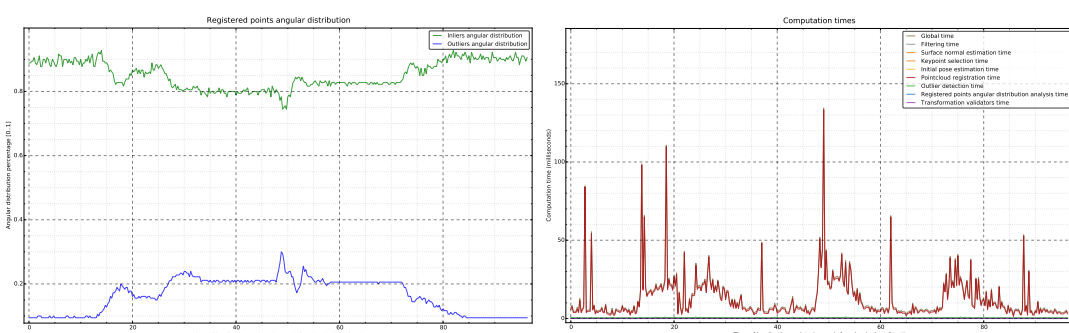


Figure 5.71: Cloud registration outlier percentage (left) and inliers angular distribution (right)

### 5.3.4 Guardian simulator tests

#### 2 5.3.4.1 Wall follower path using Guardian simulator at 5 cm/s in static environment

Figures 5.72 to 5.78 show the results of the Guardian platform using the Gazebo simulator following the lower and right wall in the static structured environment world at 5 cm/s.

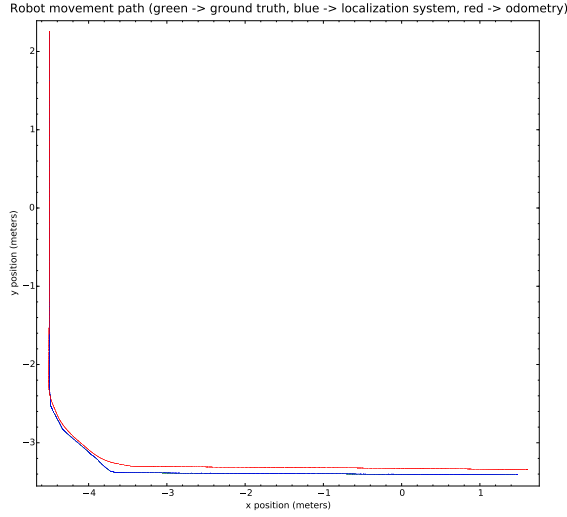


Figure 5.72: Paths from ground truth (green), localization system (blue) and odometry (red)

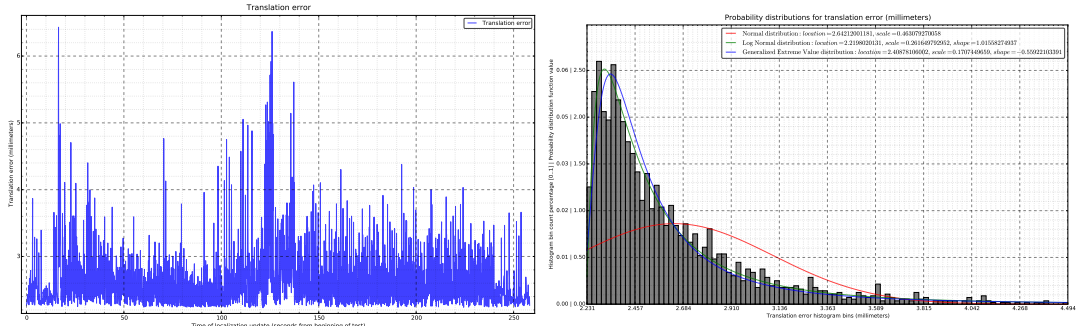


Figure 5.73: Localization system translation error (left) and its statistical distributions (right)

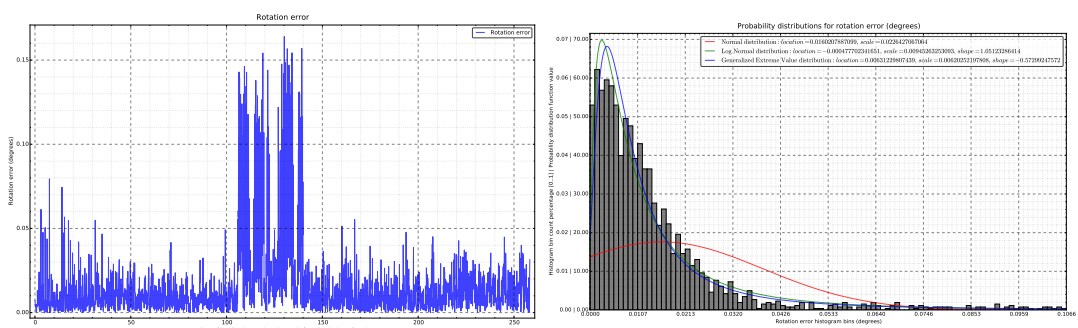


Figure 5.74: Localization system rotation error (left) and its statistical distributions (right)

## Localization system evaluation

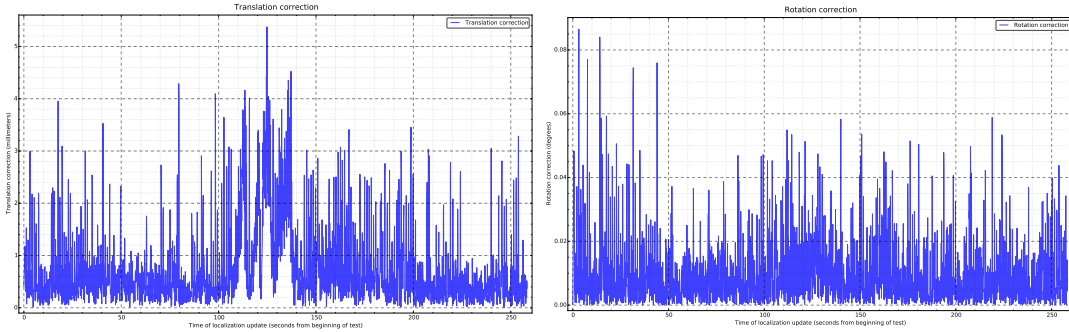


Figure 5.75: Localization system translation (left) and rotation (right) corrections

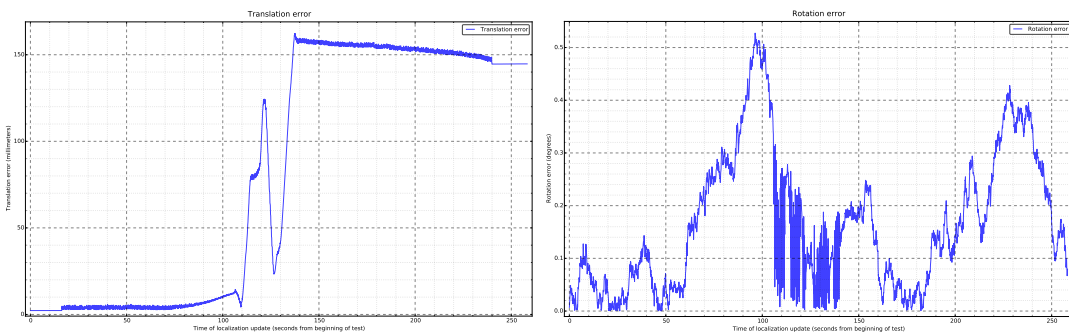


Figure 5.76: Odometry translation (left) and rotation (right) error

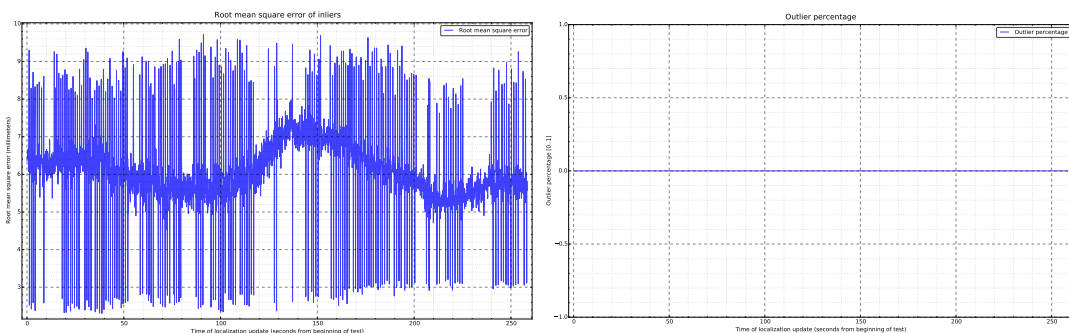


Figure 5.77: Localization system inliers root mean square error (left) and outlier percentage (right)

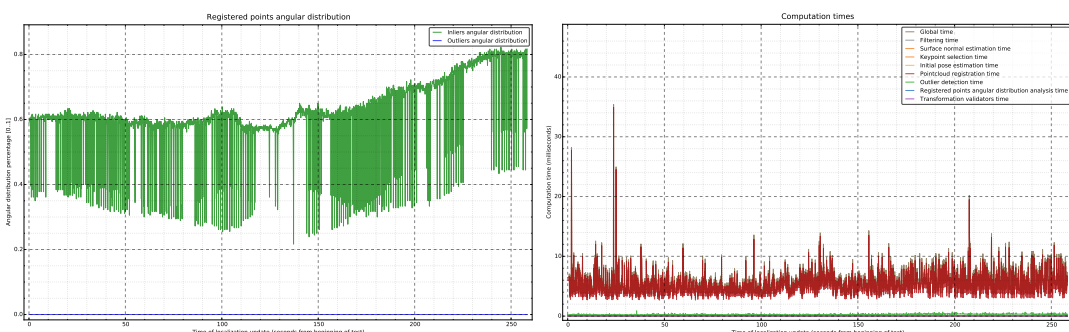


Figure 5.78: Cloud registration outlier percentage (left) and inliers angular distribution (right)

### 5.3.4.2 Wall follower path using Guardian simulator at 30 cm/s in static environment

- 2 Figures 5.79 to 5.85 show the results of the Guardian platform using the Gazebo simulator following the lower and right wall in the static structured environment world at 30 cm/s.

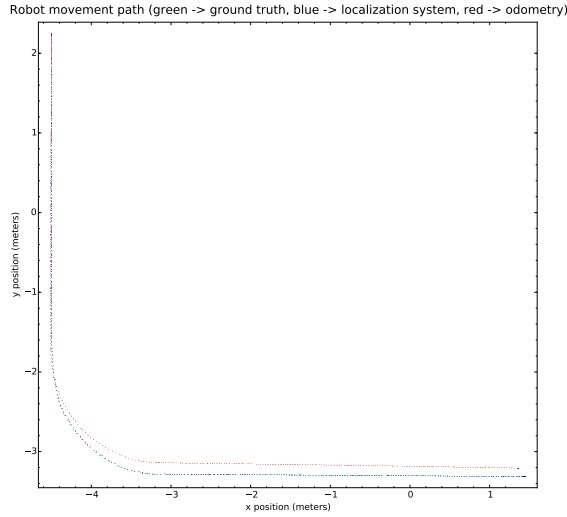


Figure 5.79: Paths from ground truth (green), localization system (blue) and odometry (red)

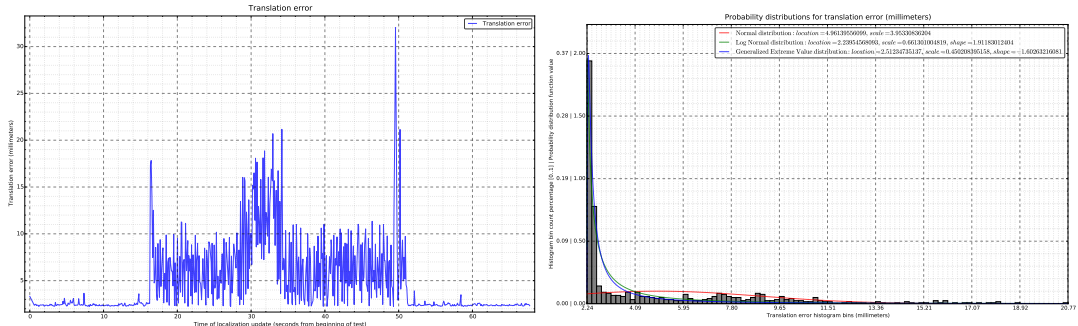


Figure 5.80: Localization system translation error (left) and its statistical distributions (right)

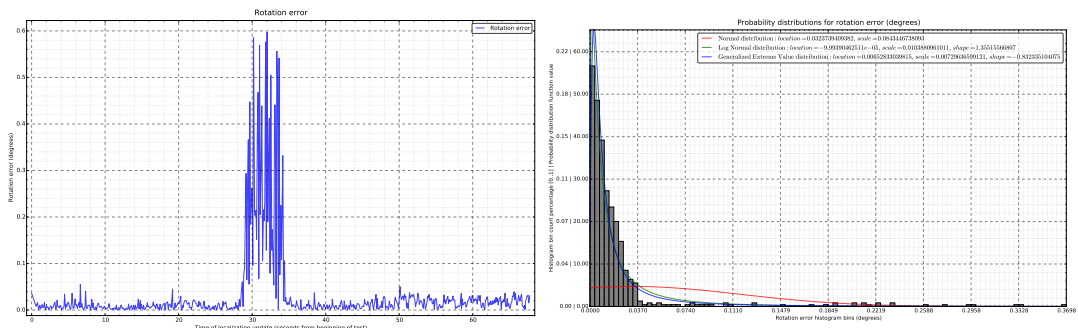


Figure 5.81: Localization system rotation error (left) and its statistical distributions (right)

## Localization system evaluation

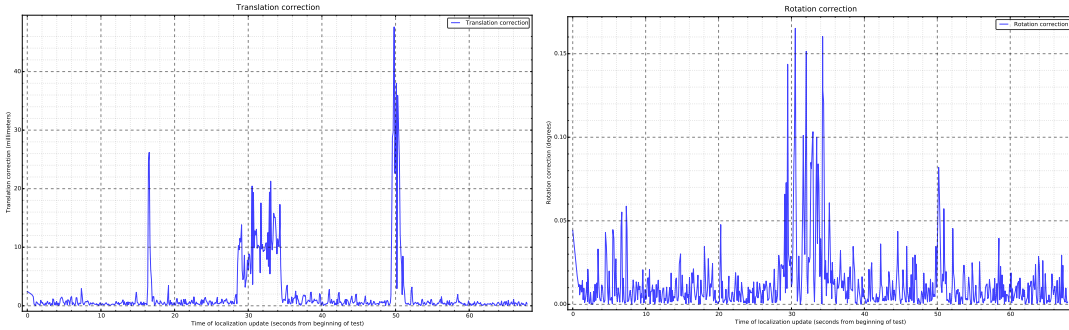


Figure 5.82: Localization system translation (left) and rotation (right) corrections

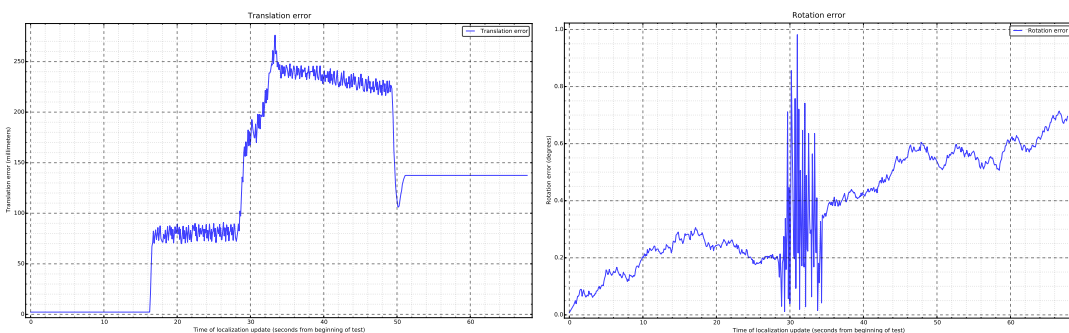


Figure 5.83: Odometry translation (left) and rotation (right) error

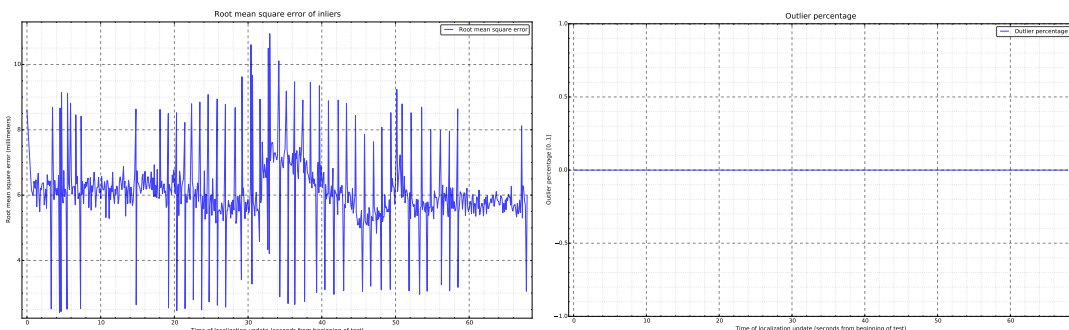


Figure 5.84: Localization system inliers root mean square error (left) and outlier percentage (right)

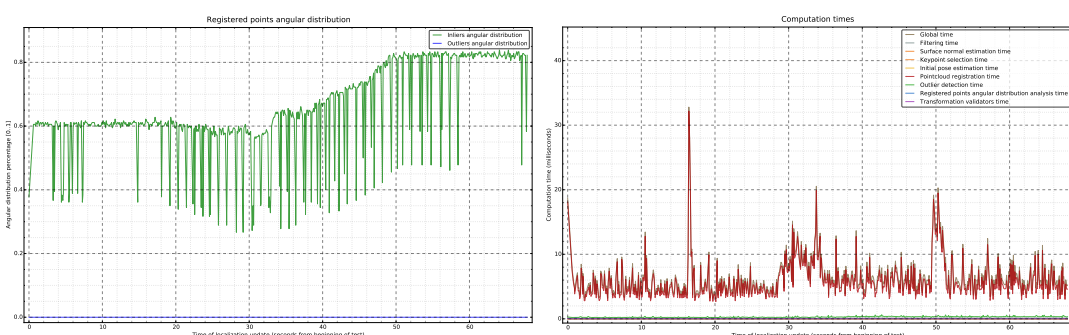


Figure 5.85: Cloud registration outlier percentage (left) and inliers angular distribution (right)

### 5.3.4.3 Wall follower path using Guardian simulator at 5 cm/s in static cluttered environment

2

Figures 5.86 to 5.92 show the results of the Guardian platform using the Gazebo simulator following the lower and right wall in the static cluttered structured environment world at 5 cm/s.

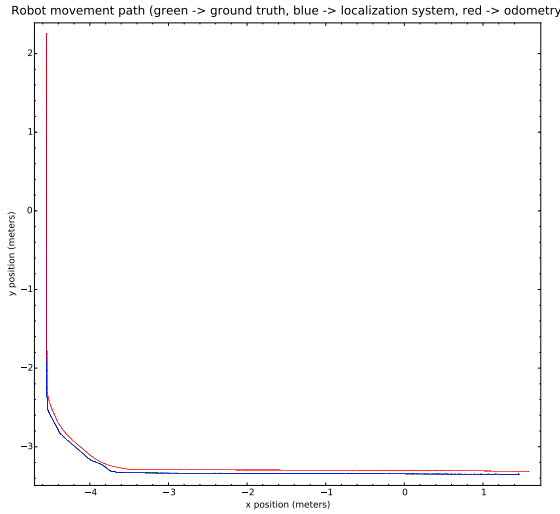


Figure 5.86: Paths from ground truth (green), localization system (blue) and odometry (red)

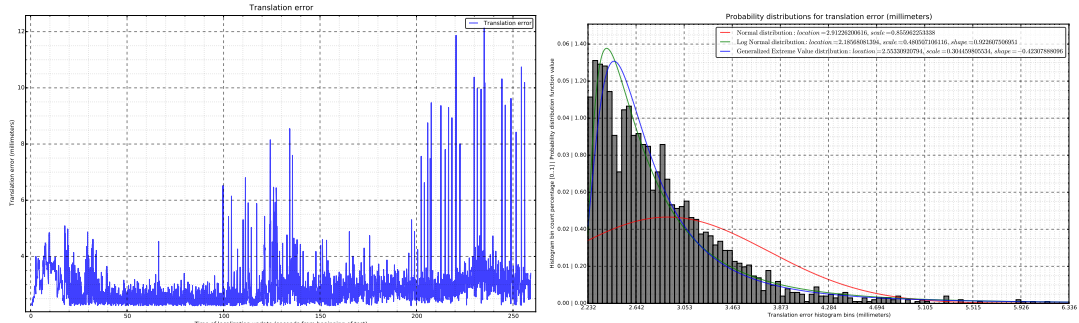


Figure 5.87: Localization system translation error (left) and its statistical distributions (right)

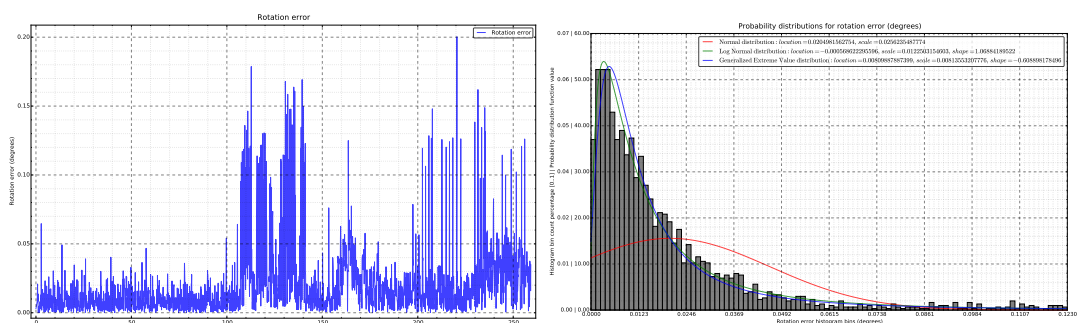


Figure 5.88: Localization system rotation error (left) and its statistical distributions (right)

## Localization system evaluation

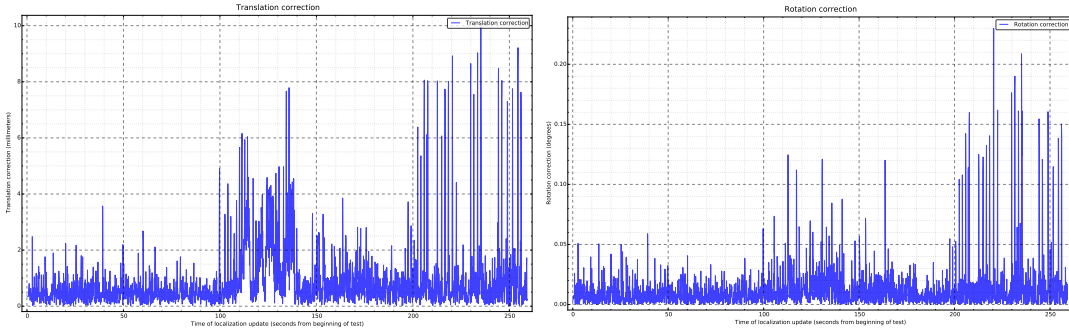


Figure 5.89: Localization system translation (left) and rotation (right) corrections

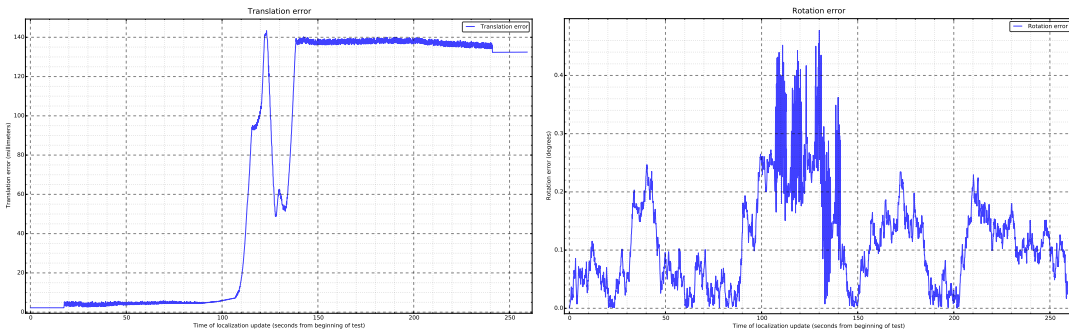


Figure 5.90: Odometry translation (left) and rotation (right) error

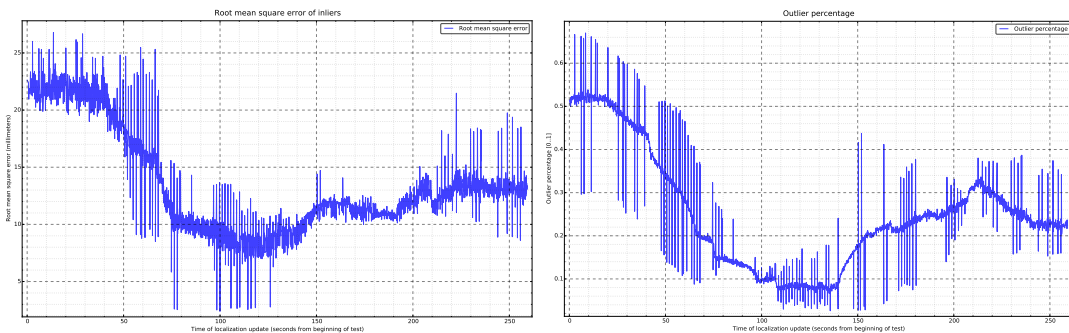


Figure 5.91: Localization system inliers root mean square error (left) and outlier percentage (right)

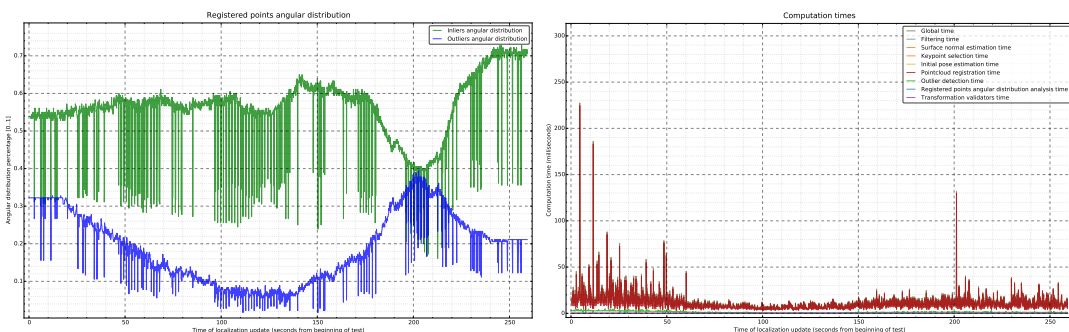


Figure 5.92: Cloud registration outlier percentage (left) and inliers angular distribution (right)

#### 5.3.4.4 Wall follower path using Guardian simulator at 30 cm/s in static cluttered environment

2

4 Figures 5.93 to 5.99 show the results of the Guardian platform using the Gazebo simulator following the lower and right wall in the static cluttered structured environment world at 30 cm/s.

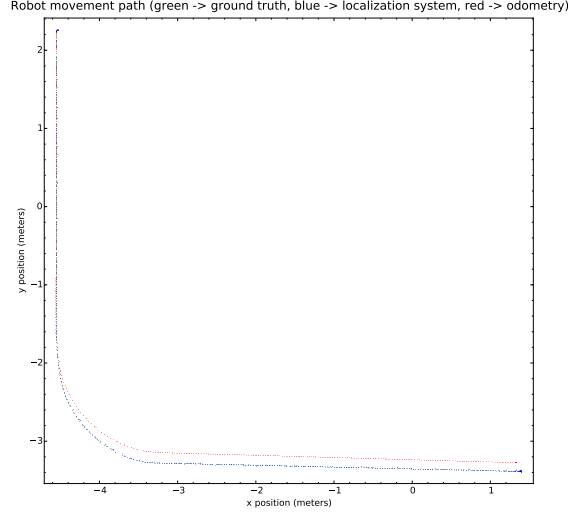


Figure 5.93: Paths from ground truth (green), localization system (blue) and odometry (red)

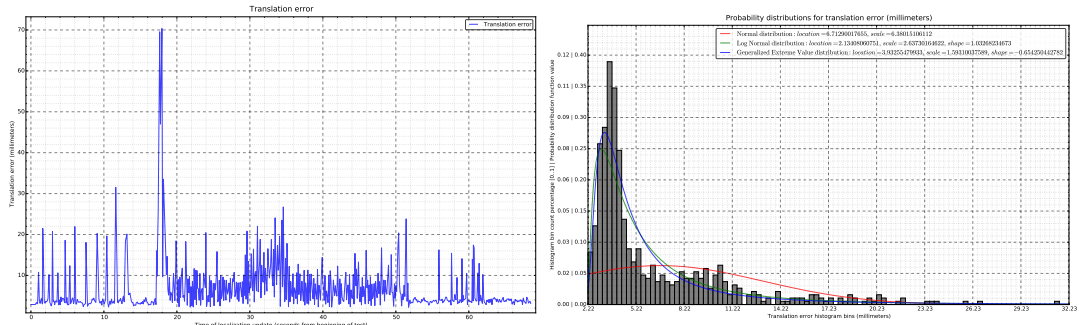


Figure 5.94: Localization system translation error (left) and its statistical distributions (right)

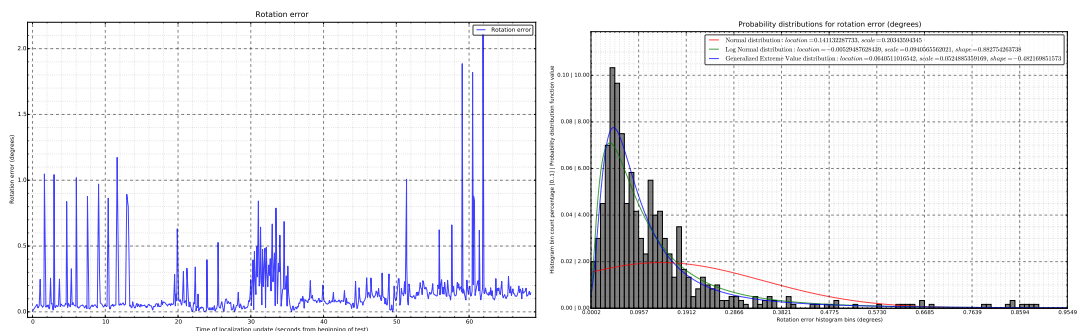


Figure 5.95: Localization system rotation error (left) and its statistical distributions (right)

## Localization system evaluation

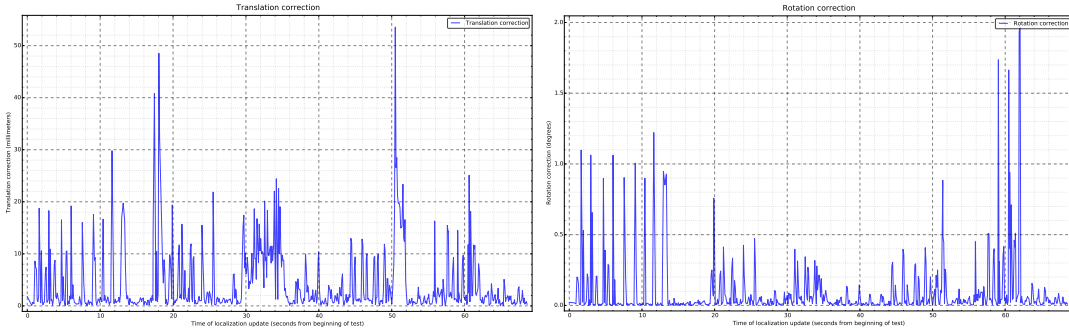


Figure 5.96: Localization system translation (left) and rotation (right) corrections

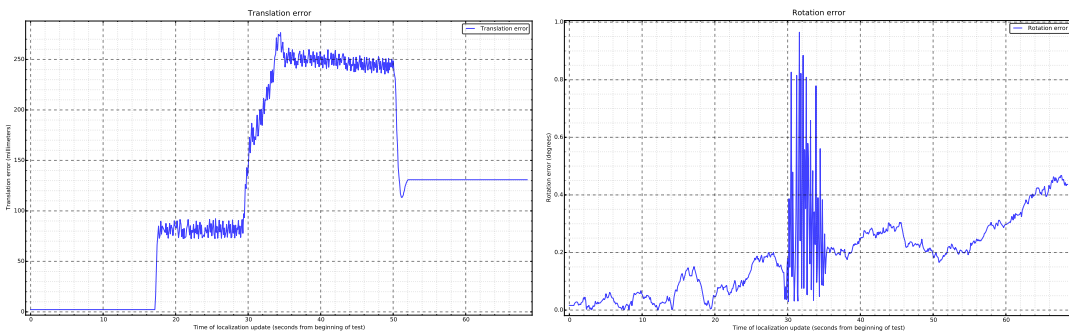


Figure 5.97: Odometry translation (left) and rotation (right) error

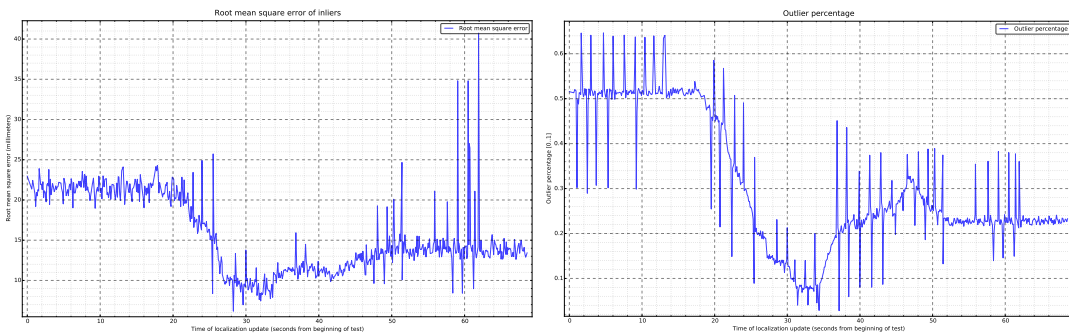


Figure 5.98: Localization system inliers root mean square error (left) and outlier percentage (right)

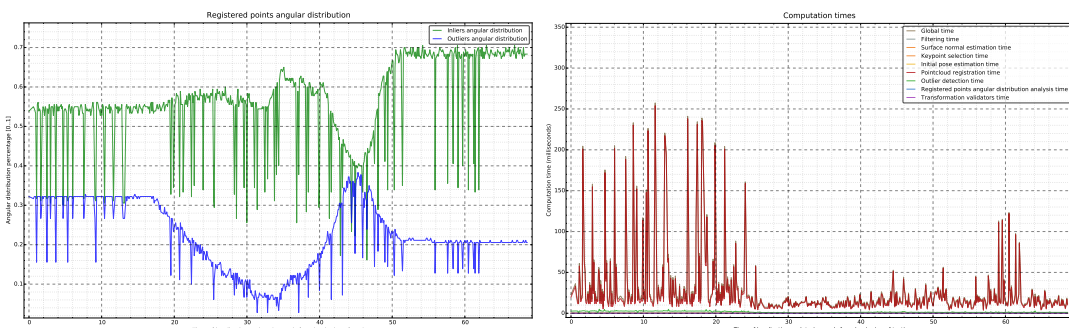


Figure 5.99: Cloud registration outlier percentage (left) and inliers angular distribution (right)

### 5.3.4.5 Wall follower path using Guardian simulator at 5 cm/s in dynamic cluttered environment

Figures 5.100 to 5.106 show the results of the Guardian platform using the Gazebo simulator following the lower and right wall in the dynamic cluttered structured environment world at 5 cm/s.

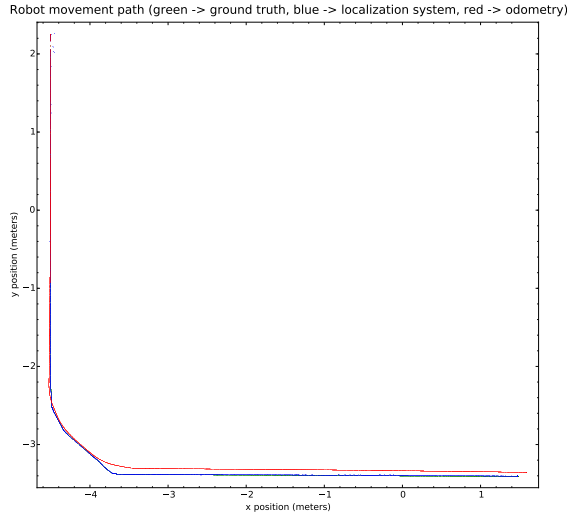


Figure 5.100: Paths from ground truth (green), localization system (blue) and odometry (red)

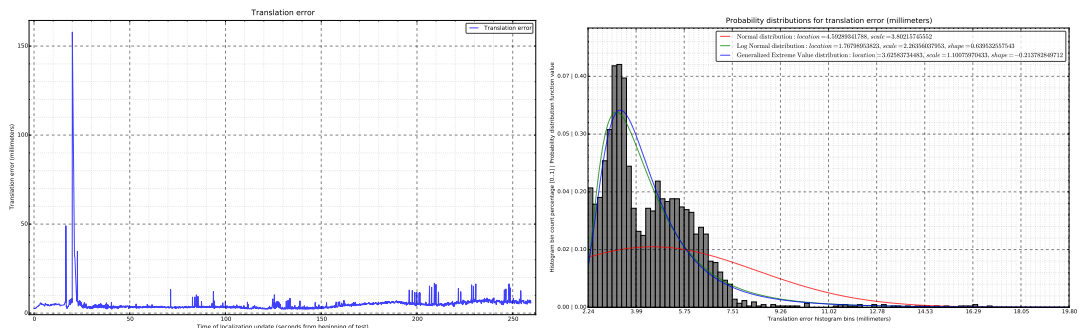


Figure 5.101: Localization system translation error (left) and its statistical distributions (right)

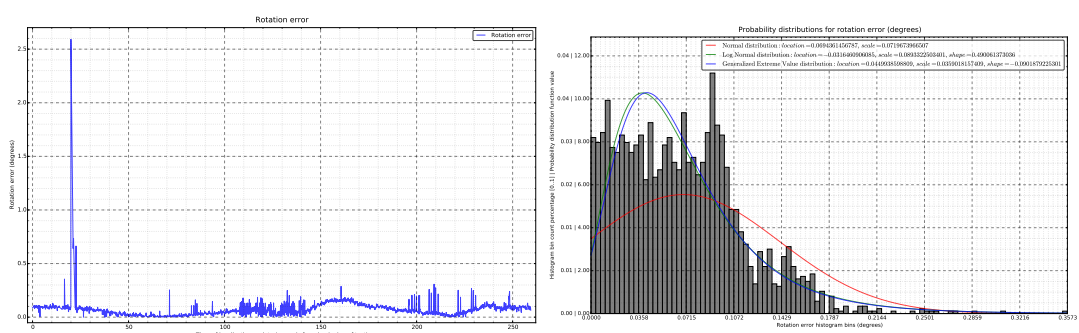


Figure 5.102: Localization system rotation error (left) and its statistical distributions (right)

## Localization system evaluation

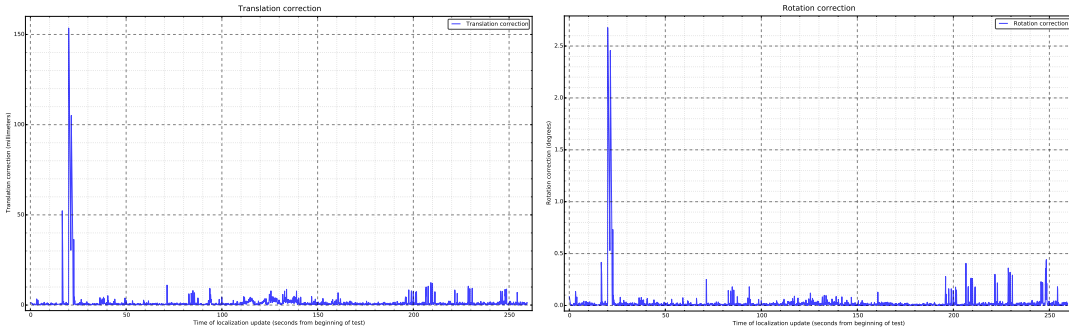


Figure 5.103: Localization system translation (left) and rotation (right) corrections

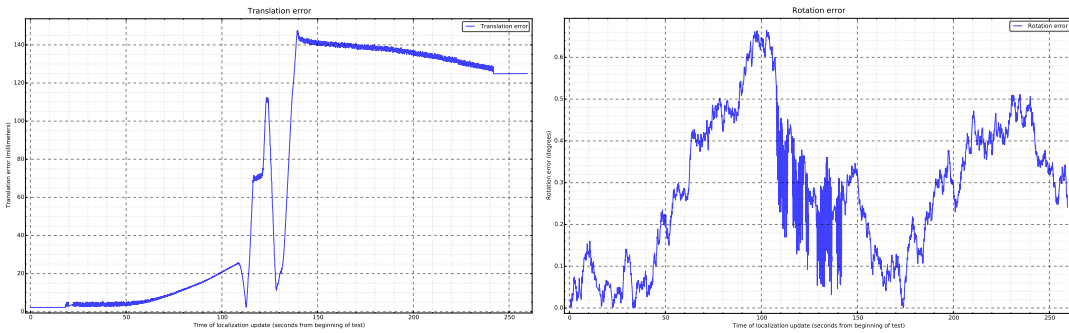


Figure 5.104: Odometry translation (left) and rotation (right) error

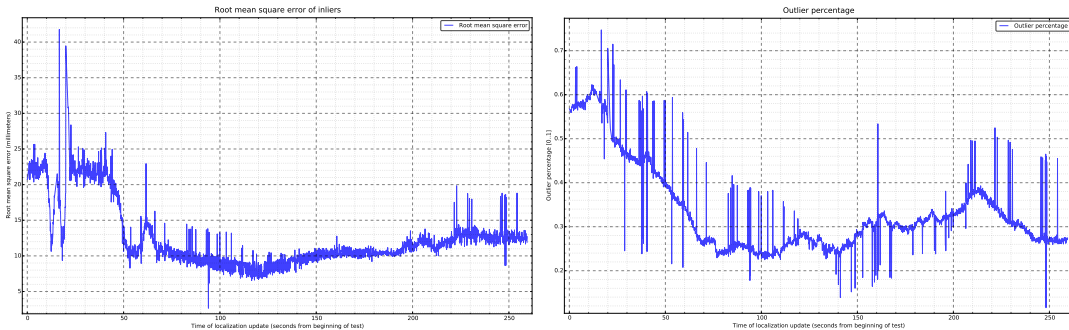


Figure 5.105: Localization system inliers root mean square error (left) and outlier percentage (right)

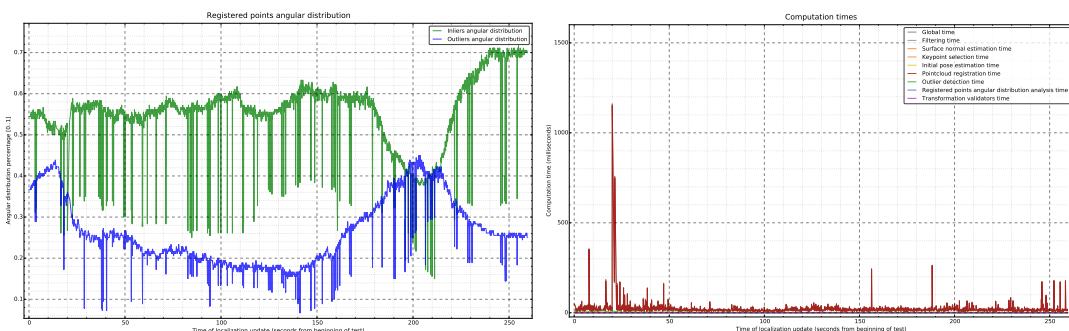


Figure 5.106: Cloud registration outlier percentage (left) and inliers angular distribution (right)

### 5.3.4.6 Wall follower path using Guardian simulator at 30 cm/s in dynamic cluttered environment

Figures 5.107 to 5.113 show the results of the Guardian platform using the Gazebo simulator following the lower and right wall in the dynamic cluttered structured environment world at 30 cm/s.

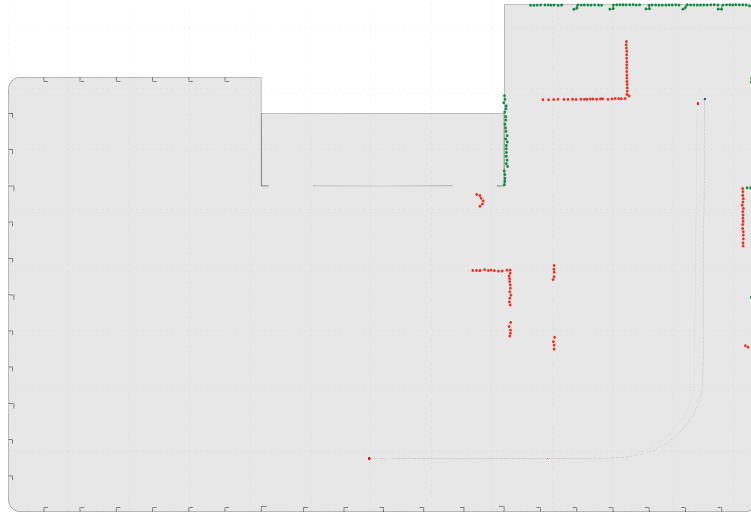


Figure 5.107: Paths from ground truth (green), localization system (blue) and odometry (red)

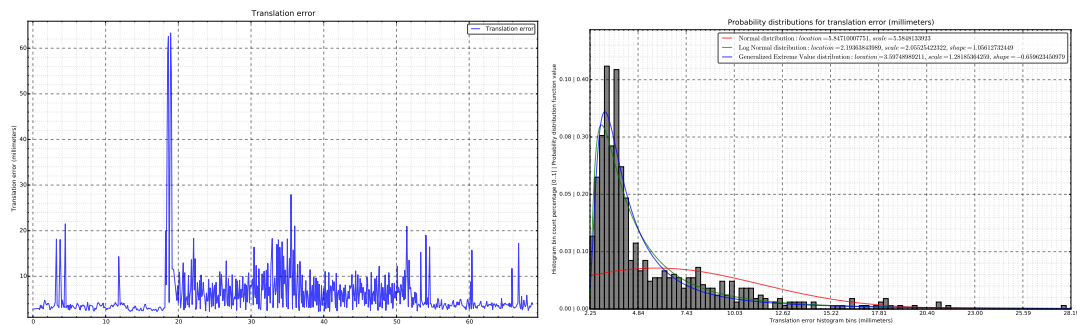


Figure 5.108: Localization system translation error (left) and its statistical distributions (right)

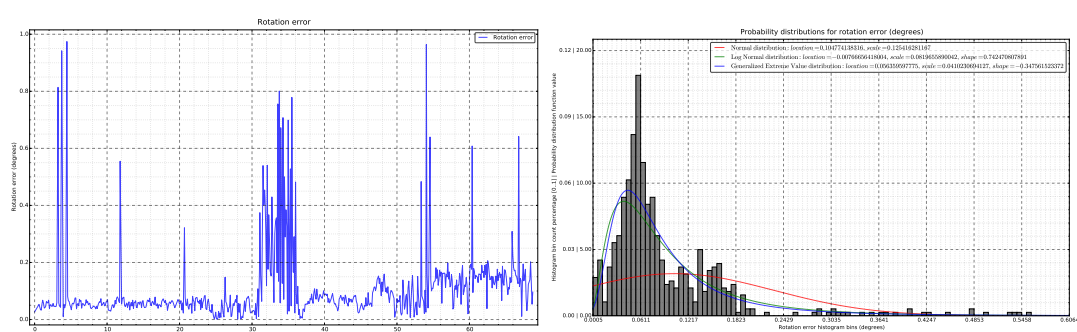


Figure 5.109: Localization system rotation error (left) and its statistical distributions (right)

## Localization system evaluation

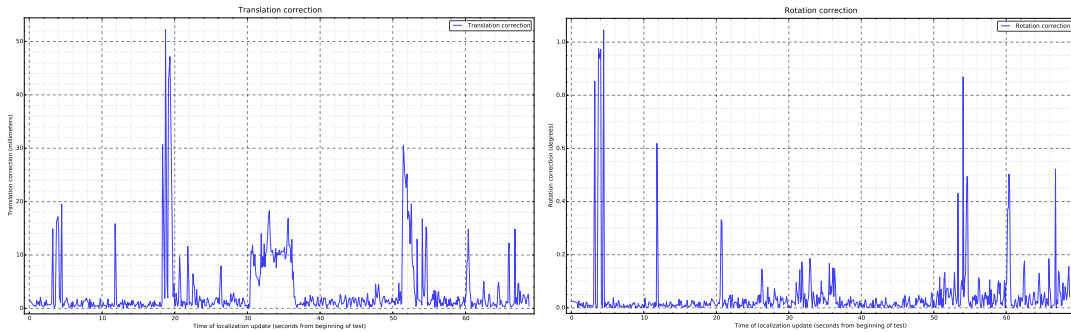


Figure 5.110: Localization system translation (left) and rotation (right) corrections

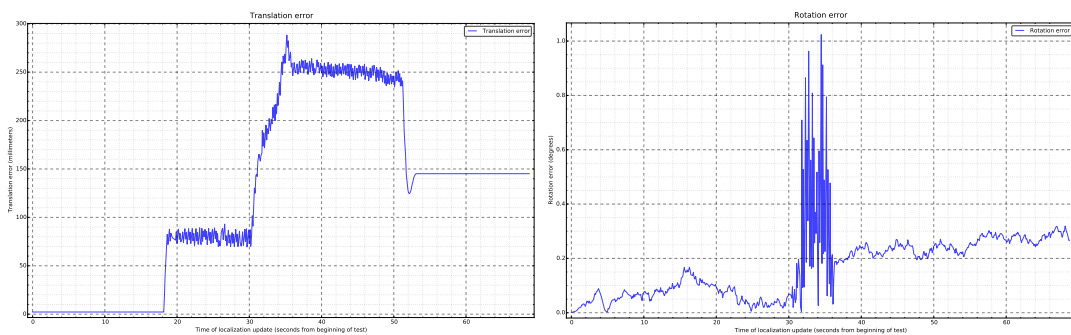


Figure 5.111: Odometry translation (left) and rotation (right) error

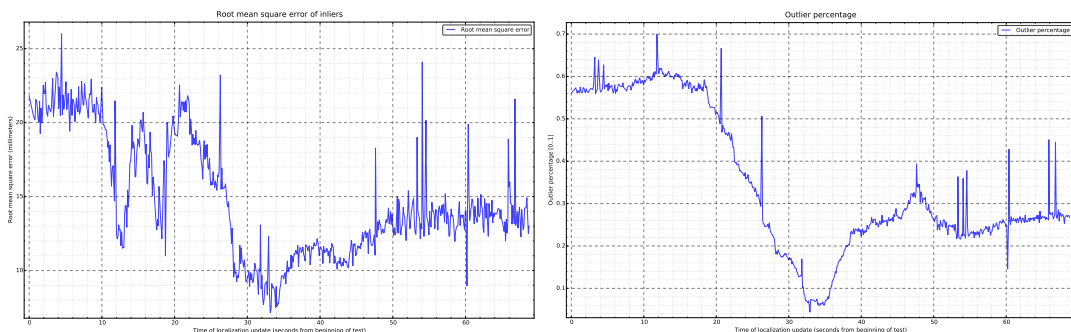


Figure 5.112: Localization system inliers root mean square error (left) and outlier percentage (right)

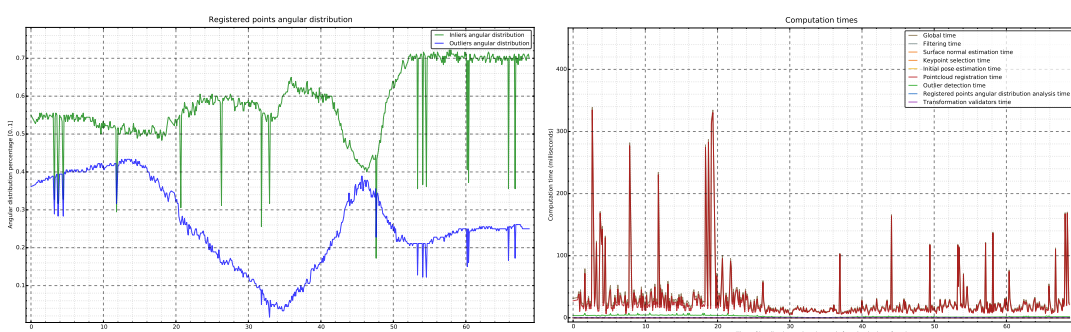


Figure 5.113: Cloud registration outlier percentage (left) and inliers angular distribution (right)

### 5.3.5 Initial pose estimation tests

- 2 Figures 5.114 to 5.116 show the accepted initial pose estimations using the global localization subsystem presented in section 4.10.1.
- 4 The blue circles presented in figure 5.115 represent the keypoints of the ambient point cloud in the robot start up position, while the violet circles are the reference point cloud keypoints. The
- 6 green circles are the ambient point cloud laser measurements after performing the initial pose estimation and registration refinement.

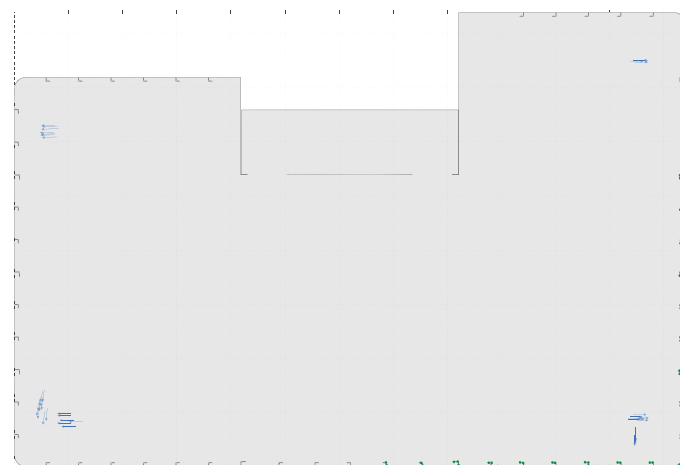


Figure 5.114: Initial pose estimation using feature matching in Guardian static environment

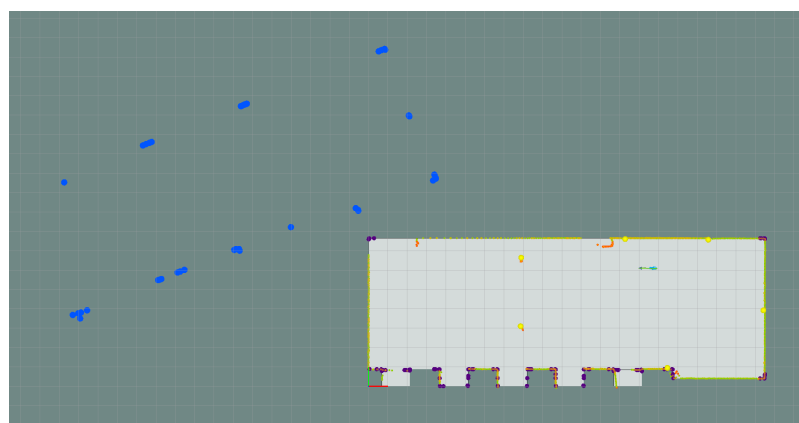


Figure 5.115: Initial pose estimation using feature matching in Jarvis environment

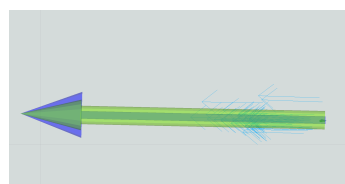


Figure 5.116: Initial pose estimation distribution in Jarvis environment

### 5.3.6 Results discussion

The results achieved with the proposed 3 DoF localization system showed sub centimeter pose tracking and reliable initial pose estimation. As expected, the simulator tests at lower velocities had less mean error than the ones at higher speeds while requiring slightly less computation time. Also, the tests on the Jarvis robot had more mean error than the corresponding simulator tests. This is due to laser scan deformation that couldn't be simulated and also because the simulators were only able to add Gaussian noise to the laser measurements. To compensate the simulators limitations, the error in odometry and laser measurements in simulation was deliberately higher than the expected values for the physical platforms. This explains why the localization system needed more time to perform the pose estimations in the simulator tests. It can also be seen that adding unknown objects increased the mean error and required computation time while adding dynamic objects increased these values even further (given that a moving object appears in a laser scan as a deformed version of its static shape).

The ability to switch registration algorithms at runtime based on the quality of the estimated pose proved to be an efficient and flexible architecture choice, since it allowed high precision pose tracking with fast registration algorithms and occasional pose tracking recovery with more robust methods (which happened more often in the tests at higher velocities, in which the odometry was significantly worse). The initial pose estimation using feature matching was very reliable and successfully found the robot location even in low feature surroundings (as can be seen in figure 5.114). Moreover, the output of the accepted initial pose estimations allows the detection of similar map locations by a navigation supervisor, which can then plot a path to disambiguate the initial pose guess and avoid dangerous operations at a wrong position. The statistical error of the lasers was mitigated by merging several laser scans before performing a point cloud registration. This is based on the fact that a considerable amount of laser noise follows a Gaussian distribution, and as such, the effective measurement error can be significantly reduced by retrieving the centroids of a voxel grid applied over the laser data. However, assembling too much laser scans can lead to worse pose tracking if the robot is moving at high speeds, because the lasers would be projected into the map frame with a high position error (because odometry accuracy decreases when the robot speed increases and the localization system will not correct it). As such, the laser assembler has dynamic reconfiguration of the number of laser scans to assemble (or the period of assembly time) based on the robot estimated velocity. This feature besides improving the pose tracking it also allows a navigation supervisor to regulate the rate at which the localization system operates. This can be very useful for mobile manipulators because the localization system can have a high update rate when the robot is moving fast and a low update rate when it is moving slower or when it is stopped. This allows a more efficient usage of the platform hardware resources while also improving the localization system accuracy. The dynamic map update capability helped lowering the point cloud registration time while also increasing the accuracy by a small margin. Moreover, it improved the robustness of the initial pose estimations and allowed better path planning for the navigation system.

## **5.4 6 DoF localization system tests**

### **2 5.4.1 Overview**

FF.

### **4 5.4.2 Results**

FF.

### **6 5.4.3 Results discussion**

FF.

## Localization system evaluation

# Chapter 6

## 2 Conclusions and future work

- 4    The proposed localization system is able to maintain pose tracking with less than one cm in trans-
- 5    lation error at several velocities even in cluttered and dynamic environments. Moreover, when
- 6    tracking is lost or no initial pose is given, the system is able to find a valid global pose estimate by
- 7    switching to more robust registration algorithms that use feature matching. This approach achieved
- 8    fast pose tracking and reliable initial pose estimation while also providing the distribution of the
- 9    accepted initial poses before registration refinement, which can be very valuable information for
- 10   a navigation supervisor when the robot is in an ambiguous region that can be registered in similar
- 11   zones in the known map. The system also allows dynamic reconfiguration of the number of laser
- 12   scans to assemble in order to mitigate laser measurement errors and can adapt its rate of operation
- 13   according to the robot estimated velocity.
- 14   The sub centimeter accuracy achieved by the proposed localization system along with the dy-
- 15   namic map update capability and the need of no artificial landmarks will allow the fast deployment
- 16   of mobile manipulators capable to operate safely and accurately in cluttered environments.

The current implementation of the self-localization system can be further improved with loop  
18 closing algorithms [GSK12] and [Graphics Processing Unit \(GPU\)](#) support [TARK10] in order  
19 to become a true [SLAM](#) system and allow the creation of accurate maps of very large environ-  
20 ments. Moreover, it could be extended to support image based localization [Lab14] and semantic  
perception [Rus10] and mapping of the environment [San13].

## Conclusions and future work

# References

- 2 [ABCO<sup>+</sup>03] Marc Alexa, Johannes Behr, Daniel Cohen-Or, Shachar Fleishman, David Levin,  
and Claudio T. Silva. Computing and rendering point set surfaces. *IEEE Transactions on Visualization and Computer Graphics*, 9(1):3–15, January 2003.
- 4 [AMGC02] M. Sanjeev Arulampalam, Simon Maskell, Neil Gordon, and Tim Clapp. A tutorial  
on particle filters for online nonlinear/non-Gaussian Bayesian tracking. *IEEE Transactions on Signal Processing*, 50(2):174–188, 2002.
- 6 [BGFM10] J.-L. Blanco, J. Gonzalez, and J.-a. Fernandez-Madrigal. Optimal Filtering for Non-  
parametric Observation Models: Applications to Localization and SLAM. *The International Journal of Robotics Research*, 29(14):1726–1742, May 2010.
- 8 [BM92] Paul J. Besl and Neil D. McKay. A method for registration of 3-D shapes. *IEEE Transactions on Pattern Analysis and Machine Intelligence*, 14(2):239–256, 1992.
- 10 [BOG<sup>+</sup>10] Mussa Bshara, Umut Orguner, Fredrik Gustafsson, Leo Van Biesen, and Student Member. Fingerprinting Localization in Wireless Networks Based on Received-Signal-Strength Measurements : A Case Study on WiMAX Networks Fingerprinting Localization in Wireless Networks Based on Received-Signal-Strength Measurements : A Case Study on WiMAX Network. ... *IEEE Transactions on*, 59(1):283–294, 2010.
- 12 [BTP13] Sofien Bouaziz, Andrea Tagliasacchi, and Mark Pauly. Sparse iterative closest point. *Computer Graphics Forum*, 32(5):113–123, August 2013.
- 14 [Che03] Z H E Chen. Bayesian Filtering : From Kalman Filters to Particle Filters , and Beyond VI Sequential Monte Carlo Estimation : Particle Filters. *Statistics*, 182(1):1–69, 2003.
- 16 [CK02] Yongguang Chen Yongguang Chen and H. Kobayashi. Signal strength based indoor geolocation. *2002 IEEE International Conference on Communications. Conference Proceedings. ICC 2002 (Cat. No.02CH37333)*, 1(1):436–439, 2002.
- 18 [CSSK02] D. Chetverikov, D. Svirko, D. Stepanov, and P. Krsek. The Trimmed Iterative Closest Point algorithm. *Object recognition supported by user interaction for service robots*, 3:545–548, 2002.
- 20 [DKU<sup>+</sup>07] Zhen Dai, Stefan Knedlik, Pakorn Ubolkosold, Junchuan Zhou, and Otmar Loffeld. Integrated GPS navigation for civilian vehicles in challenging environment. *2007 IEEE International Conference on Vehicular Electronics and Safety, ICVES*, pages 1–6, December 2007.

## REFERENCES

- [DZA<sup>+</sup>13] M. Djehaich, H. Ziane, N. Achour, R. Tiar, and N. Ouadah. SLAM-ICP with a Boolean method applied on a car-like robot. *Proceedings of the 2013 11th International Symposium on Programming and Systems, ISPS 2013*, pages 116–121, 2013. 2
- [EW99] Garry a. Einicke and Langford B. White. Robust extended Kalman filtering. *IEEE Transactions on Signal Processing*, 47(9):2596–2599, 1999. 4
- [FA14] S. Filipe and L. a. Alexandre. A Comparative Evaluation of 3D Keypoint Detectors in a RGB-D Object Dataset. *9th International Conference on Computer Vision Theory and Applications*, 2014. 6
- [FB81] Martin a Fischler and Robert C Bolles. Random Sample Consensus: A Paradigm for Model Fitting with Applications to Image Analysis and Automated Cartography. *Communications of the ACM*, 24(6):381 – 395, 1981. 10
- [FBDT99] Dieter Fox, Wolfram Burgard, Frank Dellaert, and Sebastian Thrun. Monte Carlo Localization: Efficient Position Estimation for Mobile Robots. *American Association for Artificial Intelligence, (Hanschin 1970)*:1–6, 1999. 12
- [FHK<sup>+</sup>04] Andrea Frome, Daniel Huber, Ravi Kolluri, Thomas Bülow, and Jitendra Malik. Recognizing Objects in Range Data Using Regional Point Descriptors. *Computer Vision - ECCV 2004*, 3023:224–237, 2004. 16
- [GIRL03] N. Gelfand, L. Ikemoto, S. Rusinkiewicz, and M. Levoy. Geometrically stable sampling for the ICP algorithm. *Fourth International Conference on 3-D Digital Imaging and Modeling, 2003. 3DIM 2003. Proceedings.*, pages 260–267, 2003. 18
- [GSK12] Giorgio Grisetti, Hauke Strasdat, and Kurt Konolige. g 2 o: A general Framework for (Hyper) Graph Optimization. (1):1–19, 2012. 22
- [GWG13] Francesco Guarato, James F C Windmill, and Anthony Gachagan. A new sonar localization strategy using receiver beam characteristics. *IEEE International Ultrasonics Symposium, IUS*, pages 445–448, July 2013. 24
- [HWB<sup>+</sup>13] Armin Hornung, Kai M. Wurm, Maren Bennewitz, Cyrill Stachniss, and Wolfram Burgard. OctoMap: An efficient probabilistic 3D mapping framework based on octrees. *Autonomous Robots*, 34(3):189–206, February 2013. 26
- [Ibr10] Modar Ibraheem. Gyroscope-enhanced dead reckoning localization system for an intelligent walker. In *ICINA 2010 - 2010 International Conference on Information, Networking and Automation, Proceedings*, volume 1, pages 67–72, 2010. 30
- [IKP10] Edouard Ivanjko, Andreja Kitanov, and I Petrovic. Model based Kalman Filter Mobile Robot Self-Localization. *Robot Localization and Map . . . , (1996)*:59–91, 2010. 32
- [Jez08] O Jez. Evaluation of a factorized ICP based method for 3D mapping and localization. *Atpjournal.Sk*, pages 29–37, 2008. 34
- [Jol02] Jolliffe. *Principal component analysis*, volume 2. 2002. 36
- [JU97] Simon J Julier and Je K Uhlmann. A New Extension of the Kalman Filter to Non-linear Systems. *System Identification*, 3:3–2, 1997. 38

## REFERENCES

- [Kac13] Witold Kaczurba. FPGA-Based System Combines Two Video Streams to Provide 3D Video. *Analog Dialogue*, pages 1–5, 2013.
- [Kal60] R. E. Kalman. A New Approach to Linear Filtering and Prediction Problems. *Journal of Basic Engineering*, 82(Series D):35, 1960.
- [KKOO07] Yong Shik Kim, Bong Keun Kim, Kohtaro Ohba, and Akihisa Ohya. Bias estimation of DGPS multi-path data for localization of mobile robot. *Proceedings of the SICE Annual Conference*, pages 1501–1505, September 2007.
- [KL04] Scale-invariant Keypoints and David G Lowe. Distinctive Image Features from. *International journal of computer vision*, 2004.
- [Lab14] Mathieu Labb. Online Global Loop Closure Detection for Large-Scale Multi-Session Graph-Based SLAM. *Proceedings of the IEEE/RSJ International Conference on Intelligent Robots and Systems*, 2014.
- [LKP06] Sukhan Lee Sukhan Lee, Eunyoung Kim Eunyoung Kim, and Yeonchool Park Yeonchool Park. 3D object recognition using multiple features for robotic manipulation. *Proceedings 2006 IEEE International Conference on Robotics and Automation, 2006. ICRA 2006.*, (May):3768–3774, 2006.
- [LLRM06] Martin Lauer, Sascha Lange, Martin Riedmiller, and Martin Riedmiller Martin Lauer, Sascha Lange. Calculating the perfect match: an efficient and accurate approach for robot self-localization. *Robocup 2005: Robot soccer world cup* ..., 4020(c):142–153, 2006.
- [LYL11] Jianshen Liu, Baoyong Yin, and Xinxing Liao. Robot self-localization with optimized error minimizing for soccer contest. *Journal of Computers*, 6(7):1485–1492, July 2011.
- [Mag09] Martin Magnusson. *The Three-Dimensional Normal-Distributions Transform — an Efficient Representation for Registration, Surface Analysis, and Loop Detection*. PhD thesis, Örebro University, 2009.
- [MCB10] Julien Moras, Véronique Cherfaoui, and Phillippe Bonnifait. A lidar perception scheme for intelligent vehicle navigation. In *11th International Conference on Control, Automation, Robotics and Vision, ICARCV 2010*, number December, pages 1809–1814, 2010.
- [PM63] Miguel Pinto and Ap Moreira. Novel 3D matching self-localization algorithm. *International Journal of* ..., 5(1):1–12, 1963.
- [Pom13] François Pomerleau. *Methodology and Tools for ICP-like Algorithms*. PhD thesis, ETH Zürich, 2013.
- [QCG<sup>+</sup>09] Morgan Quigley, Ken Conley, Brian Gerkey, Josh FAust, Tully Foote, Jeremy Leibs, Eric Berger, Rob Wheeler, and Andrew Mg. ROS: an open-source Robot Operating System. *Icra*, 3:5, 2009.
- [R.48] W. R. Introduction to Wireless. *Nature*, 162:911–911, April 1948.

## REFERENCES

- [RBB09] Radu Bogdan Rusu, Nico Blodow, and Michael Beetz. Fast Point Feature Histograms (FPFH) for 3D registration. *2009 IEEE International Conference on Robotics and Automation*, pages 3212–3217, May 2009. 2
- [RBMB08] Radu Bogdan Rusu, Nico Blodow, Zoltan Csaba Marton, and Michael Beetz. Aligning point cloud views using persistent feature histograms. *2008 IEEE/RSJ International Conference on Intelligent Robots and Systems, IROS*, pages 3384–3391, September 2008. 4
- [RC11] Radu Bogdan Rusu and Steve Cousins. 3D is here: Point Cloud Library (PCL). *Proceedings - IEEE International Conference on Robotics and Automation*, pages 1–4, May 2011. 8
- [Rib04] Maria Isabel Ribeiro. Kalman and Extended Kalman Filters : Concept , Derivation and Properties. *Institute for Systems and Robotics Lisboa Portugal*, (February):42, 2004. 10
- [RKZ13] Michal Reinstein, Vladimir Kubelka, and Karel Zimmermann. Terrain adaptive odometry for mobile skid-steer robots. In *Proceedings - IEEE International Conference on Robotics and Automation*, pages 4706–4711, 2013. 14
- [RL01] Szymon Rusinkiewicz and Marc Levoy. Efficient variants of the ICP algorithm. In *3-D Digital Imaging and Modeling, 2001. Proceedings. Third International Conference on. IEEE*, pages 145–152. IEEE Comput. Soc, 2001. 18
- [Rus10] Radu Bogdan Rusu. *Semantic 3D Object Maps for Everyday Manipulation in Human Living Environments*. PhD thesis, Technische Universität München, August 2010. 20
- [San13] Filipe Baptista Neves dos Santos Santos. *A collaborative, non-invasive hybrid semantic localization and mapping system*. PhD thesis, 2013. 22
- [SHT09] a Segal, D Haehnel, and S Thrun. Generalized-ICP. *Robotics: Science and Systems*, 2009. 26
- [Sot06] S Sotoodeh. Outlier Detection in Laser Scanner Point Clouds. *Iaprs*, Volume XXX(September):297–302, 2006. 28
- [SS09] Ptm Saito and Rj Sabatine. An analysis of parallel approaches for a mobile robotic self-localization algorithm. *International Journal of . . .*, 2(4):49–64, 2009. 30
- [STD09] Giovanna Sansoni, Marco Trebeschi, and Franco Docchio. State-of-the-art and applications of 3D imaging sensors in industry, cultural heritage, medicine, and criminal investigation. *Sensors*, 9:568–601, 2009. 32
- [TARK10] Toru Tamaki, Miho Abe, Bisser Raytchev, and Kazufumi Kaneda. Softassign and EM-ICP on GPU. *Proceedings - 2010 1st International Conference on Networking and Computing, ICNC 2010*, pages 179–183, November 2010. 34
- [TGCV12] Gurkan Tuna, Kayhan Gulez, V. Cagri Gungor, and T. Veli Mumcu. Evaluations of different Simultaneous Localization and Mapping (SLAM) algorithms. *IECON Proceedings (Industrial Electronics Conference)*, pages 2693–2698, 2012. 38
- [Thr02] Sebastian Thrun. *Probabilistic robotics*, volume 45. 2002. 40

## REFERENCES

- [TSD10] Federico Tombari, Samuele Salti, and Luigi Di Stefano. Unique shape context for 3d  
2 data description. *Proceedings of the ACM workshop on 3D object retrieval - 3DOR*  
'10, page 57, 2010.
- [TSD11] Federico Tombari, Samuele Salti, and Luigi Di Stefano. A combined texture-shape  
4 descriptor for enhanced 3D feature matching. *Proceedings - International Conference*  
6 on *Image Processing, ICIP*, pages 809–812, 2011.
- [Vit84] Jeffrey Scott Vitter. Faster methods for random sampling. *Communications of the*  
8 *ACM*, 27(7):703–718, 1984.
- [WM00] E.a. Wan and R. Van Der Merwe. The unscented Kalman filter for nonlinear es-  
10 timation. *Proceedings of the IEEE 2000 Adaptive Systems for Signal Processing,*  
*Communications, and Control Symposium (Cat. No.00EX373)*, 7:153–158, 2000.
- [WV11] Walter Wohlkinger and Markus Vincze. Ensemble of shape functions for 3D object  
12 classification. *2011 IEEE International Conference on Robotics and Biomimetics*,  
14 pages 2987–2992, December 2011.
- [WY07] Shun-xi Wu Shun-xi Wu and Ming Yang Ming Yang. Landmark Pair based Local-  
16 ization for Intelligent Vehicles using Laser Radar. *2007 IEEE Intelligent Vehicles*  
*Symposium*, pages 209–214, June 2007.
- [WYY<sup>+</sup>13] Bin Wu, Bailang Yu, Wenhui Yue, Song Shu, Wenqi Tan, Chunling Hu, Yan Huang,  
20 Jianping Wu, and Hongxing Liu. A voxel-based method for automated identification  
and morphological parameters estimation of individual street trees from mobile laser  
scanning data. *Remote Sensing*, 5(2):584–611, January 2013.
- [YPH<sup>+</sup>14] Hong-seok Yang, Ji-man Park, Jung-suk Han, Jai-bong Lee, Sung-hun Kim, and In-  
22 sung Yeo. Measuring abutment convergence angles using stereovision dental image  
24 processing system. pages 259–265, 2014.
- [Yu09] Zhong Yu. Intrinsic shape signatures: A shape descriptor for 3D object recognition.  
26 *2009 IEEE 12th International Conference on Computer Vision Workshops, ICCV*  
*Workshops 2009*, pages 689–696, September 2009.
- [YXL11] Peng Yang, Li Xie, and Jilin Liu. Angular velocity current statistical model based  
28 real-time celestial navigation for lunar rover. *Proceedings of the 30th Chinese Con-*  
30 *trol Conference*, pages 4011–4016, 2011.
- [Zha94] Z Zhang. Iterative point matching for registration of free form curves and surfaces.  
32 *International Journal of Computer Vision*, 12:119–152, 1994.
- [ZL11] Jia Heng Zhou and Huei Yung Lin. A self-localization and path planning technique  
34 for mobile robot navigation. *Proceedings of the World Congress on Intelligent Con-*  
*trol and Automation (WCICA)*, pages 694–699, 2011.
- [ZMH10] Yang Zhang Yang Zhang, N. Meratnia, and P. Havinga. Outlier Detection Tech-  
36 niques for Wireless Sensor Networks: A Survey. *IEEE Communications Surveys &*  
38 *Tutorials*, 12:159–170, 2010.